Available online at www.joac.info

ISSN: 2278-1862

Journal of Applicable Chemistry

2016, 5(1): 21-110

(International Peer Reviewed Journal)

Perspective Review

Computational Quantum Chemistry (CQC)
Part 2: Anticancer/anti-HIV drugs and DFT studies with Jaguar

K. Ramakrishna[1*], B. Venkata Sasidhar[1] andR. Sambasiva Rao[2]

1. Department of Chemistry, Gitam Institute of Science, Gitam University, Visakhapatnam, 530 017, **INDIA**

2 School of Chemistry, Andhra University, Visakhapatnam 530 003, **INDIA**

Email: karipeddirk@gmail.com, rsr.chem@gmail.com

Accepted on 10th January2016

ABSTRACT

Background: The FDA approved marketeddrugs for cancer and HIV increased the life span and comfort of patients. The motto of inventing better molecules to render AIDS-free and cancer-free human life and reducing the suffering is key in looking for new leads and toxic free/ high potency molecules for clinical trials. The results of CQC, structure activity relationships (SXR), HTS/virtual libraries, docking and conformer generators lead to complimentary and supplementary information in drug discovery to routine prescription through clinical trials. Earlier, we carried out the synthesis of substituted Uracil-5-Sulphonamides and confirmed their structures from spectral studies.

Scope of study: The quantum chemical investigations and biological (anti-cancer/anti-HIV) activity in vitro of four synthesized substituted Uracil-5-sulphonamides derivatives are reported.

Chemical models with CQC: The geometry optimization, chemical validity of CQC model, single point electronic point energies and physico-chemical properties of substituted aroyl sulphonamides are computed with Jaguar package of Schrodinger software suit. The level of theory employed is DFT with B3LYP hybrid functional for both optimization and vibrational frequency analysis. The anti-cancer and anti-HIVS activities of N-cyclobutyl-2,4-dioxo-1,2,3,4-tetrahydropyrimidine-5-sulfonamide, Ethyl,1-((2,4-dioxo-1,2,3,4-tetrahydropyrimidin-5-yl)sulfonyl)piperidine-4-carboxylate, ((2,4-dioxo-1,2,3,4-tetrahydro pyrimidin-5-yl)sulfonyl)-L-proline,(4aS,7aS)-6-benzyl-1-((6-methyl-2,4-dioxo-1,2,3,4-tetrahydropyrimidin-5yl) sulfonyl)tetrahydro-1H-pyrrolo[3,4-b]pyridine-5,7(6H,7aH)-dioneetc are reported here. A peda gogical research frame for pseudospectral method for solving PDFs (partial differential equations) and functional features of Jaguar in first order knowledge form are discussed. An intelligent database of drugs for cancer and HIV is under rigorous testing and passive form of a part of it is in supplementary material. The features of Schrodinger are described from an in-house hierarchical information/knowledge/method base for CQC with G09, HyperChem, ADF, Schrodinger and GAMESS for gaseous and solvent media.

Biological activity: The anticancer activity against survival of the colon carcinoma HCT-116 cell lines and anti-HIV data compared to Zidovudine (AZT) are experimentally determined. These second order tensors arecorrelated with quantum chemical derived parameters.

Conclusions: The present set of substituted sulphonamides show promising anti-cancer and anti-HIV activity. The results are valuable insights into the role in a multi-facet probing into the chemical properties of these new ligands and their physical-/bio-physical interaction energetics expanding assessment of the capabilities of molecules to explorative search in the drug-discovery pursuit. Further, detailed

investigations of toxicity, membrane permeability and protein-ligand interactions will throw light on the suitability for the next phase.

Keywords: Synthesis, Substituted Sulphonamides, CQC models, Gas phase, Jaguar package, 3D-Geo metric optimization, vibrational frequencies, Properties, biological activity, HIV, Cancer.

Contents

Anticancer/anti-HIV drugs and DFT studies with Jaguar

INTRODUCTION

Pediatric and geriatric treatment and research of cancer/HIV are challenging for medical professionals and interdisciplinary scientists. One reason is the available data is yet limited in all aspects of metabolic implications, unprecedented complications in developing and decaying phases of life processes. Further, comorbidities, opportunistic diseases, mindset in life style, surrounding environment and economic backdrop impair the health system. The lower quality of life for rest of period of children and unbearable perturbations for the remaining life span in the case of geriatric patients are of recent concern in addition to palliative care for minimum possible suffering. Some of the infections viz. HBV/HCV and HPV also cause cancer prevalent in low- and middle-income countries. At this rate, the projected annual cancer cases will go up to 22 million within next two decades from around 14 million in 2012. Here, typical research output in cancer/HIV drugs and computational quantum chemistry modeling with Jaguar are described [1-193]. We recently reviewed diagnosis of cancer cell proliferation in different organs and HIV by neural network models in a series of publications [181-186]. The applications of nature inspired algorithms viz. big bang big crunch, bat/mosquito mimics found a niche in research and clinical diagnostic tool kit [181-192]. The immediate and long term goal is to achieve as much health as possible for patients suffering from malignant neoplasms through non-invasive diagnostic tools and non-toxic medicines along with knowledge based awareness counselling for the compromised life style.

1.1 Molecules-to-Medicines-to-Materials (MtMtM, pronounced as empty-empty-em)

During evolution, simple molecules are transformed into polymers, macromolecules, molecules of life, metabolic networks and living cells. Also, simultaneously, toxic materials, poisons, materials of comfort and discomfort (to whom is a big question) are also the products of nature's laboratory, in other words, nature itself. Thus, at the fundamental level, life sustaining, disease causing and curative agents are all chemical molecules, but of different sizes, characteristics and environment. Science is a paradigm of collection of direct or indirect observables through human senses and/or state-of-art-instruments. It is also a frame to explore how they are best linked in complicated net together. This involves several checks, confirmations, re-confirmations up to even six sigma error limits and also finding out rational reasons for even a lone contradictory case of experimental/theoretical instance. Chemistry, biology, physics and mathematics (BCPM) are wings of science. The metrics, omics etc. are hybrids, while engineering and technology are means of producing prototype products in large numbers, of course with conflicting sub goals of high quality, low price tag/ durability etc. Mathematics and logic condense data through data/dimension reduction procedures. Information theory extracts maximum innate information in the data. The software/firm ware and hardware are fast number crunchers in yesteryears and now silicon machines of extracting knowledge and developing intelligent sparkles. Cloud is an internet based environment to share hardware/software resources and store data/information/knowledge/intelligence in a smart and secure manner. It is similar to a pool of LANs, WANs, magnetic/optical storage media of last century.

1.1.1 Cancer

The normal cells are fundamental units of life and they grow and die when aged or damaged. The normal cells divide forming whenever new cells are needed. The total number of molecules constituting cells is in the range of a billion. Each type of molecules viz. DNA, RNA, proteins, glycans and lipids possess a distinct biological function. The cells react to the environment and negotiate with others in developing tissues, organs and for that matter the whole organism.

Cancer is due to abnormal cells capable of division in an uncontrollable fashion and their invasion on other tissues propagated both in blood and lymph circulatory systems. When a single cell in the tissue is extensively damaged genetically and produces damaged cells in very large numbers, the malignant growth is termed as cancer. The mitosis results in proliferation of cells with a consequence of primary heterogenic tumor. The consequence of follow up metaplasia, dysplasia and anaplasia is malignant phenotype. But, the exponential growths of cells many a time result in (solid) growths/ tumors. These benign tumors may be very large, but never spread/invade nearby tissues. The surgical removal is the end

and they usually don't grow back. The exception is benign brain tumors as they are mostly life threatening. When cancer develops, this orderly cell balance collapses. In fact, cancer can develop where ever there are cells i.e. skin to brain or anywhere in the entire body. When cancer starts, damaged and old cells do survive when they should die. Further new cells proliferate resulting in tumors, but malignant. Most of malignant growths are solid masses, except leukemia (chart 1). Cancerous and normal cells are similar to a large extent, except that the former host mutated genes. Further, they share the same DNA and metabolic path ways. This is main difficulty in diagnosis and therapy. The resulting mutated proteins in cancerous cells affecting the cell division are the cause of oncogenesis. Angiogenesis inhibitors perceive specific contrast between tumor and normal tissues/ cells and thus have lower toxicities. Dona [17] compares the scenario with 'we identified the enemy (disease causing agent), but he is one among us (normal cells)'.

Metastasis: If the cancer cells at a site (say breast) cross the walls of lymphatic and/or blood vessels and circulate in the body, this is referred as lymphatic or hematogenous spread. With time, the tumor cells re-penetrate the vessel or walls and start multiplying at another organ. The new cancerous tumor at the another organ say lung is called metastatic (or secondary) tumor. But, the tumor cells at lung now are similar to breast cancer cells and it is referred as meta-static breast cancer at lung and not lung cancer.

Chart 1:Most prevalent cancers

Males	Females	Dietary risks
▶ Lung ▶ Stomach ▶ Colorectum ▶ Prostate ▶ Liver cancer	▶ Lung ▶ Stomach cancer ▶ Colorectum ▶ Breast ▶ Cervix	– High body mass index – Low fruit/ vegetable intake – Lack of physical activity – Tobacco use – Alcohol use.

Diagnosis of cancer: After the era of myths and (mis)beliefs about diseases and curative procedures, medical practices and exploration of drugs reached a state-of-maturity over half a century of time. The state-of-knowledge of modern medicine over the last quarter century changed the scenario in the detection/control/eradication of frightening ill-health problems. But unfortunately, most of the cancer patients reach metastatic stage by the time they are diagnosed and thus becomes beyond cure by even with state-of-art treatment protocols. From basic research stand point, the diagnosis of cancer, diabetes, cardiomyopathies, retinal degeneration, muscular dystrophy, cystic fibrosis, mental retardation and their treatment are now in the realm of cell/molecular biology/genetic editing/omics/metrics in 21st century. This interdisciplinary research comprises of chemistry, biology, physics and structure. Still in cancer therapy the nomenclature -- surgery, radiation/chemical therapy are in practice due to historical reasons. Another instance is the term MRI (magnetic resonance imaging) against the popular NMR (nuclear magnetic resonance) in medical diagnosis. Further, there is tremendous research progress in detection of cancer at molecular level and it will change scenario in the coming decades.

ॐ Anti-Cancer drugs

The recent progress of probing more into cancer-stem-cells in malignant tumors will open new vistas into a takeoff in therapeutic strategies with a lower toll of discomfort for cancer patients.Yet, some cancers still continue to be challenging even in 21st century and drug-discovery-research is now in the direction of molecules selectively killing/ terminating (or inhibiting) proliferation and not at all harming normal cells present even nearer to tumor cells. Cis platinum compounds were in use for treatment of testicle cancer. The characteristics of antimetabolites of pyrimidine and purine are studied as anti-tumor and tumor-growth inhibiting agents. The chloriocarcinomas, testes cancer and Hodgkin's diseases for example are curable even when detected at advanced stage. The chemotherapy or hormone adjustment treatment lowered the severity of growth and increased the patients' comfort.

An in-depth knowledge of similarities/contrast of cancerous cells from normal/non-cancerous malignant ones and their metabolic path ways pin point the direction of potential drug leads. The drug

molecule is an outcome with smart features like bioavailability, ADME, low toxicity, pharmacokinetics, non-toxic metabolites, selectively reaching to target and not accumulating elsewhere. The multi-drug (in a single tablet form) regime and combined anti-drug therapeutic protocols avoided patient's discomfort, resistance to a drug and toxic side effects of conventional cytotoxic compound.

First wave (Alkylating agents): Prior to 1940s, surgery was the treatment of (cancerous) tumors. Nitrogen mustard compounds which are alkylating agents were the first set of drugs in efforts to cure cancer. The alkylating action of these compounds on bases in DNA results in killing cancer cells.
Second wave (antimetabolites): Aminopterin and amethopterin are antimetabolites and interfere with folate synthesis. Thus, unlike nitrogen mustards, these molecules obstruct replication or promote mistakes (mutation) in replication of DNA with a consequence of death of cancer cells. This inspired to bring out chemical moieties targeting DNA and microtubules present in cell responsible for cell division. The drug resistance became a limitation of this approach.

- The classical drugs attacking DNA replication/cell division in a cancer cell also hinder normal cells. This consequence is bone marrow or gastrointestinal toxicity
- Remedy: Combination therapy

Third wave (Combination therapy): The drug becoming resistant to a single target is an artefact of few mutations. But, multiple agents attacking different parts/phases in the development of disease causing/developing virus/bacteria/process definitely need large number of mutations. This is less probable at least over an extended period of time compared to single-drug-protocol. The natural immune system follows this strategy of simultaneously waging war against large number of targets on recognized-non-self-components i.e. virus/bacteria. In 1960s, this approach of combination of chemotherapeutic agents benefited the treating cancerous patients. Of course, even now a cocktail of drugs is still in practice in chemotherapeutic regimens with several benefits and lessened limitations.

A perusal of history of anti-cancer drugs (Appendix 1) reveals nitrogen containing heterocyclic systems (which are bio-isosteric analogs of natural compounds) have a key role in therapeutic activity. 5-fluorouracil, an anti-metabolite, is a standard anticancer agent. Uracil, thymine and pyrimidine based nucleotide moieties exist in cancerous drugs. A brief synopsis of typical categories of cancer inhibiting molecules follows.

Pyridin dione: Lattmann et al. [1] studied cytotoxicity against murine carcinoma cell lines (MAC13 and MAC16) using the standard MTT assay in-vitro cultures and in-vivo growth in mice.

Fig.1:Lead Structures

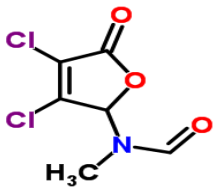

Amidofuranone N-(3 4-Dichloro-5-oxo-2 5-dihydro-2-furanyl)-N-methylformamide

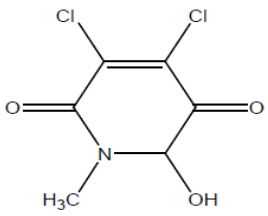

pyidindione lead structure

Lead structures with substituents	
Dichloro-5-oxo-2 5-dihydro-furan-2-yl-acetamides	4 5-Dichloro-3-pyridazones
Dichloro-5-oxo-2 5-dihydro-furan-2-yl)-N-methyl-acetamide AAF	4 5-Dichloro-2-p-methoxy-phenyl-3-pyridazone R=p-MeOPh
3-4-dichloro-5-oxo-2 5-dihydrofuran-yl(methyl)-formamide R=H	4 5-Dichloro-2-pyridazin-3(2H)-one DCPYR

In vitro - in vivo studies on mice (**IC50 µM**)

murine colon adenocarcinoma

% [inhibition] = Treated weight / control weight x 100

- MAC 13
- MAC 16

Pyrimidine derivatives: Xiong et al. [19] synthesized and studied anti-leukaemia and anti-liver-cancerous tumor activity in vitro of amino acid ester derivatives containing 5-fluorouracil (chart 2).

Chart 2: substituted fluorouracil derivatives

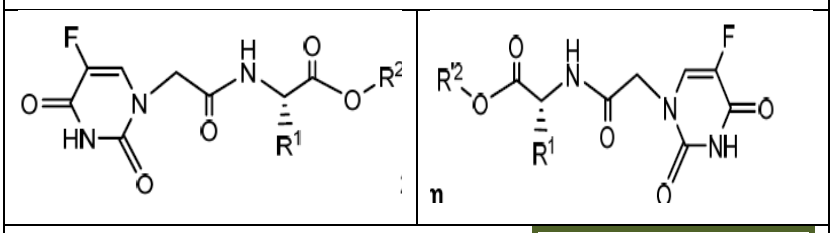

In vitro antitumor activity	
HL-60	leukaemia
BEL-7402	liver cancer

	R^1	R^2		R^1	R'^2
a	$CH(CH_3)_2$	CH_3	b	$CH(CH_3)_2$	CH_2CH_3
c	$CH_2CH(CH_3)_2$	CH_3	d	$CH_2CH(CH_3)_2$	CH_2CH_3
e-1	$CH_2CH_2SCH_3$	CH_3	e-2	$CH_2CH_2SCH_3$	CH_3
f-1	CH_2OH	CH_3	f-2	CH_2OH	CH_3
g	CH_2COOCH_3	CH_3	h	CH_2COOCH_3	CH_2CH_3
i	$CH_2CH_2COOCH_3$	CH_3	j	$CH_2CH_2COOCH_2CH_3$	CH_2CH_3
k-1	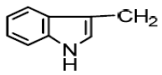	CH_3	k-2	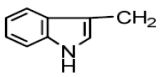	CH_3
l	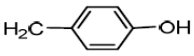	CH_3	m	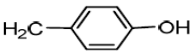	CH_3CH_3

5-fluoro-2'-deoxyuridine (floxuridine) and 5'-deoxy-5-fluorouridine (doxifluidine) are used in the treatment of kidney carcinoma and digestive system cancer respectively. Some coenzymes contain pyrimidine derivatives and thus, molecules containing a bio-target fragment would be a better drug lead. The adrenolytics containing pyrimidine and cholinesterase inhibitors are sought after moieties in the frontline of new-drug-exploration program. Semenov [21] studied in vitro antibacterial and antifungal activity of pyrimidinophanes with varying substituents. The molecules contain quaternized or not quaternized nitrogen atoms in the bridges, one/two uracil units, cis- or trans-arrangement of carbonyl groups at different pyrimidine rings (chart 3). The limited reports with pyrimidinophanes are due to their insolubility in water and other polar solvents to probe more into biological investigations.

Chart 3: Isomeric pyrimidinophanes

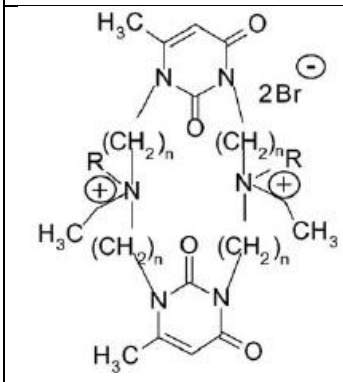

Isomeric pyrimidinophanes with quaternized N in spacers

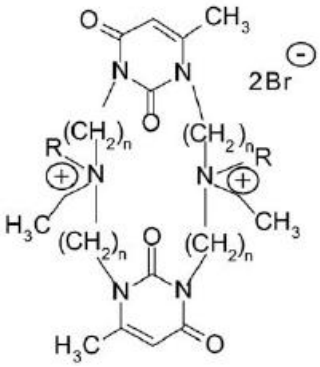

quaternized N in spacers

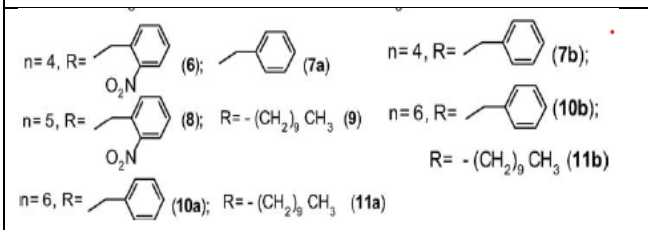

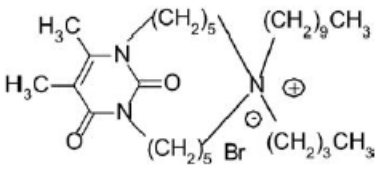

in vitro activity in mice

- Minimal inhibitory concentrations (MICs)
- LD50

Antibacterial	Antifungal
Pathogenic representative Gram-negative bacteria Pseudomonas aeruginosa 9027 Escherichia coli F-50 Gram-positive bacteria Staphylococcus aureus 209p Bacillus subtilis 6633 Enterococcus faecalis ATCC 8043	Pathogenic fungi Aspergillus niger BKMF-1119 Trichophyton mentagrophytes var. gypseum 1773 Aspergillus fumigatus AF-27 yeast Candida Albicans 885-653

Anand and Kalpana [6] carried out synthesis and in vitro biological activities of a series of substituted 6-amino-5- [2-(5-substituted-2-phenyl-1H-indol-3-yl)-4- oxothiazolidin-3-yl]- 1,3-dimethylpyrimidine- 2,4-diones (chart 4). Melatonin, serotonin, tryptophan are some of the naturally occurring indole derivatives playing a key role in many biochemical processes, for instance as antioxidant and in functioning of immune system.

Chart 4: Pyrimidine-diones

Bacteria				Fungi	
Gram-positive	Staphylococcus aureus	ATCC-29513		Aspergillus niger	MTCC-281
Gram-negative	Pseudomonas aeruginosa	MTCC-1688		Aspergillus flavus	MTCC-1973
	Standard Drug	Gentamycin		Standard drug	Flucanazole

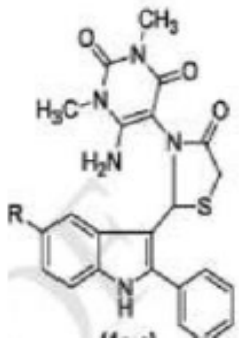

R
Cl
Me
H

Standard drug : Gentamycin

(2R 3S 4R 6S)-4 6-Diamino-3-{[3-deoxy-4-C-methyl-3-(methylamino)-L-arabinopyranosyl]oxy}-2-hydroxycyclohexyl 2-amino-2 3 4 6 7-pentadeoxy-6-(methylamino)-β-L-lyxo-heptopyranoside

Sulphonamides: Arylsulphonamides have anticancer activity and HIV-1 integrase inhibiting action. Brzozowski et al. [22] synthesized and probed into antitumor activities of 2-mercaptobenzene sulphonamides /guanidines in human patients (Fig. 2,chart 5).

Fig. 2a: Typical structures with heteroatoms (S or N)

Sulfuric diamide
Sulfamide

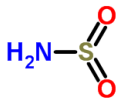

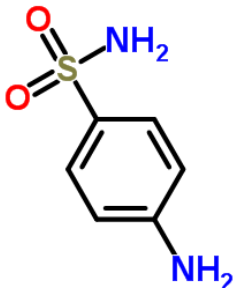

Sulfanilamide
4-Aminobenzenesulfonamide

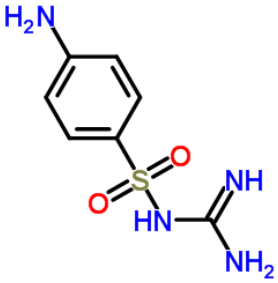

sulfaguanidine

4-Amino-N-carbamimidoylbenzenesulfonamide

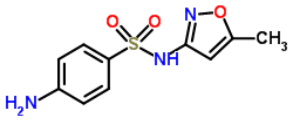

Sulfamethoxazole
4-Amino-N-(5-methyl-1,2-oxazol-3-yl)benzenesulfonamide

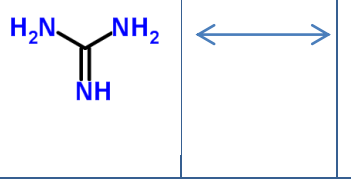

Guanidine

Fig. 2b: Sulphonamides in drug discovery line

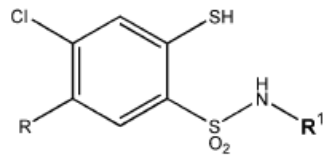

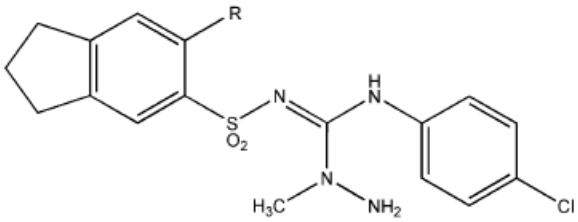

R^1

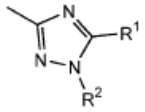

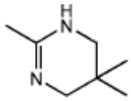

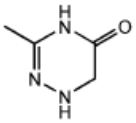

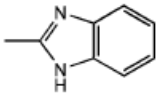

Chart 5: Substituted arylsulphonamides

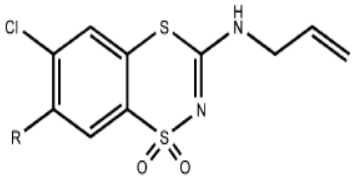

a	CH3
b	CH3OCO
c	C6H5NHCO
d	4-Cl_C6H4NHCO
e	4-F_C6H4NHCO

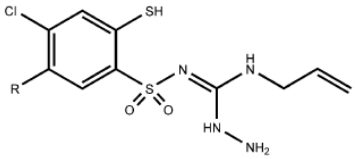

a	CH3
b	CH3OCO
c	C6H5NHCO
d	4-Cl_C6H4NHCO
e	4-F_C6H4NHCO

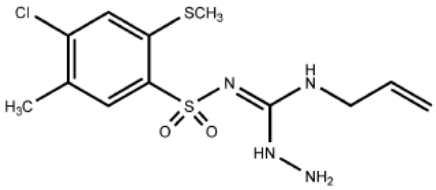

	CH3

Leukemia lung Colon CNS Melanoma	Ovarian Renal Prostate Breast

GI50	molar concentration of the compound that inhibits 50% net cell growth
TGI	Molar concentration of the compound leading to total inhibition
LC50	Molar concentration of the compound leading to 50% net cell death

Prostate cancer	PC-3
Colon cancer	HCC-2998, KM-12
Non-small cell lung cancer	NCI-H522
Melanoma	

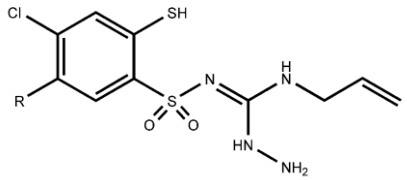

1 -allyl-3 -amino-2 -(4 -chloro-2 -mercaptobenzenesulphonyl)guanidines

Chart 5b: Guanidines

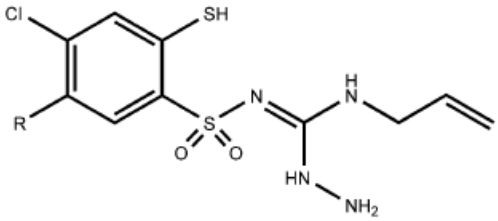

R	Anticancer activity In vitro
Me	61 human tumour Cell lines
CH3OCO	
PhNHCO	
4-Cl-PhNHCO	
4-F-PhNHCO	

Prostate	Lung
Colon	Breast.
Ovarian	Cns
Renal	Melanoma
Leukemia	

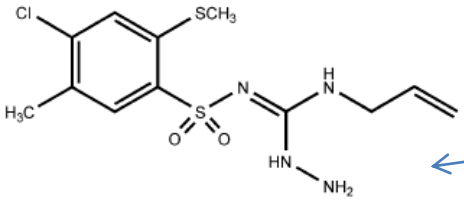

E = -2093.420884 a.u.
μ = 4.82 D

4 isomers
[22]

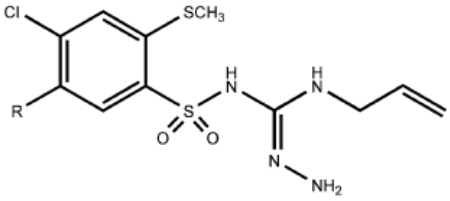

E = -2093.408158 a.u.
μ = 4.51 D

Tautomeric forms of benzenesulphonylguanidine

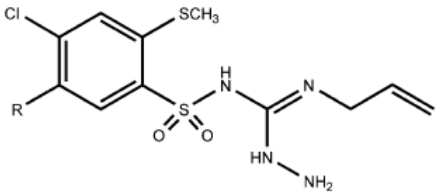

E = -2093.396946 a.u.
μ = 1.94 D

Substituted uracil moieties: Michel Nuevo, Ames Research Center, NASA reported formation of uracil, cytosine, and thymine (components of molecules of life viz. RNA, DNA) non-biologically in the

laboratory. Pyrimidine with nitrogen atoms in the benzene ring structure is wimpy [w(eakly) i(nteracting) m(assive) p(article)]. An ice sample of pyrimidine is on a substrate at -440°F and irradiated with high energy UV photons from hydrogen lamp. The photons break chemical bonds and result in fragments which recombine into many molecules including uracil, cytosine, and thymine. There is yet no undisputed evidence how life got started on Earth. But it might be many of the building blocks of life were likely present from the beginning of formation of earth and atmosphere.

Uracil (U), Cytosine (C) adenine (A) or guanine (G) (Fig.3) is attached to each nucleotide in ribonucleic acid (RNA). Adenine and guanine are purines, while cytosine and uracil are pyrimidines. Between uracil and adenine, there are two hydrogen bonds in RNA. In DNA, the uracil nucleobase is replaced by thymine. Uracil could be considered as a demethylated form of thymine. It undergoes amide-imidic acid tautomeric shifts. The amide and imidic acid tautomer are known as lactam and lactim structures. The lactam structure is the most common form of uracil. Many compounds containing uracil are used in the treatment of cancer and HIV diseases. 5-Fluorouracil (5-FU) is an antimetabolite of the pyrimidine analogue and employed in treating solid tumors such as colorectal gastric tract and liver carcinomas. 5-trifluoromethyluracil and 5-mercaptomethyluracil are effective as inhibitors of cell growth. But, the clinical applications of 5-FU are limited by poor tumor affinity, myelosuppression, strong intestinal toxicity and short pl5-fluorouracil as anticancer drug. The N1-substituted derivatives, nucleoside analogs of 5-iodouracil and 5-trifluoromethyluracil possess antiviral activity. Acyclic 5 6-disubstituted uracils are anti HIV-1 agents. N1 N3-disubstituted uracils were reported to exhibit antibacterial and antifungal activities. A cinnamoyl group at the 5-position of 1 3-dimethyl-6-aminouracil derivatives promote intercalation with DNA base pairs.

Fig. 3: Cytosine, Uracil, Adenine, Guanine

pyrimidines

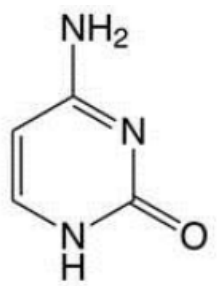

Cytosine

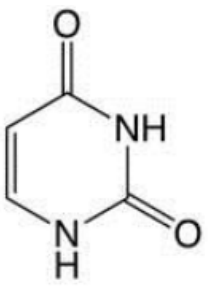

Uracil

purines

Adenine
3H-Purin-6-amine

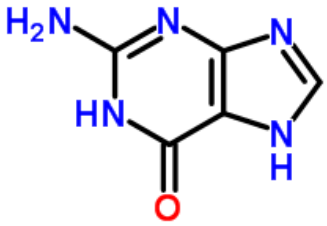

Guanine
2-amino-3,7-dihydro-6H-purin-6-one

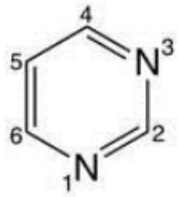

Pyrimidine

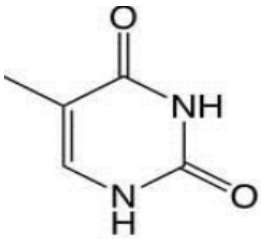

Thymine

Prachayasittikul et.al [18] investigated anticancer activity of N-substituted 5-idouracils (chart 6) against B. catarrhalis N. mucosa and S. pyogenes.

Chart 6: Substituted 5-idouracils

R

- CH2CH2CH2CH3
- CH3CHCH2CH3
- *t*-C4H9
- 1-Adm
- CH2CH2□OH

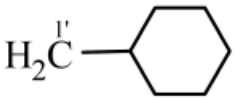

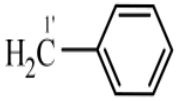

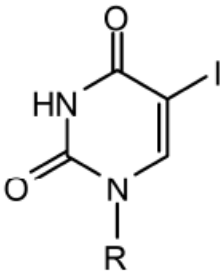

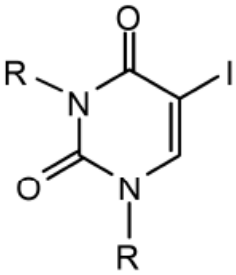

In vitro

B. catarrhalis
N. mucosa
S. pyogenes

Uracil C-Mannich bases: Mannich bases possess antineoplastic, diuretic, antipsychotic, anticonvulsant and central acting muscle relaxant, antibacterial, antimalarial and antiviral activities. Istanbullu et al. [14] synthesized and assessed biological activities using MTT assays [21] on human cell lines of cancer (chart 07).

Cancer-07-Substituted MTT

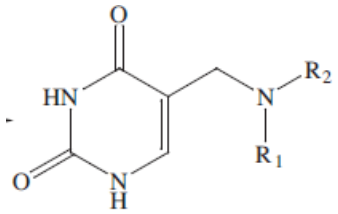

Antiproliferative activity on 3 human cell lines: in vitro	
Cervix adenocarcinoma	HeLa
Breast adenocarcinoma	MCF7
Skin epidermoid carcinoma	A431

II	**-C2H4OC2H4 -**	**morpholinomethyl**	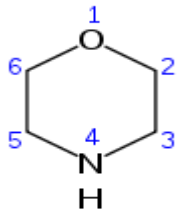 **morpholine**	**IV**	**-C4H8 -**	**pyrrolidinomethyl**	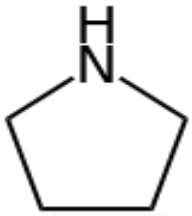 **Pyrrolidine**
			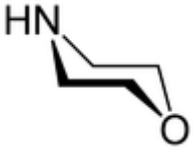	**VIII**	**-C2H4NHC2H4**	**piperazinomethyl**	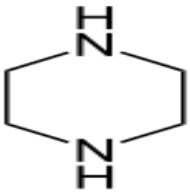
III	**-C5H10 -**	**piperidinomethyl**	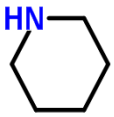 **Piperidine**				

	R1 = R2=
I	$-CH_2CH_2Cl$
V	$-CH_2CH_2OH$
VI	$-CH_2CH_3$
VII	$-CH_3$

Piperazines: The piperazines form an important template for anti-cancer, antifungal, antibacterial, antimalarial, antipsychotic agents, as well as HIV protease inhibitors and antidepressants. MST-16 [4,4-1,2-(ethanediyl)bis(1-isobutoxycarbonyloxy-methyl-2,6-piperazinedione)] is recently approved an oral anticancer drug for application in Japan. Piperazine derivatives inhibit growth of human erythroleukemia K562 cells and myeloid leukemia HL-60 cells and also hinder topoisomerase II activity. The interaction of DNA with an unfused aromatic system containing terminal piperazino substituents is reported. N-Alkyl, N-sulfonyl and N-benzoyl derivatives of benzhydrylpiperazine show anticancer and antimicrobial activity. Yarim et al. [12] reported the inhibitive activity of substituted pyrazine derivatives for cancer cells from liver, gastric and breast tumor samples (chart 8).

Chart 8: Substituted Piperazines

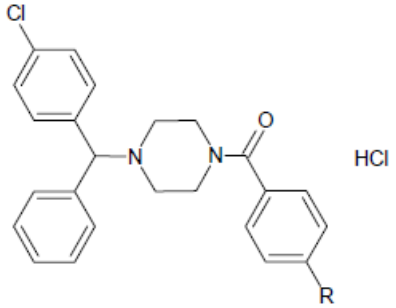

1-(4-substitutedbenzoyl)-4-(4-chlorobenzhydryl)piperazine

	GI50 In vitro
R X: [F Cl Br] OCH3 NO2 Ph 2 4-diF	

Liver	HUH7 FOCUS MAHLAVU HEPG2 HEP3B
Breast	MCF7 BT20 T47D CAMA-1
Colon	HCT116
Gastric	KATO-3
Endometrial	MFE-296

Normal breast epithelial cell SRB assay	MCF-12A

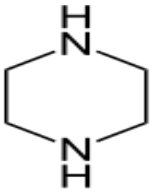

Piperazine

Hexahydropyrazine; Piperazidine; Diethylenediamine

1.1.2 Human immunodeficiency virus (HIV)

HIV, a lentivirus belonging to a subgroup of retrovirus (Sup.Knowledge:02) which can be killed with domestic bleach, turns into tyrant devil in vivo of humans producing acquired immunodeficiency syndrome (AIDS). The consequences of this disease are progressive impairment of immune system making vulnerable for life-threatening opportunistic infections as well as cancers curtailing life span. The first clinical evidence of this dreaded disease was in 1980s and the number of patients exponentially grew to 35 to 40 million including 2.6 million children with HIV by now (year 2014). In spite of global commitment for treatment and control, around 25 million patients died and even now 13 million only are under treatment to control multiplication of virus in their bodies enabling them to have relatively normal life. During the first two decade period, it was rated as a deadliest and life termination disease. The latency period for HIV infection for full development to AIDS, if left untreated, is

9 to 11 years. The worldwide drug discovery ventures (Appendix 2) spending trillions of dollars and noble prize winning results brought a new hope for relatively comfortable health with a new compromised lifestyle. Now, it is considered just like any other chronic ailment, if the comorbidities and life style is taken care of. Yet, the research communities of cross disciplines have a single target of a few more drugs further diminishing side effects and increased control of multiplication of HIV virus in the infected patients.

$$$Virus		
Epstein-Barr	:	EBV
hepatitis B	:	HBV
human cytomegalovirus	:	HCMV
hepatitis C	:	HCV
Human immunodeficiency	:	HIV
herpes simplex	:	HSV-1

Anti HIV vaccines: The discovery of a fool proof vaccine was a dream in 1990's [180]. But, the laudable report of Michael Farzan (The Scripps Research Institute, TSRI) of a potent and universally effective unconventional vaccine successful in monkeys awaits trials in humans will make it a reality in near future. The new drug candidate is an effective HIV vaccine alternative and it blocks every strains of HIV-1, HIV-2, SIV (simian immunodeficiency virus) isolated from humans or rhesus macaques and also hardest-to-stop variants of these viruses. After injection of vaccine, it protects at least eight month even in larger doses of virus compared to that occurring in human transmission. A direct mimic of receptors is prepared without many chances for the HIV virus to escape from being caught. A small and relatively innocuous virus which does not cause disease is used as a vehicle for delivery into the test animal. After injecting into the muscle tissue, the vehicle turns those cells into factories producing enough of new protective protein to last for years and may be for even decades. And the data from nonhuman primates is encouraging and outstanding. With this vaccine and future drug course in the next decade, HIV will also come down to a less harmful category of diseases for human race, provided no new ventures of food, life style are tried just for a change/newness.

HIV infection:CD4 lymphocyte is an integral part of immune system of the human body. HIV infects and fuses with a normal cell; then inserts its single stranded RNA (genetic material) transforming the otherwise normal cell of body into HIV manufacturing suite. HIV is present as free virus in blood, semen, vaginal fluid, pre-ejaculate, or breast milk, and also within infected immune cells. The major route of transmission of this sleeping demon is through blood transfusion, sex with HIV infected or repeated indiscriminate use of skin piercing devices including needles in HIV infected drug addicts. The pediatric HIV cases are through transmission through infected mother before/after conception or during breast feeding period. Even a normal baby gets infected through breast feeding of HIV infected fostered mother. Another route is even an initially normal fetus also becomes a victim in case of women bearing surrogate pregnancy get infected during the child-bearing period. HIV infects and destroys CD4 T cells.

Immuno pathogenesis of AIDS: The consequences of interplay between HIV and the immune system to the loss of immune control of multiple pathogens and cancers are termed as Immuno pathogenesis of AIDS.

Replication cycle: HIV-1 virus is more complex compared to other retroviruses. The reverse transcription of its HIV's genomic RNA to DNA by the enzyme reverse transcriptase is the hallmark of this virus. HIV-1 has genes that encode the structural proteins of the virus.

Firstly HIV virus binds with the dendritic cells of host and this has a key in the initiation of the viral infection. Replication cycle of HIV begins with gp120 protein via a portion of its V1 region. The interactions of a number of cellular and viral factors drive the activation of HIV expression. After transcription, HIV m-RNA is translated into proteins. HIV-1 is one of the species of HIV virus depends upon human host cell proteins in all phases of its life cycle. During divergence from founder to chronically replicating virus, it accumulates N-linked glycosylation sites. HIV-1 integrase catalyzes the terminal cleavage at each end of proviral DNA. This occurs removing a pair of bases and the transfer of strand of each end of 50-phosphates in the target DNA. This is mandatory for continual progeny viruses. Any

molecule inhibiting this process is an effective therapeutic/anti_HIV agent. The major steps along with bio chemical pathway of replication are in BiochemicalPathway of HIV-replication (SK2).

- Anti HIV drugs

In general, making binding site unreactive or inhibiting any one/more steps in viral replication pathway is a key to cure a disease. The drug molecules are searched in direction with success [25, 31] for HIV, hepatitis B and C virus (HBV and HCV), the herpes simplex viruses (HSV-1 and -2), Epstein-Barr virus (EBV), and human cytomegalovirus (HCMV) etc. On this score,each of the steps in replication cycle of HIV is a potential break point for therapeutic intervention. On the other hand, neutralizing antibodies have little effect on virus replication, cytotoxic T lymphocytes (CTL) limit and also do not stop HIV replication completely. The naturally occurring nucleosides with beta-configurations inhibit HIV replication in addition to their antiviral andantitumor activities as evident from SXR studies [26]. HIV-IN is a safe target against HIV as no similarenzymes are involved in human cellular function.

Non-nucleoside reverse transcriptase inhibitors (NNRTIs):

They are structurally diverse group of compounds binding at the same site (palm domain of the p66 subunit) of reverse transcriptase (RT), a viral enzyme. Thereby NNRTIs control replication of genetic material of HIV. The binding of nevirapine, first generation NNRTI is the butterfly-like shape (Fig.5). The factors viz. conformational flexibility and positional adaptability or the ability to 'wiggle and jiggle' in a binding site are critical for non-nucleoside HIV-1-RT inhibitors [25]. Zidovudine and sanilvudine are popular anti-HIV drugs and exhibit reverse transcriptase inhibitory activity. Sakakibara et al. [30] synthesized derivatives of uracil with a 3,5-dimethylbenzyl group at the N3-position and measured non- inhibiting action on nucleoside HIV-1 reverse transcriptase. The SXR [chart 9] and molecular modeling shed light on interactions between HIV-1 reverse transcriptase and the molecules in the present study. The stable conformer out of 3000 studied with AMBER force field has a hydrogen bond of 6-amino group to amide group of Lys101 residue (NH ... O=C) and orientation of 3,5 dimethyl dibenzyl moiety around hydrophobic area (Tyr181,Tyr188, Trp229, and Leu234 residues) of HIV-1 RT. Hydrogen-bonding was observed in many NNRTIs with backbone of the amino acids Lys101.

Fig. 5: butterfly-like shape structure

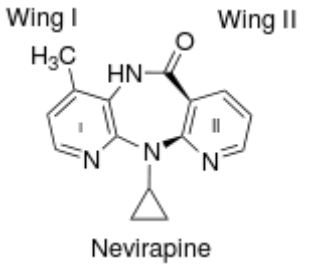

Chart 9: Substituted uracils

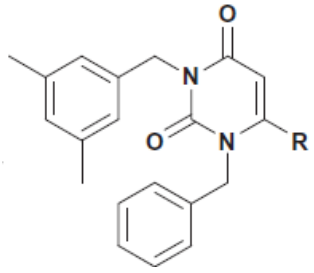

3-(3,5-dimethylbenzyl)uracil

R
NHAc
NHMe
Nme2
Pyrrolidinyl
Piperidinyl
Piperazinyl
Morpholyl
Cyclopropylamino
Cyclohexylamino
Benzylamino

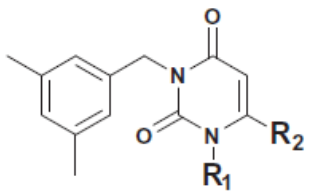

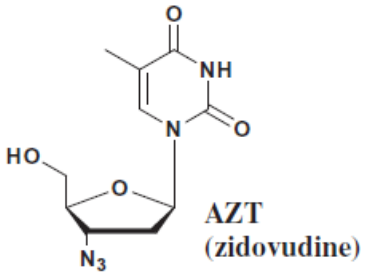

R1	R2
Bn	NHAc
Bn	NHAc
Bn	Nme2
Bn	Pyrrolidinyl
Bn	Piperidinyl
Bn	Piperidinyl
Bn	Morpholyl
Bn	Cyclo-propylamino
Bn	Cyclo-hexylamino
Bn	NHBn
Cyano-methyl	N3
2-Picolyl	N3
4-Picolyl	N3
Cyanomethyl	NH2
2-Picolyl	NH2
4-Picolyl	NH2
S#: Substituent	

MT-4 cells	Inhibition of virus-induced cytopathogenicity
Standard	Zidovudine (AZT)

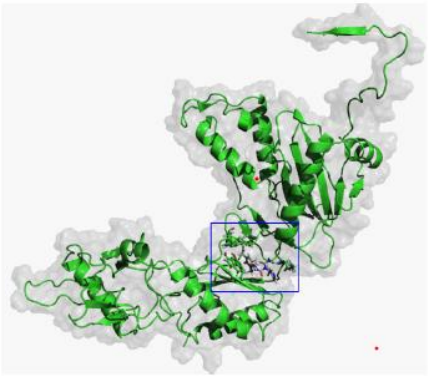

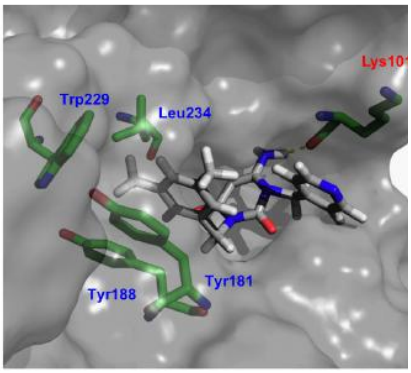

hydrophobic interaction
(Tyr181, Tyr188, Trp229, Leu234)

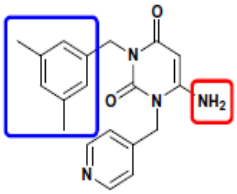

hydrogen bond (Lys101

Malik et al. [29] assessed anti-HIV activities of substituted pyrimidine derivatives after synthesizing the compounds (chart 10)

Chart 10: Substituted pyrimidine derivatives

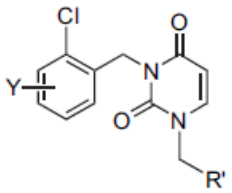

1,3-Bis(2-chlorobenzyl)-1H-pyrimidine-2,4-dione (6a)

	R' ; Y=H
a	-CH=CH2
b	-CH=CHC6H5
c	-CH3
d	-(CH2)2CH3
e	-(CH2)6CH3
f	-CO2C2H5

	R'	
a	-CH=CH2	4-Cl
b	-CH3	4-Cl
c	-(CH2)2CH3	4-Cl
d	-CO2C2H5	4-Cl
a	-CH=CH2	6-Cl
b	-(CH2)2CH3	6-Cl
c	-CO2C2H5	6-Cl

MT-4 cells	HIV cytopathic effects and 50% inhibitory concentration for cell growth
T4 lymphocytes (CEM-SS cell line)	HIV-1 replication in

Earlier, we reviewed the sparkles in the transformation of a mathematical model of computational quantum chemistry into an experimental probe. The results of SEMO/ab initio chemical models of hydrazides, DFT studies of small molecules [173-179] were published during the last one decade. In this communication, the primary results of model chemistries and quantum chemical parameters at DFT level in gaseous phase are briefly described. The full details of CQC and SXR with molecular descriptor studies for all the molecules with multiple quantum chemistry/neural network packages are under way and the information will be in future publications.

2. Experimental

Hardware & software

The Dell laptop with Intel(R) Core(TM)i7-2670QM CPU @2.20GHz processor (8.GB RAM) under Windows 7 Ultimate operating system was used to run Jaguar version 8.5 (release 13) of Schrodinger, Inc., New York, NY, 2014 (appendix.3).

Results

In this study, geometric optimizations are carried out in redundant internal coordinates at UDFT level of theory with the basis sets, B3LYP (Becke_3_Parameter/HF+Slater+Becke88+VWN+LYP) 6-31G**. The optimized geometric structures for the compounds (synthesized in our laboratory [179]) are summarized in chart 11. The vibrational frequency analysis is performed to check the chemical validity of optimized 3D-geometric structure on the potential energy surface.

Chart 11: Optimized structures and biological activities of substituted sulfonamides etc.

Chemical name	Input Structure	Optimized structure	Cancer cell survival (%)	Anti-HIV activity (%)
N-cyclobutyl-2,4-dioxo-1,2,3,4-tetrahydropyrimidine-5-sulfonamide			3.7	32.78
N-cyclopentyl-2,4-dioxo-1,2,3,4-tetrahydropyrimidine-5-sulfonamide			1.92	22.64
N-(3,3-dimethylbutyl)-2,4-dioxo-1,2,3,4-tetrahydropyrimidine-5-sulfonamide			4.94	2.40
N-isopropyl-2,4-dioxo-1,2,3,4-tetrahydropyrimidine-5-sulfonamide			0	21.53
(R)-N-(1-(naphthalen-1-yl)ethyl)-2,4-dioxo-1,2,3,4-tetrahydropyrimidine-5-sulfonamide			2.33	2.71
N-(2,3-dihydro-1H-inden-1-yl)-2,4-dioxo-1,2,3,4-tetrahydropyrimidine-5-sulfonamide			2.88	11.92
(S)-2,4-dioxo-N-(1-phenylethyl)-1,2,3,4-tetrahydropyrimidine-5-sulfonamide			9.87	14.46

N-(1-methoxyethyl)-2,4-dioxo-1,2,3,4-tetrahydropyrimidine-5-sulfonamide			3.15	4.80
Ethyl,1-((2,4-dioxo-1,2,3,4-tetrahydropyrimidin-5-yl)sulfonyl)piperidine-4-carboxylate			0.68	51.2
5-((4-(2,3-dihydrobenzo[b][1,4]dioxine-2-carbonyl)piperazin-1-yl)sulfonyl)pyrimidine-2,4(1H,3H)-dione			2.06	7.7
N-butyl-N-methyl-2,4-dioxo-1,2,3,4-tetrahydropyrimidine-5-sulfonamide			3.43	34.1
5-((4-(4-fluorophenyl)piperazin-1-yl)sulfonyl)pyrimidine-2,4(1H,3H)-dione			0.55	41.2
5-((4-(2,3-dichlorophenyl)piperazin-1-yl)sulfonyl)pyrimidine-2,4(1H,3H)-dione			0	55.8
(S)-N-(3-methyl-1-(2-(piperidin-1-yl)phenyl)butyl)-2,4-dioxo-1,2,3,4-tetrahydropyrimidine-5-sulfonamide			3.84	92.12
(S)-5-((1-(4-methoxybenzyl)-3,4,5,6,7,8-hexahydroisoquinolin-2(1H)-yl)sulfonyl)pyrimidine-2,4(1H,3H)-dione			25.24	73.25
(4aS,7aS)-6-benzyl-1-((6-methyl-2,4-dioxo-1,2,3,4-tetrahydropyrimidin-5-yl)sulfonyl)tetrahydro-1H-pyrrolo[3,4-b]pyridine-5,7(6H,7aH)-dione			3.29	78.25

(S)-5-((4-((4-chlorophenyl)(phenyl)methyl)piperazin-1-yl)sulfonyl)pyrimidine- 2,4(1H,3H)-dione			3.57	43.94
((2,4-dioxo-1,2,3,4-tetrahydropyrimidin-5-yl)sulfonyl)-L-alanine			3.57	53.9
((2,4-dioxo-1,2,3,4-tetrahydropyrimidin-5-yl)sulfonyl)-glycine			0.27	55
N-cyclobutyl-1-((2R,3R,4S,5R)-3,4-dihydroxy-5-(hydroxymethyl) tetrahydrofuran-2-yl)-2,4-dioxo-1,2,3,4-tetrahydropyrimidine-5-sulfonamide			0.14	30.30
N-cyclopentyl-1-((2R,3R,4S,5R)-3,4-dihydroxy-5-(hydroxymethyl) tetrahydrofuran-2-yl)-2,4-dioxo-1,2,3,4-tetrahydropyrimidine-5-sulfonamide			4.94	20.30
N-butyl-1-((2R,3R,4S,5R)-3,4-dihydroxy-5-(hydroxymethyl)tetrahydrofuran-2-yl)-N-methyl-2,4-dioxo-1,2,3,4-tetrahydropyrimidine-5-sulfonamide			2.6	34.10

The non-linear trend (Fig 6) of variation of activity against elecctronic energy shows only brad dependence. The linear correlation is inadequate and one variable is too restrictive for quantitative assessment. Work is in progress for detailed analysis with quantum chemical, geometric and charge based descriptors using neural networks (NN), support vector regression (SVR) and nature inspired modeling procedures.

Fig 6: Variation of biological activity versus CQC energies.

Scatter diagram	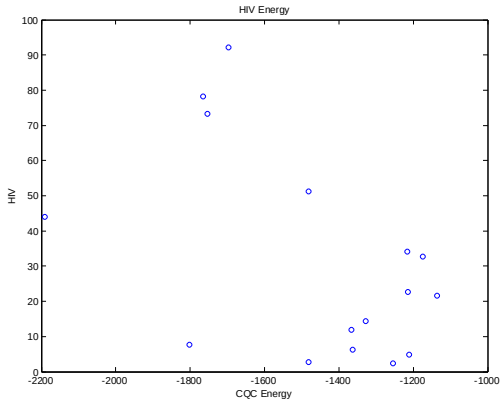 y : Anti HIV activity (%) x: Energy	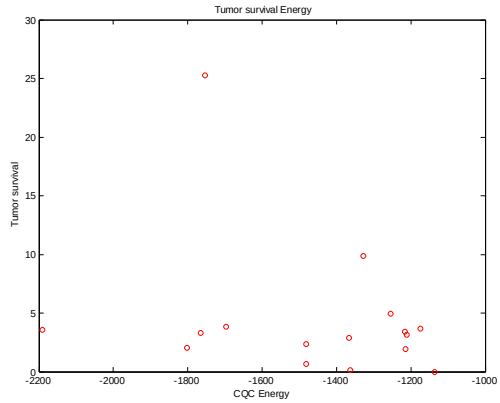 y:Tumor survival (%) x: Energy
	Correlation matrix for Linear trend	
	1.0000 -0.5030 -0.5030 1.0000	1.0000 -0.2469 -0.2469 1.0000

3. Theory

The Hamiltonian operator of Schrodinger wave equation for electronic energy of a chemical moiety is a second order PDE. Before 1950s, the bottle neck in solving Schrodinger wave equation for multi-electron systems (non-hydrogen like atoms) was computing multi-electron integrals. The simplest case among them is repulsion between two electrons. In 1950, Boys put forward use of Gaussian orbitals instead of Slater orbitals to express wave function. The computer software started with calculation of ERIs for even poly atomic molecules containing s and p orbitals. The limitation is that they are painfully slow. Pople broke the fence with Pople-Hehre axis-switch method with a consequence of hundred fold speed. The angular momentum (L) and contraction (K) are handled to cope up with increase in speed. Over six decades, computational quantum chemistry groups used and improved and well tested numerical solution methods. BFGS algorithm and other quasi- (or pseudo-) Gauss-Newton methods have been successfully employed in software packages (Appendix 4). Gaussian XX series started using Berny algorithm [173] with many adaptive features for almost sure convergence optimization of a variety of moieties in ground/excited states and in all three phases of matter. Jaguar employed pseudo-spectral approach to solve PDEs and a brief account follows.

Jaguar for CQC

Pseudo_spectral methods

The spectral and pseudo spectral algorithms are methods of choice for functions with smooth solution hyper surfaces. If there are deviations (viz. discontinuities, breaks) (KB.1, KB.2), spectral collocation approaches using spectral differentiation of matrices are the correct choice.

A large number of available basis functions, choice to estimate coefficients result in wide scope of spectral solutions with different properties (or flavors). Schrödinger wave equation for a particle in a potential well is a simple PDE. The equation of interest consists of a term containing derivatives (eg. kinetic energy component) multiplied by the function (potential). In spectral methods, the solution is expanded say as plane waves (basis functions). By truncating the expansion to desired level, the solution is arrived. Here, by numerical method like Runge–Kutta methods is used. The limitation iscalculation of RHS of ODE at of each time step.

$$fn(x) \;\; ; \;\; fnBS = \sum_{j=0}^{\#BS} coef_j * Bfn_j(x)$$

In spectral representation based methods, product of function with scalar transforms into vector-matrix multiplication. It scales up only to N^2

- Additional step of calculation for solution of differential equation for the coefficients
- Matrix elements need to be evaluated explicitly at each iteration

But, calculation atdiscrete grid points and inverse discrete Fourier transform results in the value of the function. At these grid points, the function is multiplied with vector and result is Fourier-transformed back.

- FFT scales up O(Nlog(N)) and thus more efficient than matrix multiplication
- The function is used without additional integral evaluations.

Thus, pseudo-spectral method involves only multiplication of V(x) and f(x) as part of a differential equation with three steps.

KB. 1: Choice of Basis functions

KB: Type of quadrature based on type of basis functions	
If	Polynomials
Then	Gaussian quadrature
If	Plane waves
Then	Discrete Fourier Transform
If	Product can be represented with the given finite set of basis functions
Then	Equation is exact due to adequate quadrature

Alg. Pseudo spectral solution of PDF

- Spectral method: Expansion into a finite set of basis functions
  - For a given set of basis functions
    - Quadrature is sought
    - Converts scalar products of these basis functions into a weighted sum over grid points
  - End for
- Calculation of product at each grid point

Orszag, Steven A. (1972). Studies in Applied Mathematics 51 (1972): 253–259. "Comparison of Pseudospectral and Spectral Approximation".

Steven A. Orszag (1969) Phys. Fluids Supp. II, 12, 250-257 Numerical Methods for the Simulation of Turbulence,

D. Gottlieb and S. Orzag (1977) "Numerical Analysis of Spectral Methods : Theory and Applications", SIAM, Philadelphia, PA

J. Hesthaven, S. Gottlieb and D. Gottlieb (2007) "Spectral methods for time-dependent problems", Cambridge UP, Cambridge, UK

Lloyd N. Trefethen (2000) Spectral Methods in MATLAB. SIAM, Philadelphia, PA

Bengt Fornberg (1996) A Practical Guide to Pseudospectral Methods. Cambridge University Press, Cambridge, UK Press.

WH; Teukolsky, SA; Vetterling, WT; Flannery, BP (2007). "Section 20.7. Spectral Methods". Numerical Recipes: The Art of Scientific Computing (3rd ed.). New York: Cambridge University Press.

KB. 2: Necessary conditions, limitations and remedial measures of Pseudo spectral approach for solution of PDFs

Subtle differences between finite difference and spectral methods	
Finite difference methods	Spectral method
Equation to be solved is approximated	Expected solution is approximated
Differencing replaces the continuum equation by an equation on Grid points	Spectral method expresses solution as a truncated expansion in a set of basis functions

Finite differences vs spectral method	
If	Finite differencing
Then	Continuum equation replaced by equation on grid points
If	Spectral method
Then	Solution expressed as a truncated expansion in a set of basis functions

Pseudo spectral solution of PDF	
If	Smooth solutions
Then	Spectral methods work well
If	Discontinuities like shocks Or bad
Then	spectral methods fail
If	Even mild non-smoothness (like a discontinuity in some high-order derivative of the solution)
Then	Spoils the convergence of spectral methods
If	Discontinuities &
	spectral methods need to be used
Then	Spectral collocation methods Spectral differentiation of matrices Spectral Differencing with a Twist

Baltensperger, R., and Trummer, M.R. SIAM J. Scientific Computing, 24, **2003**, 1465–1487
Spectral Differencing with a Twist

Alg. Pseudo spectral method
For each SCF iteration

- Cal density matrix from the wave function
- Cal the values of the integrals on the grid points
- Manipulate them to produce the necessary operators on the grid
- Assemble Fock matrix by transforming these components back into spectral space
- Fock matrix is used in the usual way to generate the wave function for the next iteration

End For % iteration

Discussion

Optimization of geometric structure

In geometric optimization, an initial guess structure, some or all of bond characteristics (BL, BA and DHA), level of theory, basis sets, optimization algorithm, convergence criteria are inputted either through GUI or an ASCII file. Jaguar uses redundant internal co-ordinate system by default, which has been proved to be most efficient among Z-matrix, XYZ Cartesian coordinates etc. (KB.3). A utopian coordinate system representing 3D-chemical structure of a molecule is one where the change in energyalong each coordinate is maximized while coupling between coordinates is minimized.

KB.3: Advantages and Limitations of co-ordinate systems in CQC	
Redundant internal coordinates + Most efficient	
If	Group of atoms becomes collinear

Cartesian
+ avoid the problems of collinear coordinate sets
− but an optimization in Cartesian coordinates is likely

Then	Internal coordinates become ill-defined &
	Jaguar chooses a new set of redundant internal coordinates
If	Auto correction fails
Then	Software warns
	Remedy : User chosen co-ordinate system & rerun

to take

longer than one in redundant internal coordinates

Z-matrix

- efficient optimization is not a trivial task
- requires an understanding of the coupling between simple internal coordinates.

Cleaning initial structure

Ligand Prepartion (LigPrep): The module, LigPrep, uses advanced rules to correct Lewis structures and arrives at energy minimized 3D-molecular structure accurately reducing computational errors down the stream of multiple phases of calculations. It also expands tautomeric and ionization states, ring conformations/ stereoisomers leading to structural diversity.

Search for optimized geometry: The search direction in Jaguar is calculated by gradient of energy with initial Hessian.Similar to any other ab initio electronic structure software, Jaguar finds a solution to Schrodinger wave equation in an iterative manner employing self-consistent field (SCF) jargon to arrive at lowest energy wave function within the space spanned by basis set of choice. The XYZ coordinates corresponding to structure on PES is the optimized geometric configuration of the moiety with a chosen point group.

For molecules with a large number of atoms, most of fundamental integrals are computed with pseudospectral procedure in physical space on a grid. In other words, it is not in spectral space defined by basis functions. Due to high costs of storage, in each SCF iteration, both pseudospectral and conventional algorithms recalculate key integral terms. Jaguar calculates one-electron and some of the largest two-electron terms analytically. Also uses the pseudospectral method for the majority of the computationally intensive two-electron integral terms.

The progress and final of geometric optimization (KB.4) iteration is used to test chemically valid 3D-strucuture, transition state, scanning for conformers and IRC. However geometry optimization is not required for rigid coordination scan.

SCF convergence tests

The convergence of HF wave functions is fast for simple organic molecules compared to open shell molecules or at higher level theory and complex basis sets. Molecules with transition metal ions are invariably slow and care is to be taken in the initial guess and increasing the number of iterations.

Convergence in G[xx>94]: Four criteria viz. maximum force component, root-mean square force, maximum step component and root-mean-square step are to be passed for completion of optimization in G03. For large molecules, geometry is accepted if forces are less than $1/100^{th}$ of cutoff value.

Convergence in Jaguar: Jaguar (version > 7.0) automatically sets to ultrafine mode when it detects non-convergence of SCF. In this case, denser pseudo spectral grids and tighter cuts-of are employed. Unlike many other software packages, it adapts dynamic strategy for convergence criteria for SCF calculation. In the initial phase a quick accuracy level is employed except for transition metal moieties. After sufficient number of iterations, the convergence level is raised to 'accurate'. Here, cutoffs are tighter and pseudospectral grids are denser compared to Quick criteria.

KB. 4: Test for geometry optimzation		
	If Geometry_optimization & Jaguar Geometry_converged = .False.	
If	energy of successive geometries <= convergence_criteria	&
	elements of the analytic gradient of the energy < = convergence_criteria	&
	displacement< = convergence_criteria	
Then	Geometry_converged = .True.	
If	Iterations performed > Max.Itertions	&
	Geometry_converged = .False.	
Then	Start with a different geometry	&|Or
	Change [Level of theory, BasisSets, Orbital characteristics,.....]	
		&
If	Keyword = 'Loose' OR 'default5	
Then	Conv.Criteria.Geopt.Loose = 5* Conv.Criteria.Default	
If	Jaguar & geometry optimizaton & solution_Phase	
Then	Conv.Criteria. Geopt.Soln = 3* Conv.Criteria.Default	

If	Energy change criterion is met	
	gradient and displacement criteria not met	
Then	Geometry_converged = .True.	
	See P199 Sec 8.5.10	
If	poor initial geometries, or poor initial Hessians	
Then	Increase MaxIt to higher than defaultValue(100)	
If	Bad systems	
	[It > MaxIt & Geo_opt = .false]	
Then	Restart geo.opt in Maesto using one of best opt_geometries	
If	Jaguar & geometry optimizaton	
	Keyword = ' Save intermediate geometries in output structure file'	
Then	Geometries available for each iteration	
If	Minimum energy structures OR TS	
Then	Conv.Criteria. Geopt.Soln= .Accurate. such that analytic gradients accurate	

	If	Bad systems | TS | Minimum energy structures
		wave function . converged = .False.
If	RMS_ change in density matrix < RMS_ density matrix element change criterion[5.0 x 10–6]	
Then	wave function . converged = .True.	&
	pretend	
case 0		
	Cal compute analytic derivatives of energy	
case 1		
	compute numerical derivatives of energy (obtained from calculations on 6 Natom perturbed geometries by moving each atom **pretend** bohr in positive or negative x, y, or z direction)	
case 2		
	Calculate frequencies numerically	
otherwise		
	Invalid option	
end		

Default values of convergence in Jaguar	
Convergence Criterion For	**Default value**
Maximum element of gradient	4.5□ 10-4
rms of gradient elements	3.0□ 10-4
Maximum Newton-Raphson step (not currently used)	1.0□ 10-2
rms Newton-Raphson step (not currently used)	1.0□ 10-2
Maximum element of nuclear displacement	1.8□ 10-3
rms of nuclear displacement elements	1.2□ 10-3
Difference between final energies from previous and current geometry optimization iterations	5.0□ 10-5

Hessian matrix: Either user given or software generated initial Hessian (second derivative matrix or force constant matrix) along with gradient defines the search direction on PES to traverse to a lowering of

energy (KB.5 and KB.6). In the case of restarting a run, the software picks up Hessian from the inputted file.

KB.5: Hessian calculation in Jaguar

If Jaguar & Hessian

If Rerun_file inputted
Then Hessian is read from input file

If Initial Hessian option menu chosen
Then Best choice
- + Fischer-Almlöf
- + Schlegel Hessian
- + Option
  - o Unit matrix.12
  - o Quantum mechanical

If Refinement of initial Hessian
Then Methods : [Powell updates, mixed Murtagh-Sargent/Powell updates or Murtagh-Sargent updates]

Jaguar computing the initial Hessian Quantum mechanically
- + Best option for cases where the other Hessian choices are inadequate
- – Most time-consuming

Remedy: Alternate steps to improve optimizations
- + More cost-effective

KB. 6: Analysis of output of frequency calculations

Consequent	Antecedent
Perform frequency analysis	if Converged geometry
Stable and chemically valid structure (local/global) with minimum energy	if NIMAG = 0
Transition State (TS)	if NIMAG = 1
Saddle point	if NIMAG =2
Higher order saddle point	if NIMAG >2

NIMAG: Number of imaginary frequencies

Fischer, T. H.; Almlöf, J. *J. Phys. Chem.* **1992,** *96*, 9768. General methods for geometry and wave function optimization

Schlegel, H. B. *Theor. Chim. Acta* **1984,** *66*, 333-340., Estimating the Hessian for gradient-type geometry optimizations.

Identification of chemically valid moieties from vibrational frequency analysis

The prime focus of vibrational frequency analysis is to ascertain whether the stationary point on PES corresponds to a chemically valid structure adhering to the rules of chemical bonding (valence and bond types), transition state or higher order saddle point. The object function in vibrational analysis is a multi-dimensional complex surface in normal coordinates of the atoms of the moiety. Zero number of imaginary frequencies (or zero/low magnitudes of first six vibrational frequencies) affirms the chemical validity of optimum geometry of species. Only after arriving at a valid chemical structure for a chemical species/moiety, properties (now popular as descriptors exceeding 5000 in number) viz. physical/chemical/physico-chemical/spectroscopic is calculated.

The vibrational frequencies for a 3D-structure of molecule are computed in Jaguar by analytical or numerical differentiation of energies with co-ordinates in gas or solution phases (KB.7). By default, the frequencies are calculated for most abundant isotope of an atom in the molecule. The subsequent information includes infrared (IR) intensities and thermochemical properties. Mastero displays molecules with animation of vibrations. Rotational symmetry numbers identify the number of orientations of a molecule and are obtained from each other by rotation.

Scaling factors: The errors in frequencies by CQC are predictable and hence scaling factors for different basis sets and levels of theory (KB.7) are in vogue; they enhance the quality of consequent thermochemical properties. Pulay's modified scaled Quantum Mechanical Force Fields (SQM) method [81] for B3LYP/6-31G* with 11 scale factors is one option. It is based on the type of stretch, bend, or torsion and scales Hessian elements themselves (in internal coordinate's format). A parametrization is done with 30 molecules containing C, H, N, O, and Cl for B3LYP/6-31G*. In literature, scaling factors for

low frequency vibration sets, zero point vibrational energies, enthalpy and entropy are reported, apart from many other varieties.

Thermochemical quantities:By default, they are calculated at 1.0 atmosphere pressure and 298.15(^{o}K). These values can also be obtained at different temperatures with a default step_increase of 10.00 K and a step length of one.

KB. 7: Frequency calculations & scale factors for corrections

	If Vibrational frequencies& Jaguar	
If	[UHF | RHF] OR [DFT]	&
	[Gas phase | solution]	&
	BS without f functions	&
	Default option	
Then	Analytical second derivatives of Energies with respect to co-ordinates	&
	molecular symmetry is turned off only for frequencies	
If	RODFT wave functions	
	effective core potential	
Then	Numerical derivatives	
If	GVB-LMP2	
Then	Frequency calculation is not available	
If	HF, GVB, LMP2, and DFT	&
	[Gas phase | solution]	&
	User_option = 'Numerical Derivatives'	
Then	Numerical derivatives	
If	User choice = ' Average isotopic masses" % Atomic mass	
Then	average of the isotopic masses, weighted by the abundance of the isotopes,	
else	atomic mass used for each element is that of its most abundant isotope	
	+ Analytic frequency calculations are much faster than numerical frequency calculations	
If	Standard frequency scaling	
Then	Table	

Scale Factor		Basis Set	SCF Method
0.9085		3-21G	HF
0.8953		6-31G*	
0.8970		6-31+G*	
0.8992		6-31G**	
0.9051		6-311G**	
0.9434		6-31G*	MP2
0.9370		6-31G**	
0.9496		6-311G**	
0.9945		6-31G*	BLYP
0.9914		6-31G*	BP86
0.9614		6-31G*	B3LYP
0.9558		6-31G*	B3P86
0.9573		6-31G*	B3PW91

Default thermochemical quantities	
Heat capacity at constant volume	(C*v*) cal/mol K
internal energy	(U)
entropy	(S) kcal/mol
enthalpy	(H) kcal/mol
Gibbs free energy	(G) kcal/mol
Rotational symmetry numbers	Rot.Sym.#
zero point energies	ZPE

Baker, J.; Jarzecki, A. A.; Pulay, P. *J. Phys. Chem A* **1998,** *102,* 1412. Harmonic Vibrational Frequencies: An Evaluation of Hartree-Fock, Møller-Plesset,

Scott, A. P.; Radom, L. *J. Phys.Chem.* **1996,** *100,* 16502. Quadratic Configuration Interaction, Density Functional Theory, and Semiempirical Scale Factors

Discussion

Accurate energies: In Jaguar, a multistep geometry optimization and single point energy are followed by corrections for BS, electron pairing and temperature effects (Alg. 1). A database of synopsis of recent literature titles with accurate computations in CQC is available with the authors [179].

Alg.1: Accurate (J2) energies in Jaguar	
geometry optimization	B3LYP/6-31G*
frequency calculation	
single point energy (SPE)	GVB/LMP2 BS: ccpvtz(-f) and cc-pvtz++
basis set correction energy	CE_BS
A parameterized electron-pair correction energy is also added	CE_EP
Energy.J2 = absolute enthalpy at 298K	SPE + CE_BS + CE_EP
temperature effects from B3LYP frequencies	
– do not include standard heat of formation	

If	Atomic number of atoms < atomic number (Argon)	&
	Accurate energy	&
	Jaguar suite	
Then	J2 theory calculations	

Dunietz, B. D.; Murphy, R. B.; Friesner, R. A. *J. Chem. Phys.* **1999,** *110*, 1921.
Calculation of enthalpies of formation by a multi-configurational localized perturbation theory - application for closed shell cases.

GAUSSIAN XX: One of widely employed quantum mechanical packages is from group of Pople, Nobel laureate. The initial version of package dates back to 1970s (chart 12).

Chart 12: Evolution of Gaussian CQC package into Gaussian09

Gaussian70	Gaussian76	Gaussian77		Gaussian78
Gaussian80	Gaussian82	Gaussian83	Gaussian85	Gaussian86
Gaussian88	Gaussian90	Gaussian92	Gaussian93	Gaussian94
Gaussian95	Gaussian96	Gaussian98	Gaussian03	Gaussian09

Gaussian80 : First version published on Quantum Chemical Program Exchange (QCPE) running on IBM mainframe

GAMESS: It is an outcome of academic endeavor in CQC with competing features of Gxx, HYPERCHEM etc.

Q-Chem:Pople with his postdocs brought out initial commercial version of Q-chem in 1997. The present size of code grew to 3.3 million lines including 1.5 million lines of machine generated programs. The good speed and efficiency arose from Atomic Orbital INTegralS (AOINTS) package, which is invisible to the user. AOINTS is most advanced ERI algorithm technology.

Jaguar:It is an ab initio computational quantum chemistry (CQC) package for gas and solution (basically water) research of macro molecules and systems containing transition metal ions. Schrödinger suit is one of commercial software packages with a core of knowledge based work flow designs for complicated tasks. It is the brainchild in the research groups of Richard Friesner and William Goddard. The initial commercial version PS-GVB (referring to the so-called pseudospectral (PS) generalized valence bond method) has unique feature of pseudospectral approximation. This approach is speed enhancing tool for computationally expensive integral operations present in most quantum chemical calculations. As a result, calculations complete much faster but with a negligible loss of accuracy.

Chart 13 : Different versions of Jaguar of Schrodinger

Jaguar 15.4	**2015**	**Jaguar 8.5**		**Jaguar 7.6**	**2009**	**Jaguar 5.5**	**2004**
Jaguar 14.x	2014	**Jaguar 8.0**	2013	**Jaguar 7.5**	2008	**Jaguar 5.0**	2003
Jaguar 13.x	2013	**Jaguar 7.9**	2012	**Jaguar 7.0**	2007	**Jaguar 4.2**	2002
		Jaguar 7.8	2011	**Jaguar 6.5**	2006	**Jaguar 4.1**	2001
		Jaguar 7.7	2010	**Jaguar 6.0**	2005	**Jaguar 4.0**	2000
						Jaguar 3.5	
						Jaguar 3.0	

Typical research studies with Jaguar package: Jaguar, a module of Schrodinger suit is widely employed in medicinal chemistry, drug-discovery, macro-molecular (protein-protein, protein-ligand, protein-enzyme-

ligand/protein) interactions both in presence and absence of water molecule(s) (clusters) at active sites. The applications extended also to material science, industrial chemicals, mechanism of organic reactions, stable molecules under extreme conditionsand synthesis of pure chemicalsand moieties not yet synthesized. Typical results from top-tier research journals include the role of water at the active site [87,85,69], selectivity of kinase inhibitors [51], high energy water sites [113] through measurement of free energy of solvation [171], thermodynamics of hydration of active site [40], hydrophobic effect [86,172,137,92] of biomolecules. SXR (structure X [:activity, inhibition, ...] relationships [127,153,41,78], structure-function of protein convertase subtilisin/kexin [103], selection of molecules based on structuredesign [79,80,102] / virtual screening [39] resulted in high information content. The synthesis of tricyclic pyrrole-2-carboxamides in solution phase [140] , solvation mapping [54], explicit solvent effects [69], polar surface area [147], thermodynamics of properties of water [107], water molecules at the surface of proteins [68], thermodynamic driven bioprocesses [35], enthalpy-entropy compensation in protein-ligand binding through water networks [46], water map analysis in reactions of proteins [53,91,103], p38α MAP kinase inhibitors, treatment of Alzheimer's disease [61], protein-small molecule interactions in wet and dry regions [101], free energy of solvation [171], drug solubility [158] and computer aided drug design by hydration site thermodynamics [99] are researched with Schrodinger modules.

Further, docking strategies for binding in pharmacophores [36,70,77], consensus induced fit docking [58], DARS (Decoys As the Reference State) potentials in protein-protein docking [114], docking of poly peptide with GLIDE [36], FFT-based protein docking [144], pose prediction accuracy in docking [125], universal pharmacophore model for studies of drug blockade [76], shape based ligand alignment [75], investigations in virtual screening [116,141,118,132,55,47,48]and conformational search [37] with CQC employed Jaguar software.

HIV-reverse transcriptase [123,138], enzymatic production of 1-butanol from pyruvate [74], nanobodies that block the enzymatic/ cytotoxic activities [38], prediction of free energies of CK2 inhibitors [126], biostructural investigation of glutamate receptor (GluR5) agonist [110], inverse binding [37, 50], molecular determinants of selectivity at the dopamine D3 receptor [60], discovery of PARP-1 inhibitors [84], macrocycles in the treatment of myelofibrosis and lymphoma [81], inhibitors for breast cancer proliferation [42,43,51], molecular dynamics of kinases [100] and thermodynamic characterization of kinases [94] made use of Jaguar package from Schrodinger suit. The highlights of information shedding light on future course of this interdisciplinary research are under preparation [178].

Acknowledgements

RSR appreciates Voleti Sreedhara Rao, CSO, TheraXel Discoveries, Hyderabad for the keen observations in improving manuscript. We thank Mr. Atsushi Inoue, Molecular Information & Interaction Technology, Next Generation Systems Core Function Unit, Eisai Product Creation Systems (Eisai. Co., Ltd.) for the help rendered in running Jaguar software.

The popular slogan 'Learn while teaching' is a sugar coated soft pride embedded capsule. On the other hand, 'Learn hard' and 'Teach smooth' is righteous approach with long shelf-life. Yet, it is an untrodden path, obviously thorny with sharp edged curves putting back many a time in square A. Also, it is like a snail walk to reach the goal. But, this is a smart launch pad for learners in passing through 'reproduce to integrate cycle' on need basis and IQ level. The novice knows a bit of the concept and an expert does not know a bit of it. We express our gratitude from inner layers of brain to our teachers in preaching to pursue this line of commitment.

KRK planned synthesis of molecules. KRK and RSR developed a blue print of CQC experiments with Schrodinger. BVS executed experimental chemistry; full papers are from archives of RSR & KRK. Manuscript prepared by RSR and KRK with processed outputs.

Appendix.1:

Structure-IUPAC Name- Anti_Cancer drug evolution (Side)

Molecule	Structure	IUPAC Name	Brand name of drug
Abiraterone Acetate	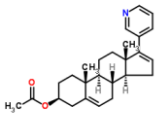	$C_{26}H_{33}NO_2$ Androsta-5,16-dien-3-ol, 17-(3-pyridinyl)-, acetate (ester), (3β)-	Zytiga
Ado-Trastuzumab Emtansine	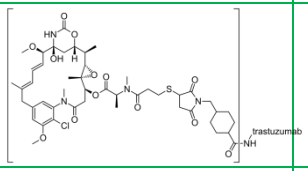	$C_{6448}H_{9948}N_{1720}O_{2012}S_{44}\cdot(C_{47}H_{62}ClN_4O_{13}S)_n$ Antibody	Kadcyla
Afatinib Dimaleate	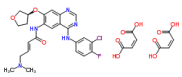	$C_{32}H_{33}ClFN_5O_{11}$ 2E)-N-{4-[(3-Chloro-4-fluorophenyl)amino]-7-[(3S)-tetrahydro-3-furanyloxy]-6-quinazolinyl}-4-(dimethylamino)-2-butenamide (2Z)-2-butenedioate (1:2)	Gilotrif
Aldesleukin	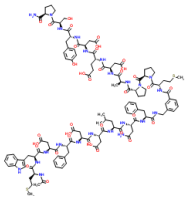	C114H147N23O36S2 N-(3-{[(N-acetyl-L-methionyl-L-tryptophyl-L-α-aspartyl-L-phenylalanyl-L-α-aspartyl-L-α-aspartyl-L-leucyl-L-asparaginyl-L-phenylalanyl)amino]methyl}benzoyl)-L-methionyl-D-prolyl-D-prolyl-L-alanyl-D-α-aspartyl-D-α-glutamyl-D-α-aspartyl-D-tyrosyl-D-seryl-D-prolinamide	Interleukin-2
Alectinib	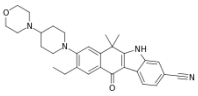	9-Ethyl-6,6-dimethyl-8-[4-(4-morpholinyl)-1-piperidinyl]-11-oxo-6,11-dihydro-5*H*-benzo[*b*]carbazole-3-carbonitrile	Alecensa
Alimta	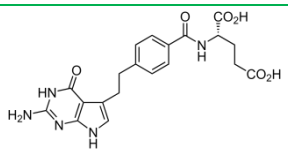	$C_{20}H_{21}N_5O_6$ (2*S*)-2-{[4-[2-(2-amino-4-oxo-1,7-dihydro pyrrolo[2,3-*d*]pyrimidin-5-yl)ethyl]benzoyl]amino} pentanedioic acid	
Aminolevulinic Acid	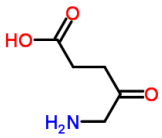	$C_5H_9NO_3$ 5-Amino-4-oxopentanoic acid	Levulan
Anastrozole	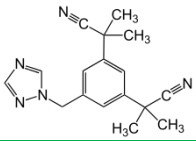	$C_{17}H_{19}N_5$ 2,2'-[5-(1*H*-1,2,4-triazol-1-ylmethyl)-1,3-phenylene]bis(2-methylpropanenitrile)[1]	Arimidex

Molecule	Structure	IUPAC Name	Brand name of drug
Anexsia	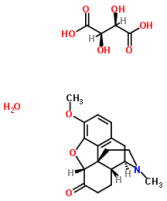	$C_{22}H_{29}NO_{10}$ (2R,3R)-2,3-Dihydroxysuccinic acid - (5alpha)-3-methoxy-17-methyl-4,5-epoxymorphinan-6-one hydrate (1:1:1)	
Anzemet	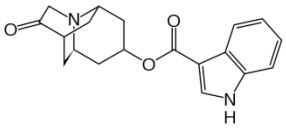	$C_{19}H_{20}N_2O_3$ (3*R*)-10-oxo-8-azatricyclo[5.3.1.0^{3,8}] undec-5-yl 1*H*-indole-3-carboxylate (Dolaserton)	
Aredia	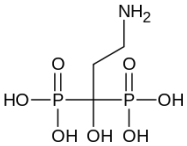	$C_3H_{11}NO_7P_2$ (pamidronate disodium for injection) (3-amino-1-hydroxypropane-1,1-diyl)bis(phosphonic acid)	
Arsenic Trioxide	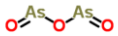	As_2O_3 Arsenic sesquioxide	Trisenox
Axitinib	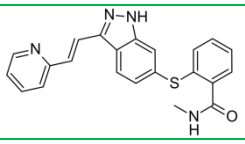	$C_{22}H_{18}N_4OS$ *N*-Methyl-2-[[3-[(*E*)-2-pyridin-2-ylethenyl]-1*H*-indazol-6-yl]sulfanyl]benzamide	Inlyta
Azacitidine	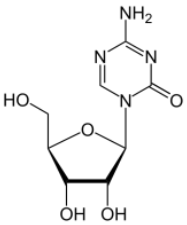	$C_8H_{12}N_4O_5$ 4-Amino-1-β-D-ribofuranosyl-1,3,5-triazin-2(1*H*)-one	Mylosar
Azacitidine	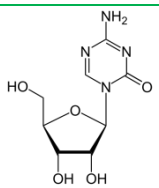	$C_8H_{12}N_4O_5$ 4-Amino-1-β-D-ribofuranosyl-1,3,5-triazin-2(1*H*)-one	Vidaza

Molecule	Structure	IUPAC Name	Brand name of drug
Bendamustine Hydrochloride	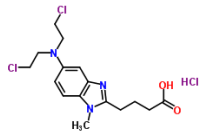	$C_{16}H_{22}Cl_3N_3O_2$ 4-{5-[Bis(2-chloroethyl)amino]-1-methyl-1H-benzimidazol-2-yl}butanoic acid hydrochloride (1:1)	Treanda
Bexarotene	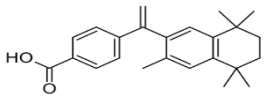	$C_{24}H_{28}O_2$ 4-[1-(5,6,7,8-tetrahydro-3,5,5,8,8-pentamethyl-2-naphthalenyl)ethenyl]benzoic acid	Targretin
Bortezomib	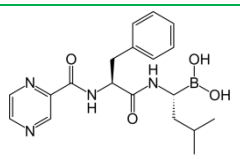	$C_{19}H_{25}BN_4O_4$ [(1*R*)-3-methyl-1-({(2*S*)-3-phenyl-2-[(pyrazin-2-ylcarbonyl)amino]propanoyl}amino)butyl]boronic acid	Velcade
Busulfan	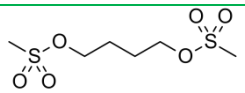	$C_6H_{14}O_6S_2$ butane-1,4-diyl dimethanesulfonate	Myleran
Cabazitaxel	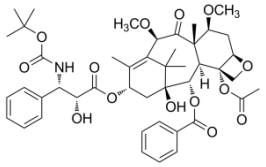	$C_{45}H_{57}NO_{14}$ (1*S*,2*S*,3*R*,4*S*,7*R*,9*S*,10*S*,12*R*,15*S*)-4-(Acetyloxy)-15-{[(2*R*,3*S*)-3-{[(tert-butoxy)carbonyl]amino}-2-hydroxy-3-phenylpropanoyl]oxy}-1-hydroxy-9,12-dimethoxy-10,14,17,17-tetramethyl-11-oxo-6-oxatetracyclo[11.3.1.0^{3,10}.0^{4,7}]heptadec-13-en-2-yl benzoate	Jevtana
Capecitabine	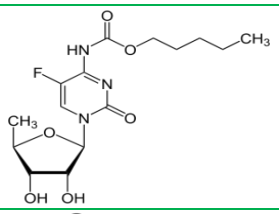	$C_{15}H_{22}FN_3O_6$ Pentyl [1-(3,4-dihydroxy-5-methyltetrahydrofuran-2-yl)-5-fluoro-2-oxo-1*H*-pyrimidin-4-yl]carbamate	Xeloda
Carboplatin	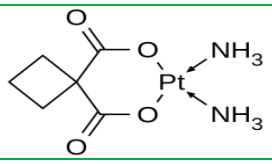	$C_6H_{12}N_2O_4Pt$ *cis*-diammine(cyclobutane-1,1-dicarboxylate-*O*,*O'*)platinum(II)	Paraplatin
Carfilzomib	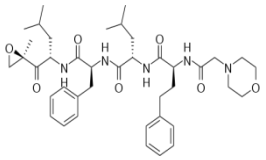	$C_{40}H_{57}N_5O_7$ (*S*)-4-Methyl-*N*-((*S*)-1-(((*S*)-4-methyl-1-((*R*)-2-methyloxiran-2-yl)-1-oxopentan-2-yl)amino)-1-oxo-3-phenylpropan-2-yl)-2-((*S*)-2-(2-morpholinoacetamido)-4-phenylbutanamido)pentanamide	Kyprolis
Carmustine Implant	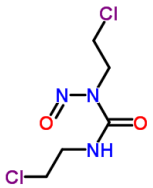	C5H9Cl2N3O2 1,3-Bis(2-chloroethyl)-1-nitrosourea	Gliadel

Molecule	Structure	IUPAC Name	Brand name of drug
Carmustine Implant	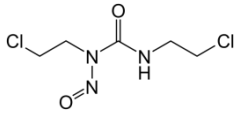	$C_5H_9Cl_2N_3O_2$ 1,3-Bis(2-chloroethyl)-1-nitrosourea	Gliadel wafer
Ceritinib	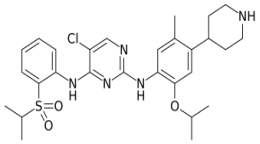	$C_{28}H_{36}ClN_5O_3S$ 5-Chloro-N^2-[2-isopropoxy-5-methyl-4-(4-piperidinyl)phenyl]-N^4-[2-(isopropylsulfonyl)phenyl]-2,4-pyrimidinediamine	Zykadia
Chlorambucil	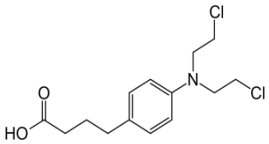	$C_{14}H_{19}Cl_2NO_2$ 4-[bis(2-chlorethyl)amino]benzenebutanoic acid	Leukeran Linfolizin
Cisplatin	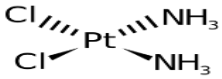	$Cl_2H_6N_2Pt$ (*SP*-4-2)-diamminedichloroplatinum(II)	Platinol-AQ
Crizotinib	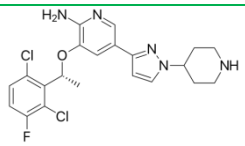	$C_{21}H_{22}Cl_2FN_5O$ 3-[(1*R*)-1-(2,6-dichloro-3-fluorophenyl)ethoxy]-5-(1-piperidin-4-ylpyrazol-4-yl)pyridin-2-amine	Xalkori
Cyclophosphamide	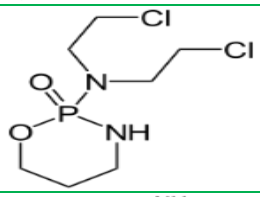	$C_7H_{15}Cl_2N_2O_2P$ (*RS*)-*N*,*N*-bis(2-chloroethyl)-1,3,2-oxazaphosphinan-2-amine 2-oxide	Neosar
Cytarabine	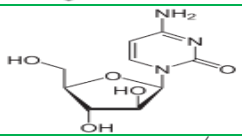	$C_9H_{13}N_3O_5$ 4-amino-1-[(2*R*,3*S*,4*R*,5*R*)-3,4-dihydroxy-5-(hydroxymethyl)oxolan-2-yl] pyrimidin-2-one	Tarabine PFS
Dabrafenib	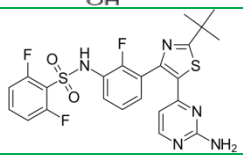	$C_{23}H_{20}F_3N_5O_2S_2$ *N*-{3-[5-(2-aminopyrimidin-4-yl)-2-*tert*-butyl-1,3-thiazol-4-yl]-2-fluorophenyl}-2,6-difluorobenzenesulfonamide	Tafinlar
Dasatinib	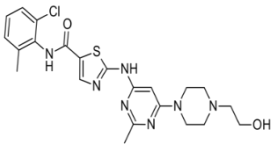	$C_{22}H_{26}ClN_7O_2S$ *N*-(2-chloro-6-methylphenyl)-2-[[6-[4-(2-hydroxyethyl)-1-piperazinyl]-2-methyl-4-pyrimidinyl]amino]-5-thiazole carboxamide monohydrate	Sprycel
Daunorubicin Hydrochloride	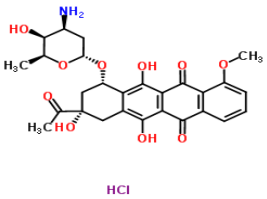	$C_{27}H_{30}ClNO_{10}$ (1S,3S)-3-Acetyl-3,5,12-trihydroxy-10-methoxy-6,11-dioxo-1,2,3,4,6,11-hexahydrotetracen-1-yl 3-amino-2,3,6-trideoxy-α-L-lyxo-hexopyranoside hydrochloride (1:1)	Rubidomycin

Molecule	Structure	IUPAC Name	Brand name of drug
Dexrazoxane Hydrochloride	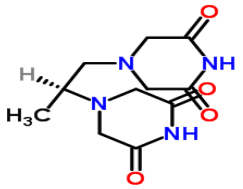	4,4'-[(2S)-1,2-Propanediyl]di(2,6-piperazinedione)	Totect Zinecard
Dexrazoxane Hydrochloride	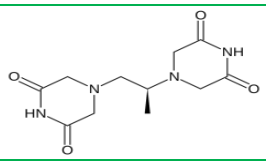	$C_{11}H_{16}N_4O_4$ 4-[(2*S*)-2-(3,5-dioxopiperazin-1-yl)propyl]piperazine-2,6-dione	Zinecard Totect
Docetaxel	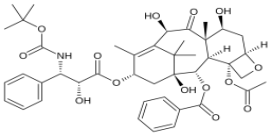	$C_{43}H_{53}NO_{14}$ 1,7β,10β-trihydroxy-9-oxo-5β,20-epoxytax-11-ene-2α,4,13α-triyl 4-acetate 2-benzoate 13-{(2*R*,3*S*)-3-[(*tert*-butoxycarbonyl)amino]-2-hydroxy-3-phenylpropanoate}	Taxotere
Doxorubicin Hydrochloride	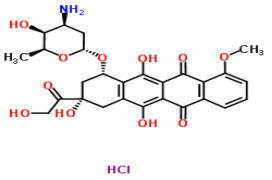	(1S,3S)-3-Glycoloyl-3,5,12-trihydroxy-10-methoxy-6,11-dioxo-1,2,3,4,6,11-hexahydro-1-tetracenyl 3-amino-2,3,6-trideoxy-alpha-L-lyxo-hexopyranoside hydrochloride (1:1)	Adriamycin Doxil Evacet
Eltrombopag Olamine	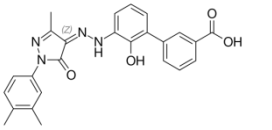 Eltrombopag	$C_{25}H_{22}N_4O_4$ 3'-{(2*Z*)-2-[1-(3,4-dimethylphenyl)-3-methyl-5-oxo-1,5-dihydro-4*H*-pyrazol-4-ylidene]hydrazino}-2'-hydroxy-3-biphenylcarboxylic acid	Promacta
Empliciti	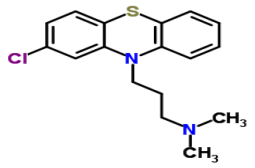	C17H19ClN2S 3-(2-Chloro-10H-phenothiazin-10-yl)-N,N-dimethyl-1-propanamine	Elotuzumab
Enzalutamide	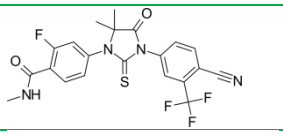	$C_{21}H_{16}F_4N_4O_2S$ 4-(3-(4-Cyano-3-(trifluoromethyl)phenyl)-5,5-dimethyl-4-oxo-2-thioxoimidazolidin-1-yl)-2-fluoro-*N*-methylbenzamide	Xtandi
Epirubicin Hydrochloride	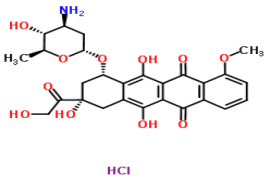	$C_{27}H_{30}ClNO_{11}$ (1S,3S)-3-Glycoloyl-3,5,12-trihydroxy-10-methoxy-6,11-dioxo-1,2,3,4,6,11-hexahydro-1-tetracenyl 3-amino-2,3,6-trideoxy-alpha-L-arabino-hexopyranoside hydrochloride (1:1)	Ellence
Eribulin Mesylate	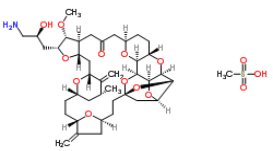	C41H63NO14S (1S,3S,6S,9S,12S,14R,16R,18S,20R,21R,22S,26R,29S,31R,32S,35R,36S)-20-[(2S)-3-Amino-2-hydroxypropyl]-21-methoxy-14-methyl-8,15-bis(methylene)-2,19,30,34,37,39,40,41-octaoxanonacyclo[24.9.2.1~3,32~.1~3,33~.1~6,9~.1~12,16~.0~18,22~.0~29,36~.0~31,35~]hentetracontan-24-one methanesulfonate (1:1)	Halaven

Molecule	Structure	IUPAC Name	Brand name of drug
Erlotinib Hydrochloride	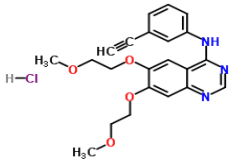	$C_{22}H_{24}ClN_3O_4$ Hydrogen chloride - N-(3-ethynylphenyl)-6,7-bis(2-methoxyethoxy)-4-quinazolinamine (1:1:1)	Tarceva
Etoposide	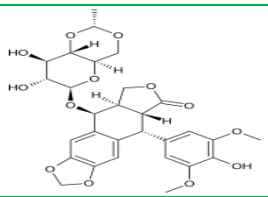	$C_{29}H_{32}O_{13}$ 4'-Demethyl-epipodophyllotoxin 9-[4,6-*O*-(*R*)-ethylidene-*beta*-D-glucopyranoside], 4' -(dihydrogen phosphate)	VePesid Toposar
Etoposide Phosphate	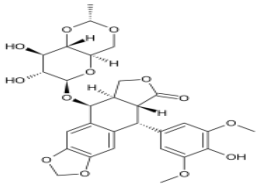	$C_{29}H_{32}O_{13}$ 4'-Demethyl-epipodophyllotoxin 9-[4,6-*O*-(*R*)-ethylidene-*beta*-D-glucopyranoside], 4' -(dihydrogen phosphate)	Etopophos
Everolimus	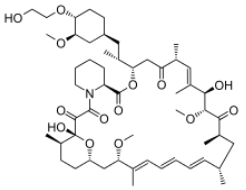	dihydroxy-12-[(2R)-1-[(1S,3R,4R)-4-(2-hydroxyethoxy)-3-methoxycyclohexyl]propan-2-yl]-19,30-dimethoxy-15,17,21,23,29,35-hexamethyl-11,36-dioxa-4-azatricyclo[30.3.1.0 hexatriaconta-16,24,26,28-tetraene-2,3,10,14,20-pentone	Afinitor
Filgrastim	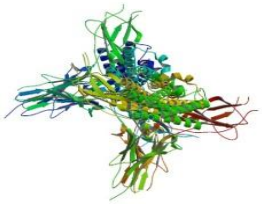	$C_{845}H_{1343}N_{223}O_{243}S_9$ Human granulocyte colony stimulating factor	Neupogen Zarxio
Fludarabine Phosphate	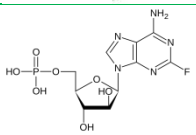	$C_{10}H_{13}FN_5O_7P$ [(2*R*,3*R*,4*S*,5*R*)-5-(6-amino-2-fluoro-purin-9-yl)- 3,4-dihydroxy-oxolan-2-yl]methoxyphosphonic acid	Fludara
Fluorouracil	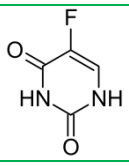	$C_4H_3FN_2O_2$ 5-Fluoro-1*H*,3*H*-pyrimidine-2,4-dione	Fluoroplex
Fulvestrant	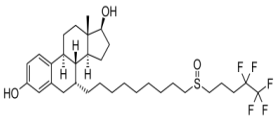	$C_{32}H_{47}F_5O_3S$ (7α,17β)-7-{9-[(4,4,5,5,5-pentafluoropentyl)sulfinyl]nonyl}estra-1,3,5(10)-triene-3,17-diol	Faslodex

Molecule	Structure	IUPAC Name	Brand name of drug
Gefitinib	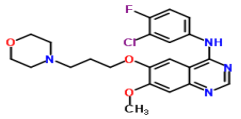	$C_{22}H_{24}ClFN_4O_3$ N-(3-chloro-4-fluoro-phenyl)-7-methoxy-6-(3-morpholinopropoxy)quinazolin-4-amine	
Gefitinib	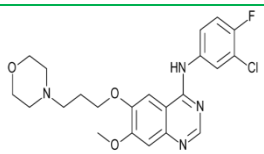	$C_{22}H_{24}ClFN_4O_3$ *N*-(3-chloro-4-fluoro-phenyl)-7-methoxy-6-(3-morpholin-4-ylpropoxy)quinazolin-4-amine	Iressa
Gemcitabine Hydrochloride	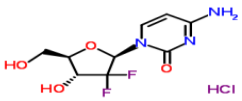	$C_9H_{12}ClF_2N_3O_4$ 2'-Deoxy-2',2'-difluorocytidine hydrochloride (1:1)	Gemzar
Gleevec	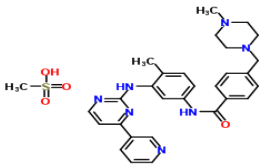	C30H35N7O4S 4-[(4-Methyl-1-piperazinyl)methyl]-N-(4-methyl-3-{[4-(3-pyridinyl)-2-pyrimidinyl]amino}phenyl)benzamide methanesulfonate (1:1)	Imatinib Mesylate
Goserelin Acetate	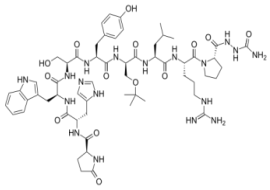	$C_{59}H_{84}N_{18}O_{14}$ N-(21-((1H-indol-3-yl)methyl)-1,1-diamino-12-(tert-butoxymethyl)-6-(2-(2-carbamoylhydrazinecarbonyl)cyclopentanecarbonyl)-15-(4-hydroxybenzyl)-18-(hydroxymethyl)-25-(1H-imidazol-5-yl)-9-isobutyl-8,11,14,17,20,23-hexaoxo-2,7,10,13,16,19,22-heptaazapentacos-1-en-24-yl)-5-oxopyrrolidine-2-carboxamide	Zoladex
Ibritumomab Tiuxetan	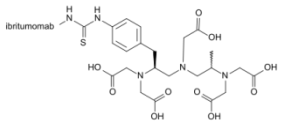	antibody	Zevalin
Ibrutinib	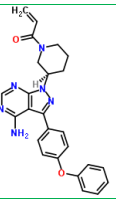	$C_{25}H_{24}N_6O_2$ 1-{(3R)-3-[4-Amino-3-(4-phenoxyphenyl)-1H-pyrazolo[3,4-d]pyrimidin-1-yl]-1-piperidinyl}-2-propen-1-one	
Ibrutinib	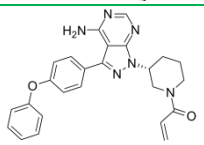	$C_{25}H_{24}N_6O_2$ 1-[(3*R*)-3-[4-Amino-3-(4-phenoxyphenyl)-1*H*-pyrazolo[3,4-*d*]pyrimidin-1-yl]piperidin-1-yl]prop-2-en-1-one	Imbruvica
ICE	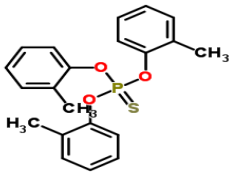	C21H21O3PS O,O,O-Tris(2-methylphenyl) thiophosphate	

Molecule	Structure	IUPAC Name	Brand name of drug
Idarubicin Hydrochloride	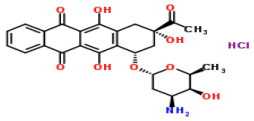	$C_{26}H_{28}ClNO_9$ (1S,3S)-3-Acetyl-3,5,12-trihydroxy-6,11-dioxo-1,2,3,4,6,11-hexahydro-1-tetracenyl 3-amino-2,3,6-trideoxy-alpha-L-lyxo-hexopyranoside hydrochloride (1:1)	Idamycin
Idelalisib	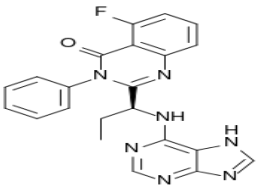	$C_{22}H_{18}FN_7O$ 5-Fluoro-3-phenyl-2-[(1*S*)-1-(7*H*-purin-6-ylamino)propyl]-4(3*H*)-quinazolinone	Zydelig
Ifosfamide	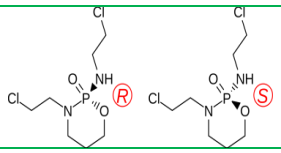	$C_7H_{15}Cl_2N_2O_2P$ *N*-3-bis(2-chloroethyl)-1,3,2-oxazaphosphinan-2-amide-2-oxide	Ifex
Imatinib Mesylate	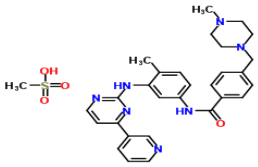	C30H35N7O4S 4-[(4-Methyl-1-piperazinyl)methyl]-N-(4-methyl-3-{[4-(3-pyridinyl)-2-pyrimidinyl]amino}phenyl)benzamide methanesulfonate (1:1)	Gleevec
Imiquimod	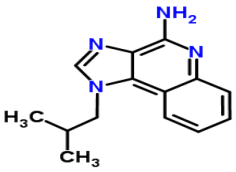	C14H16N4 1-isobutylimidazo[4,5-c]quinolin-4-amine	
Irinotecan Hydrochloride	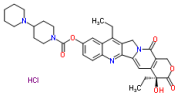	C33H39ClN4O6 (4S)-4,11-Diethyl-4-hydroxy-3,14-dioxo-3,4,12,14-tetrahydro-1H-pyrano[3',4':6,7]indolizino[1,2-b]quinolin-9-yl 1,4'-bipiperidine-1'-carboxylate hydrochloride (1:1)	
Irinotecan Hydrochloride Liposome	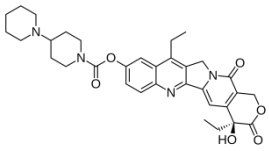 + Liposome	$C_{33}H_{38}N_4O_6$ (*S*)-4,11-diethyl-3,4,12,14-tetrahydro-4-hydroxy-3,14-dioxo1*H*-pyrano[3',4':6,7]-indolizino[1,2-b]quinolin-9-yl-[1,4'bipiperidine]-1'-carboxylate	Onivyde
Ixabepilone		C27H42N2O5S (1S,3S,7S,10R,11S,12S,16R)-7,11-Dihydroxy-8,8,10,12,16-pentamethyl-3-[(1E)-1-(2-methyl-1,3-thiazol-4-yl)-1-propen-2-yl]-17-oxa-4-azabicyclo[14.1.0]heptadecane-5,9-dione	Ixabepilone

Molecule	Structure	IUPAC Name	Brand name of drug
Ixazomib Citrate	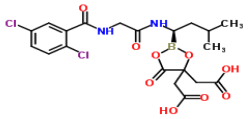	C20H23BCl2N2O9 2,2'-{2-[(1R)-1-{[N-(2,5-Dichlorobenzoyl)glycyl]amino}-3-methylbutyl]-5-oxo-1,3,2-dioxaborolane-4,4-diyl}diacetic acid	
Ixazomib Citrate	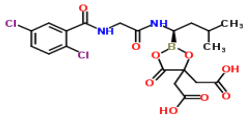	$C_{20}H_{23}BCl_2N_2O_9$ 2,2'-{2-[(1R)-1-{[N-(2,5-Dichlorobenzoyl)glycyl]amino}-3-methylbutyl]-5-oxo-1,3,2-dioxaborolane-4,4-diyl}diacetic acid	Ninlaro
Lanreotide Acetate	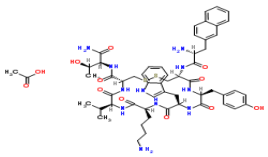	$C_{56}H_{73}N_{11}O_{12}S_2$ (4R,7S,10S,13R,16S,19R)-10-(4-Aminobutyl)-N-[(2S,3R)-1-amino-3-hydroxy-1-oxo-2-butanyl]-16-(4-hydroxybenzyl)-13-(1H-indol-3-ylmethyl)-7-isopropyl-19-{[3-(2-naphthyl)-D-alanyl]amino}-6,9,12,15,18-penta oxo-1,2-dithia-5,8,11,14,17-pentaazacycloicosane-4-carboxamide acetat	
Lanreotide (Acetate)	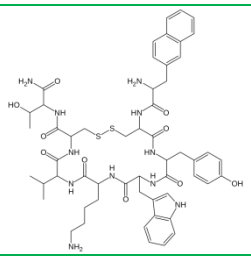	$C_{54}H_{69}N_{11}O_{10}S_2$ 3-(2-naphthyl)-D-alanyl-L-cysteinyl-L-tyrosyl-D-tryptophyl-L-lysyl-L-valyl-L-cysteinyl-L-threoninamide (2->7)-disulfide	Somatuline Depot
Lapatinib Ditosylate	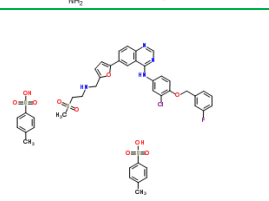	$C_{43}H_{44}ClFN_4O_{11}S_3$ N-{3-Chloro-4-[(3-fluorobenzyl)oxy]phenyl}-6-[5-({[2-(methylsulfonyl)ethyl]amino}methyl)-2-furyl]-4-quinazolinamine 4-methylbenzenesulfonate hydrate (1:2:1)	
Lapatinib Ditosylate			Tykerb
Lenalidomide	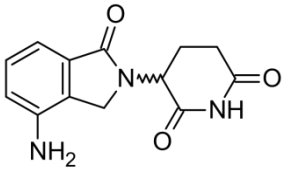	$C_{13}H_{13}N_3O_3$ (*RS*)-3-(4-Amino-1-oxo 1,3-dihydro-2*H*-isoindol- 2-yl)piperidine-2,6-dione	Revlimid
Lenvatinib Mesylate	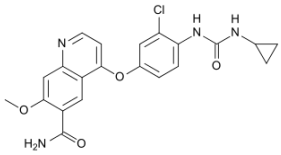	$C_{21}H_{19}ClN_4O_4$ 4-[3-chloro-4-(cyclopropylcarbamoylamino)phenoxy]-7-methoxy-quinoline-6-carboxamide	Lenvima
Letrozole	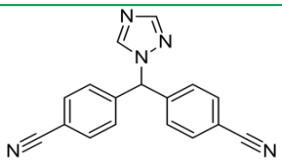	$C_{17}H_{11}N_5$ 4,4'-((1H-1,2,4-triazol-1-yl)methylene)dibenzonitrile	Femara

Molecule	Structure	IUPAC Name	Brand name of drug
Leucovorin Calcium	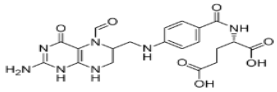	$C_{20}H_{23}N_7O_7$ (*2S*)-2-{[4-[(2-amino-5-formyl-4-oxo-5,6,7,8-tetrahydro-1*H*-pteridin-6-yl)methylamino] benzoyl]amino}pentanedioic acid	Wellcovorin
Leuprolide Acetate	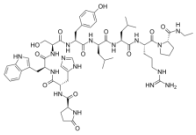	$C_{59}H_{84}N_{16}O_{12}$ *N*-[1-[[1-[[1-[[1-[[1-[[5-(diaminomethylideneamino)-1-[2-(ethylcarbamoyl)pyrrolidin-1-yl]-1-oxo-pentan-2-yl]carbamoyl]-3-methyl-butyl]carbamoyl]-3-methyl-butyl]carbamoyl]-2-(4-hydroxyphenyl)ethyl] carbamoyl]-2-hydroxy-ethyl]carbamoyl]-2-(1*H*-indol-3-yl)ethyl]carbamoyl]-2-(3*H*-imidazol-4-yl)ethyl]-5-oxo-pyrrolidine-2-carboxamide	Lupron
			Lupron Depot
			Lupron Depot-3 Month
			Lupron Depot-4 Month
			Lupron Depot-Ped
			Viadur
Mechlorethamine Hydrochloride	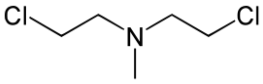	$C_5H_{11}Cl_2N$ Bis(2-chloroethyl)methylamine	Mustargen
Megestrol Acetate	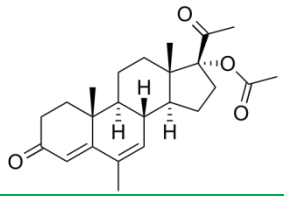	$C_{24}H_{32}O_4$ 17-(acetyloxy)-6-methyl-pregna-4,6-diene-3,20-dione	Megace
Mercaptopurine	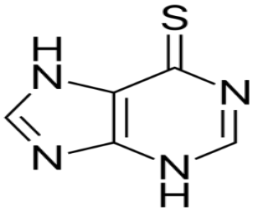	$C_5H_4N_4S$ 3,7-dihydropurine-6-thione	Purinethol
Mercaptopurine			Purixan
Mesna Methazolastone Temozolomide	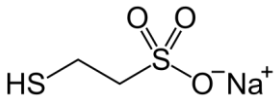 Mesna	$C_2H_5NaO_3S_2$ sodium 2-sulfanylethanesulfonate	Mesnex
	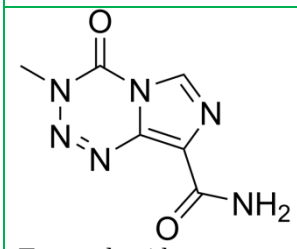 Temozolomide	$C_6H_6N_6O_2$ 4-methyl-5-oxo-2,3,4,6,8-pentazabicyclo[4.3.0]nona-2,7,9-triene-9-carboxamide	
Methotrexate	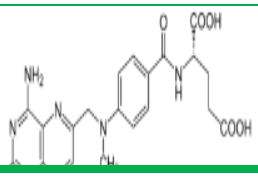	$C_{20}H_{22}N_8O_5$ (2*S*)-2-[(4-{[(2,4-Diaminopteridin-6-yl)methyl](methyl)amino}benzoyl)amino]pentanedioic acid	Folex
Methotrexate			Folex PFS
Methotrexate			Methotrexate LPF
Methotrexate			Mexate

Molecule	Structure	IUPAC Name	Brand name of drug
Methotrexate			Mexate-AQ
Methotrexate			Rheumatrex
Mitomycin C	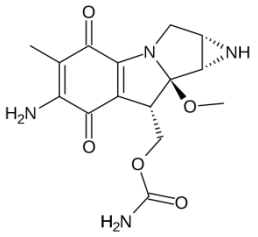	$C_{15}H_{18}N_4O_5$ {11-Amino-7-methoxy-12-methyl-10,13-dioxo-2,5-diazatetracyclo[7.4.0.0^{2,7}.0^{4,6}]trideca-1(9),11-dien-8-yl}methyl carbamate	Mitozytrex
Mitomycin C			Mutamycin
Nelarabine	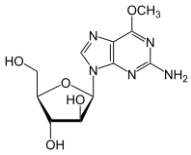	(2*R*,3*S*,4*S*,5*R*)-2-(2-amino-6-methoxy-purin-9-yl)-5-(hydroxymethyl)oxolane-3,4-diol	Arranon
Netupitant palonosetron	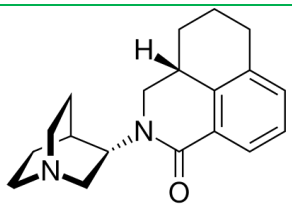	$C_{19}H_{24}N_2O$ (3*aS*)-2-[(3*S*)-1-Azabicyclo[2.2.2]oct-3-yl]-2,3,3*a*,4,5,6-hexahydro-1*H*-benz[*de*]isoquinolin-1-one	Akynzeo
	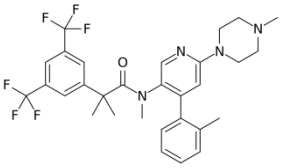 Netupitant	$C_{30}H_{32}F_6N_4O$ 2-[3,5-Bis(trifluoromethyl)phenyl]-*N*,2-dimethyl-*N*-[4-(2-methylphenyl)-6-(4-methyl-1-piperazinyl)-3-pyridinyl]propanamide	
Nilotinib	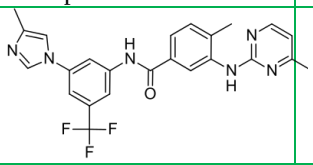	$C_{28}H_{22}F_3N_7O$ 4-methyl-*N*-[3-(4-methyl-1*H*-imidazol-1-yl)- 5-(trifluoromethyl)phenyl]-3- [(4-pyridin-3-ylpyrimidin-2-yl) amino]benzamide	Tasigna
Olaparib	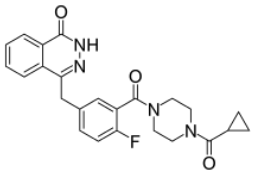	$C_{24}H_{23}FN_4O_3$ 4-(3-{[4-(Cyclopropylcarbonyl)-1-piperazinyl]carbonyl}-4-fluorobenzyl)-1(2H)-phthalazinone	Lynparza
Omacetaxine Mepesuccinate	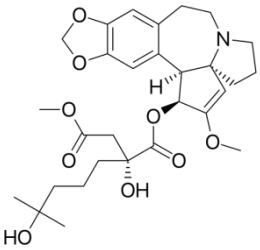	$C_{29}H_{39}NO_9$ 1-((1*S*,3a*R*,14b*S*)-2-Methoxy-1,5,6,8,9,14b-hexahydro-4*H*-cyclopenta(a)(1,3)dioxolo(4,5-*h*)pyrrolo(2,1-*b*)(3)benzazepin-1-yl) 4-methyl (2*R*)-2-hydroxy-2-(4-hydroxy-4-methylpentyl)butanedioate	Synribo

Molecule	Structure	IUPAC Name	Brand name of drug
Ondansetron Hydrochloride	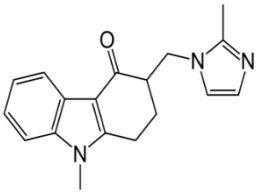	$C_{18}H_{19}N_3O$ (*RS*)-9-methyl-3-[(2-methyl-1*H*-imidazol-1-yl)methyl]-2,3-dihydro-1*H*-carbazol-4(9*H*)-one	Zofran
Osimertinib	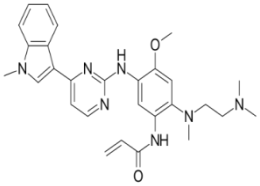	$C_{28}H_{33}N_7O_2$ *N*-(2-{2-dimethylaminoethyl-methylamino}-4-methoxy-5-{[4-(1-methylindol-3-yl)pyrimidin-2-yl]amino}phenyl)prop-2-enamide	Tagrisso
Paclitaxel	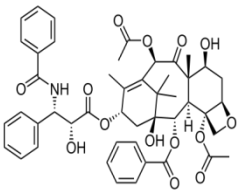	$C_{47}H_{51}NO_{14}$ (2α,4α,5β,7β,10β,13α)-4,10-Bis(acetyloxy)-13-{[(2*R*,3*S*)-3-(benzoylamino)-2-hydroxy-3-phenylpropanoyl]oxy}-1,7-dihydroxy-9-oxo-5,20-epoxytax-11-en-2-yl benzoate	Taxol
Paclitaxel Albumin-stabilized Nanoparticle Formulation	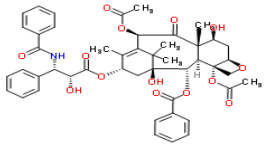	Taxol :(2alpha,5beta,7beta,10beta,13alpha)-4,10-Diacetoxy-13-{[(2R,3S)-3-(benzoylamino)-2-hydroxy-3-phenylpropanoyl]oxy}-1,7-dihydroxy-9-oxo-5,20-epoxytax-11-en-2-yl benzoate	Abraxane
Palbociclib	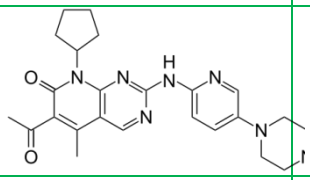	$C_{24}H_{29}N_7O_2$ 6-Acetyl-8-cyclopentyl-5-methyl-2-{[5-(1-piperazinyl)-2-pyridinyl]amino}pyrido[2,3-d]pyrimidin-7(8*H*)-one	Ibrance
Palonosetron	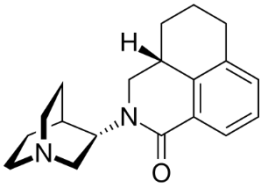	$C_{19}H_{24}N_2O$ (3*aS*)-2-[(3*S*)-1-Azabicyclo[2.2.2]oct-3-yl]-2,3,3*a*,4,5,6-hexahydro-1*H*-benz[*de*]isoquinolin-1-one	Aloxi
Panobinostat	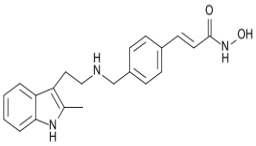	$C_{21}H_{23}N_3O_2$ (2*E*)-*N*-hydroxy-3-[4-({[2-(2-methyl-1*H*-indol-3-yl)ethyl]amino}methyl)phenyl]acrylamide	Farydak
Pazopanib Hydrochloride	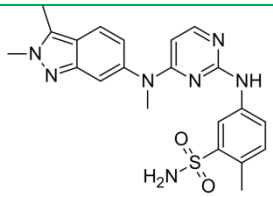	$C_{21}H_{23}N_7O_2S$ 5-[[4-[(2,3-Dimethyl-2H-indazol-6-yl)methylamino]-2-pyrimidinyl]amino]-2-methylbenzolsulfonamide	Votrient

Molecule	Structure	IUPAC Name	Brand name of drug
Pertuzumab	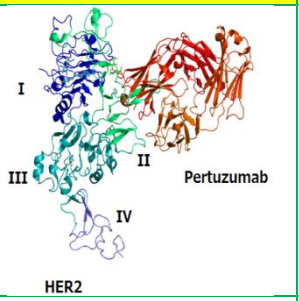	Monoclonal antibody	Perjeta
Plerixafor	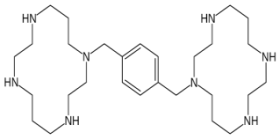	$C_{28}H_{54}N_8$ 1,1′-[1,4-Phenylenebis(methylene)]bis [1,4,8,11-tetraazacyclotetradecane]	Mozobil
Pomalidomide	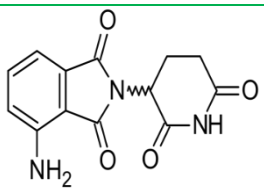	$C_{13}H_{11}N_3O_4$ (*RS*)-4-Amino-2-(2,6-dioxopiperidin-3-yl)isoindole-1,3-dione	Pomalyst
Ponatinib Hydrochloride	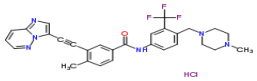	C29H28ClF3N6O 3-(Imidazo[1,2-b]pyridazin-3-ylethynyl)-4-methyl-N-{4-[(4-methyl-1-piperazinyl)methyl]-3-(trifluoromethyl)phenyl}benzamide hydrochloride (1:1)	Iclusig
Pralatrexate	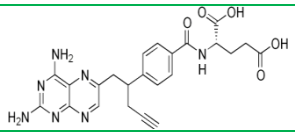	$C_{23}H_{23}N_7O_5$ *N*-(4-{1-[(2,4-diaminopteridin-6-yl)methyl]but-3-yn-1-yl}benzoyl)-L-glutamic acid	Folotyn
Procarbazine Hydrochloride	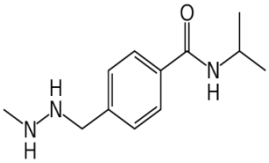	$C_{12}H_{19}N_3O$ *N*-Isopropyl-4-[(2-methylhydrazino)methyl]benzamide	Matulane
Raloxifene Hydrochloride	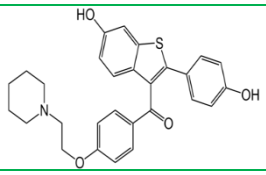	$C_{28}H_{27}NO_4S$ [6-hydroxy-2-(4-hydroxyphenyl)- benzothiophen-3-yl]- [4-[2-(1-piperidyl)ethoxy]phenyl] -methanone	Keoxifene
Regorafenib	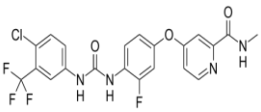	$C_{21}H_{17}ClF_4N_4O_4$ 4-[4-({[4-Chloro-3-(trifluoromethyl)phenyl]carbamoyl}amino)-3-fluorophenoxy]-*N*-methylpyridine-2-carboxamide hydrate	Stivarga

Molecule	Structure	IUPAC Name	Brand name of drug
Rituximab		C6416H9874N1688O1987S44 anti body	Rituxan
Rolapitant Hydrochloride	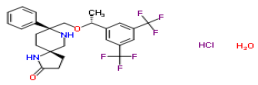	C25H29ClF6N2O3 (5S,8S)-8-({(1R)-1-[3,5-Bis(trifluoromethyl)phenyl]ethoxy}methyl)-8-phenyl-1,7-diazaspiro[4.5]decan-2-one hydrochloride hydrate	Varubi
Romidepsin	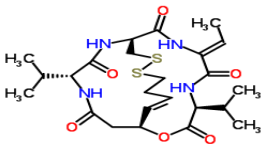	C24H36N4O6S2 (1S,4S,7Z,10S,21R)-7-Ethylidene-4,21-diisopropyl-2-oxa-12,13-dithia-5,8,20,23-tetraazabicyclo[8.7.6]tricos-16-ene-3,6,9,19,22-pentone	Istodax
Ruxolitinib (Phosphate)	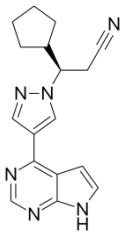	$C_{17}H_{18}N_6$ (3*R*)-3-cyclopentyl-3-[4-(7*H*-pyrrolo[2,3-d]pyrimidin-4-yl)pyrazol-1-yl]propanenitrile	Jakafi
Sonidegib	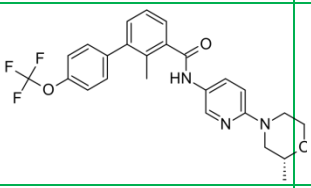	$C_{26}H_{26}F_3N_3O_3$ *N*-[6-[(2*S*,6*R*)-2,6-Dimethylmorpholin-4-yl]pyridin-3-yl]-2-methyl-3-[4-(trifluoromethoxy)phenyl]benzamide	Odomzo
Sorafenib Tosylate	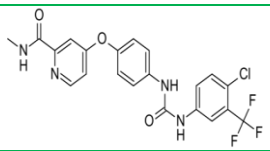	$C_{21}H_{16}ClF_3N_4O_3$ 4-[4-[[4-chloro-3-(trifluoromethyl)phenyl]carbamoylamino] phenoxy]-*N*-methyl-pyridine-2-carboxamide	Nexavar
Sunitinib Malate	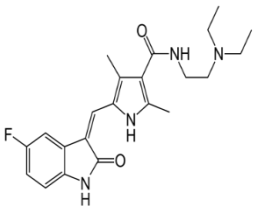	$C_{22}H_{27}FN_4O_2$ *N*-(2-diethylaminoethyl)-5-[(*Z*)-(5-fluoro-2-oxo-1H-indol-3-ylidene)methyl]-2,4-dimethyl-1*H*-pyrrole-3-carboxamide	Sutent
Talimogene Laherparepvec	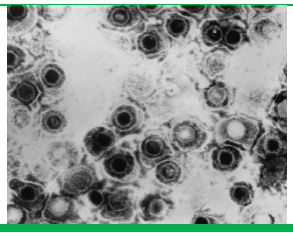	Transmission electron micrograph of an unmodified herpes simplex virus	Imlygic

Molecule	Structure	IUPAC Name	Brand name of drug
Tamoxifen Citrate	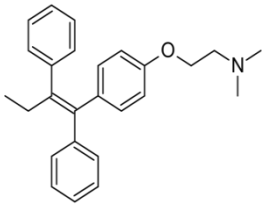	$C_{26}H_{29}NO$ (*Z*)-2-[4-(1,2-diphenylbut-1-enyl)phenoxy]-*N*,*N*-dimethylethanamine	Nolvadex
Temozolomide	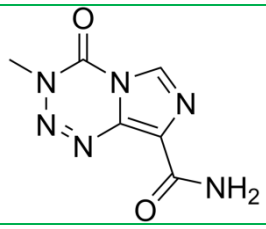	$C_6H_6N_6O_2$ 4-methyl-5-oxo-2,3,4,6,8-pentazabicyclo[4.3.0]nona-2,7,9-triene-9-carboxamide	Temodar
Temsirolimus	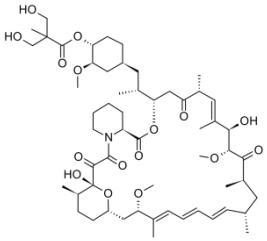	$C_{56}H_{87}NO_{16}$ (1*R*,2*R*,4*S*)-4-{(2*R*)-2-[(3*S*,6*R*,7*E*,9*R*,10*R*,12*R*,14*S*,15*E*,17*E*,19*E*,21*S*,23*S*,26*R*,27*R*,34a*S*)-9,27-dihydroxy-10,21-dimethoxy-6,8,12,14,20,26-hexamethyl-1,5,11,28,29-pentaoxo-1,4,5,6,9,10,11,12,13,14,21,22,23,24,25,26,27,28,29,31,32,33,34,34a-tetracosahydro-3*H*-23,27-epoxypyrido[2,1-*c*][1,4]oxazacyclohentriacontin-3-yl]propyl}-2-methoxycyclohexyl 3-hydroxy-2-(hydroxymethyl)-2-methylpropanoate	Torisel
Thalidomide	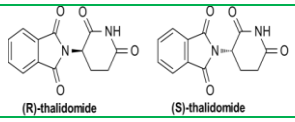	$C_{13}H_{10}N_2O_4$ (*RS*)-2-(2,6-dioxopiperidin-3-yl)-1*H*-isoindole-1,3(2*H*)-dione	Synovir Thalomid
Thioguanine	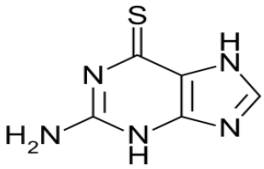	$C_5H_5N_5S$ 2-amino-1H-purine-6(7H)-thione	Tabloid
Topotecan Hydrochloride	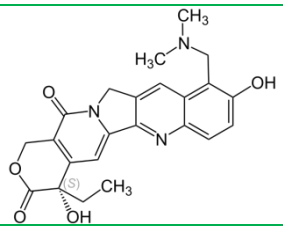	$C_{23}H_{23}N_3O_5$ •HCl (*S*)-10-[(dimethylamino)methyl]-4-ethyl-4,9-dihydroxy-1*H*-pyrano[3',4':6,7]indolizino[1,2-*b*]quinoline-3,14(4*H*,12*H*)-dione monohydrochloride	Hycamtin
Toremifene	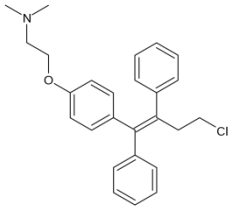	$C_{26}H_{28}ClNO$ 2-{4-[(1*Z*)-4-chloro-1,2-diphenyl-but-1-en-1-yl]phenoxy}-*N*,*N*-dimethylethanamine	Fareston

Molecule	Structure	IUPAC Name	Brand name of drug
Tositumomab and Iodine I 131 Tositumomab	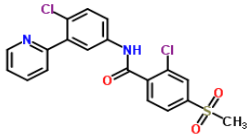	C19H14Cl2N2O3S 2-Chloro-N-[4-chloro-3-(2-pyridinyl)phenyl]-4-(methylsulfonyl)benzamide	Bexxar
Trabectedin	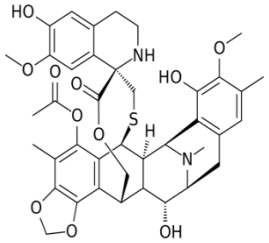	$C_{39}H_{43}N_3O_{11}S$ (1'*R*,6*R*,6a*R*,7*R*,13*S*,14*S*,16*R*)-6',8,14-trihydroxy-7',9-dimethoxy-4,10,23-trimethyl-19-oxo-3',4',6,7,12,13,14,16-octahydrospiro[6,16-(epithiopropano-oxymethano)-7,13-imino-6a*H*-1,3-dioxolo[7,8]isoquino[3,2-*b*][3]benzazocine-20,1'(2'*H*)-isoquinolin]-5-yl acetate	Yondelis
Trametinib	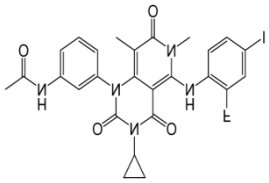	$C_{26}H_{23}FIN_5O_4$ *N*-(3-{3-Cyclopropyl-5-[(2-fluoro-4-iodophenyl)amino]-6,8-dimethyl-2,4,7-trioxo-3,4,6,7-tetrahydropyrido[4,3-d]pyrimidin-1(2*H*)-yl}phenyl)acetamide	Mekinist
Trifluridine and Tipiracil Hydrochloride	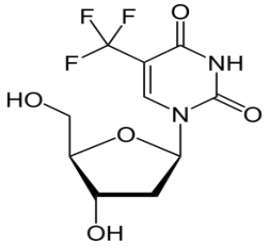 Trifluridine	$C_{10}H_{11}F_3N_2O_5$ 1-[4-hydroxy-5-(hydroxymethyl)oxolan-2-yl]-5-(trifluoromethyl) pyrimidine-2,4-dione	Lonsurf
	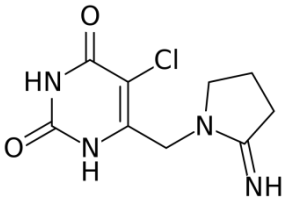 Tipiracil Hydrochloride	$C_9H_{11}ClN_4O_2$ 5-Chloro-6-[(2-imino-1-pyrrolidinyl)methyl]-2,4(1*H*,3*H*)-pyrimidinedione	
Vemurafenib	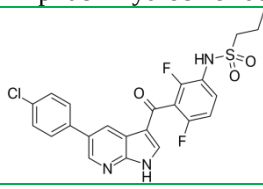	$C_{23}H_{18}ClF_2N_3O_3S$ *N*-(3-{[5-(4-chlorophenyl)-1*H*-pyrrolo[2,3-b]pyridin-3-yl]carbonyl}-2,4-difluorophenyl)propane-1-sulfonamide	Zelboraf
Vinblastine Sulfate	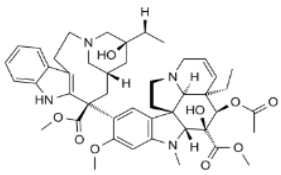	$C_{46}H_{58}N_4O_9$ dimethyl (2β,3β,4β,5α,12β,19α)-15-[(5*S*,9*S*)-5-ethyl-5-hydroxy-9-(methoxycarbonyl)-1,4,5,6,7,8,9,10-octahydro-2*H*-3,7-methanoazacycloundecino[5,4-b]indol- 9-yl]-3-hydroxy-16-methoxy-1-methyl-6,7-didehydroaspidospermidine-3,4-dicarboxylate	Velsar Velban

Molecule	Structure	IUPAC Name	Brand name of drug
Vincristine Sulfate Liposome	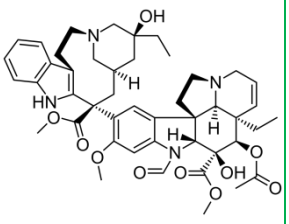	$C_{46}H_{56}N_4O_{10}$ (3a*R*,3a1*R*,4*R*,5*S*,5a*R*,10b*R*)-Methyl 4-acetoxy-3a-ethyl-9-((5*S*,7*S*,9*S*)-5-ethyl-5-hydroxy-9-(methoxycarbonyl)-2,4,5,6,7,8,9,10-octahydro-1*H*-3,7-methano[1]azacycloundecino[5,4-*b*]indol-9-yl)-6-formyl-5-hydroxy-8-methoxy-3a,3a1,4,5,5a,6,11,12-octahydro-1*H*-indolizino[8,1-cd]carbazole-5-carboxylate	Marqibo
Vinorelbine (Tartrate)	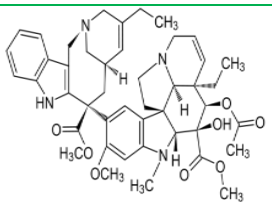	$C_{45}H_{54}N_4O_8$ 4-(acetyloxy)- 6,7-didehydro- 15-((2*R*,6*R*,8*S*)-4-ethyl- 1,3,6,7,8,9-hexahydro- 8-(methoxycarbonyl)-2,6-methano- 2*H*-azecino(4,3-*b*)indol-8-yl)- 3-hydroxy- 16-methoxy- 1-methyl- methyl ester,	Navelbine
Vorinostat	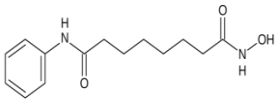	$C_{14}H_{20}N_2O_3$ *N*-Hydroxy-*N*′-phenyloctanediamide	Zolinza
Zoledronic Acid	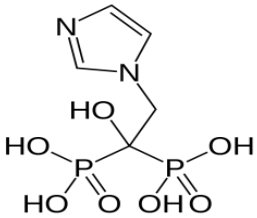	$C_5H_{10}N_2O_7P_2$ [1-hydroxy-2-(1*H*-imidazol-1-yl)ethane-1,1-diyl]bis(phosphonic acid)	Zometa

Glucarpidase	$C_{1950}H_{3157}N_{543}O_{599}S_7$(monomer) Recombinant glutamate carboxypeptidase (carboxypeptidase G2)	Voraxaze
Ipilimumab	$C_{6742}H_{9972}N_{1732}O_{2004}S_{40}$ Antibody	Yervoy
Necitumumab	$C_{6436}H_{9958}N_{1702}O_{2020}S_{42}$ Anti body	Portrazza
Nivolumab	$C_{6362}H_{9862}N_{1712}O_{1995}S_{42}$ Antibody	Opdivo
Palifermin	$C_{721}H_{1142}N_{202}O_{204}S_9$ Truncated human recombinant keratinocyte growth factor(KGF) produced in Escherichia coli.	Kepivance
Romiplostim	Protein L-methionyl[human immunogloblin heavy constant gamma 1-(227 C-terminal residues)-peptide (Fc fragment)] fusion protein with 41 amino acids peptide, (7-7′:10,10′)-bisdisulfide dimer	Nplate

Appendix.2:

Structure-IUPAC Name- Anti_HIV drug evolution (Side)

Source of information

FDA: Antiretroviral Drugs Used in the Treatment of HIV Infection

National Institute of Allergy and Infectious Diseases: Drugs That Fight HIV-1

National Library of Medicine: Drug information from the DailyMed website

Type	Molecules(Brand name)	Structure	IUPAC Name	Brand name
NRTIs	Abacavir (abacavir sulfate, ABC)	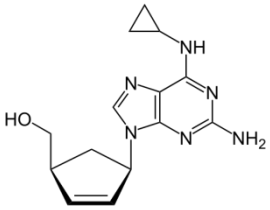	$C_{14}H_{18}N_6O$ {(1*S*,4*R*)-4-[2-amino-6-(cyclopropylamino)-9*H*-purin-9-yl]cyclopent-2-en-1-yl}methanol	Ziagen
	Didanosine (delayed-release didanosine, dideoxyinosine, enteric-coated didanosine, ddi, ddi ec)			Videx
		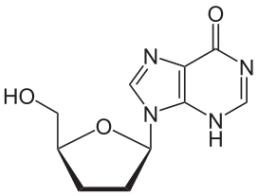	$C_{10}H_{12}N_4O_3$ 9-((2*R*,5*S*)-5-(hydroxymethyl)tetrahydrofuran-2-yl)-3*H*-purin-6(9*H*)-one	Videx EC (enteric-coated)
	Emtricitabine (FTC)	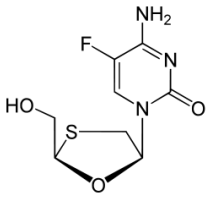	$C_8H_{10}FN_3O_3S$ 4-amino-5-fluoro-1-[(2*R*,5*S*)-2-(hydroxymethyl)-1,3-oxathiolan-5-yl]-1,2-dihydropyrimidin-2-one	Emtriva
	Lamivudine (3TC)	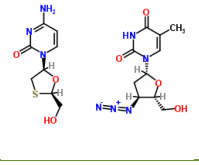	C18H24N8O7S 3'-Azido-3'-deoxythymidine - 4-amino-1-[(2R,5S)-2-(hydroxymethyl)-1,3-oxathiolan-5-yl]-2(1H)-pyrimidinone (1:1)	Epivir
	Stavudine (d4t)	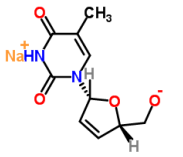	C10H11N2NaO4 Sodium [(2S,5R)-5-(5-methyl-2,4-dioxo-3,4-dihydro-1(2H)-pyrimidinyl)-2,5-dihydro-2-furanyl]methanolate	Zerit
	Tenofovir disoproxil fumarate (tenofovir DF, TDF)	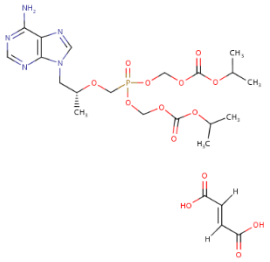	$C_{23}H_{34}N_5O_{14}P$ (2E)-2-Butendisäure - bis{[(isopropoxycarbonyl)oxy]methyl}-({[(2R)-1-(6-amino-9H-purin-9-yl)-2-propanyl]oxy}methyl)phosphonat (1:1)	Viread
	Zidovudine (azidothymidine, AZT, ZDV)	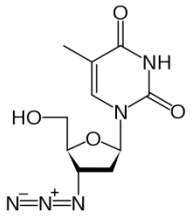	$C_{10}H_{13}N_5O_4$ 1-[(2*R*,4*S*,5*S*)-4-Azido-5-(hydroxymethyl)oxolan-2-yl]-5-methylpyrimidine-2,4-dione	Retrovir

Type	Molecules(Brand name)	Structure	IUPAC Name	Brand name
NNRTIs	Delavirdine (delavirdine mesylate, DLV)	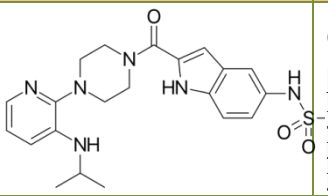	$C_{22}H_{28}N_6O_3S$ *N*-[2-({4-[3-(propan-2-ylamino)pyridin-2-yl]piperazin-1-yl}carbonyl)-1*H*-indol-5-yl]methanesulfonamide	Rescriptor
	Efavirenz (EFV)	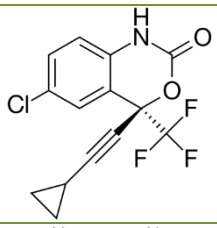	$C_{14}H_9ClF_3NO_2$ (4*S*)-6-chloro-4-(2-cyclopropylethynyl)-4-(trifluoromethyl)-2,4-dihydro-1*H*-3,1-benzoxazin-2-one	Sustiva
	Etravirine (ETR)	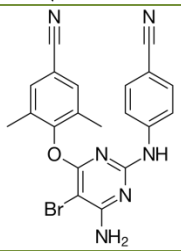	$C_{20}H_{15}BrN_6O$ 4-[6-Amino-5-bromo-2-[(4-cyanophenyl)amino] pyrimidin-4-yl]oxy-3,5-dimethylbenzonitrile	Intelence
	Nevirapine (extended-release nevirapine, NVP)			Viramune
		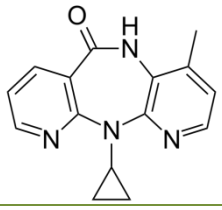	$C_{15}H_{14}N_4O$ 11-cyclopropyl-4-methyl-5,11-dihydro-6*H*- dipyrido[3,2-*b*:2′,3′-*e*][1,4]diazepin-6-one	Viramune XR (extended release)
	Rilpivirine (rilpivirine hydrochloride, RPV)	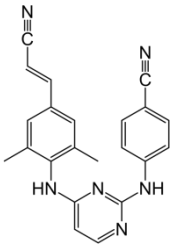	$C_{22}H_{18}N_6$ 4-{[4-({4-[(*E*)-2-cyanovinyl]-2,6-dimethylphenyl}amino)pyrimidin-2-yl]amino}benzonitrile	Edurant
Protease Inhibitors	Atazanavir (atazanavir sulfate, ATV)	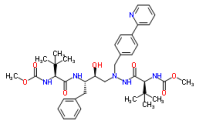	C38H52N6O7 Methyl {(5S,10S,11S,14S)-11-benzyl-10-hydroxy-15,15-dimethyl-5-(2-methyl-2-propanyl)-3,6,13-trioxo-8-[4-(2-pyridinyl)benzyl]-2-oxa-4,7,8,12-tetraazahexadecan-14-yl}carbamate	Reyataz
	Darunavir (darunavir ethanolate, DRV)	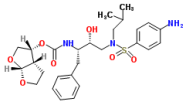	C27H37N3O7S (3R,3aS,6aR)-Hexahydrofuro[2,3-b]furan-3-yl [(2S,3R)-4-{[(4-aminophenyl)sulfonyl](isobutyl)amino}-3-hydroxy-1-phenyl-2-butanyl]carbamate	Prezista

Type	Molecules(Brand name)	Structure	IUPAC Name	Brand name
	Fosamprenavir (fosamprenavir calcium, FOS-APV, FPV)	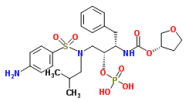	C25H36N3O9PS (3S)-Tetrahydro-3-furanyl [(2S,3R)-4-{[(4-aminophenyl)sulfonyl](isobutyl)amino}-1-phenyl-3-(phosphonooxy)-2-butanyl]carbamate	Lexiva
	Indinavir (indinavir sulfate, IDV)	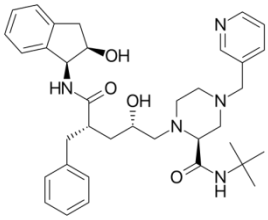	$C_{36}H_{47}N_5O_4$ (2*S*)-1-[(2*S*,4*R*)-4-benzyl-2-hydroxy-4-{[(1*S*,2*R*)-2-hydroxy-2,3-dihydro-1*H*-inden-1-yl]carbamoyl}butyl]-*N*-*tert*-butyl-4-(pyridin-3-ylmethyl)piperazine-2-carboxamide	Crixivan
	Nelfinavir (nelfinavir mesylate, NFV)	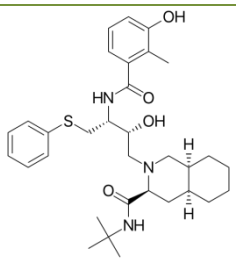	$C_{32}H_{45}N_3O_4S$ (3*S*,4a*S*,8a*S*)-*N*-*tert*-butyl-2-[(2*R*,3*R*)-2-hydroxy-3-[(3-hydroxy-2-methylphenyl)formamido]-4-(phenylsulfanyl)butyl]-decahydroisoquinoline-3-carboxamide	Viracept
	Ritonavir (RTV)	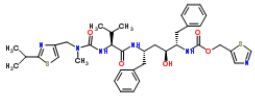	$C_{37}H_{48}N_6O_5S_2$ (1E,2S)-N-[(2S,4S,5S)-4-Hydroxy-5-{(E)-[hydroxy(1,3-thiazol-5-ylmethoxy)methylene]amino}-1,6-diphenyl-2-hexanyl]-2-[(E)-(hydroxy{[(2-isopropyl-1,3-thiazol-4-yl)methyl](methyl)amino}methylene)amino]-3- methylbutanimidic acid	Norvir
	Saquinavir (saquinavir mesylate, SQV)	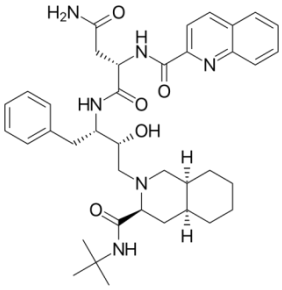	$C_{38}H_{50}N_6O_5$ (2*S*)-*N*-[(2*S*,3*R*)-4-[(3*S*)-3-(*tert*-butylcarbamoyl)-decahydroisoquinolin-2-yl]-3-hydroxy-1-phenylbutan-2-yl]-2-(quinolin-2-ylformamido)butanediamide	Invirase
	Tipranavir (TPV)	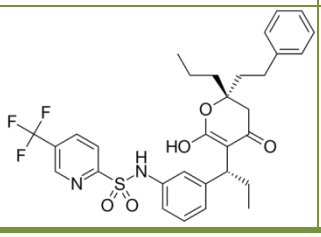	$C_{31}H_{33}F_3N_2O_5S$ *N*-{3-[(1*R*)-1-[(2*R*)-6-hydroxy-4-oxo-2-(2-phenylethyl)-2-propyl-3,4-dihydro-2*H*-pyran-5-yl]propyl]phenyl}-5-(trifluoromethyl)pyridine-2-sulfonamide	Aptivus

Type	Molecules(Brand name)	Structure	IUPAC Name	Brand name
Fusion Inhibitors	Enfuvirtide (T-20)	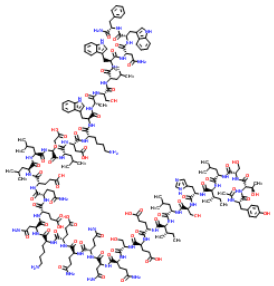	$C_{204}H_{301}N_{51}O_{64}$ acetyl-L-tyrosyl-L-threonyl-L-seryl-L-leucyl-L-isoleucyl-L-histidyl-L-seryl-L-leucyl-L-isoleucyl-L-a-glutamyl-L-a-glutamyl-L-seryl-L-glutaminyl-L-asparaginyl-L-glutaminyl-L-glutaminyl-L-a-glutamyl-L-lysyl-L-asparaginyl-L-a-glutamyl-L-glutaminyl-L-a-glutamyl-L-leucyl-L-leucyl-L-a-glutamyl-L-leucyl-L-a-aspartyl-L-lysyl-L-tryptophyl-L-alanyl-L-seryl-L-leucyl-L-tryptophyl-L-asparaginyl-L-tryptophyl-L-phenylalaninamide	Fuzeon
Entry inhibitors.	Maraviroc (MVC)	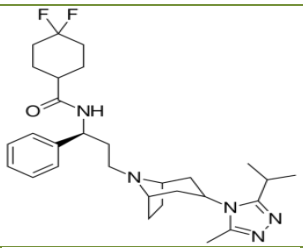	$C_{29}H_{41}F_2N_5O$ 4,4-difluoro-*N*-{(1*S*)-3-[3-(3-isopropyl-5-methyl-4*H*-1,2,4-triazol-4-yl)-8-azabicyclo[3.2.1]oct-8-yl]-1-phenylpropyl}cyclohexanecarboxamide	Selzentry
Integrase inhibitors	Dolutegravir (DTG)	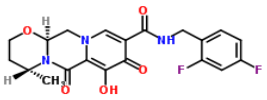	$C_{20}H_{19}F_2N_3O_5$ (4R,12aS)-N-(2,4-Difluorobenzyl)-7-hydroxy-4-methyl-6,8-dioxo-3,4,6,8,12,12a-hexahydro-2H-pyrido[1',2':4,5]pyrazino[2,1-b][1,3]oxazine-9-carboxamide	Tivicay
	Elvitegravir (EVG)	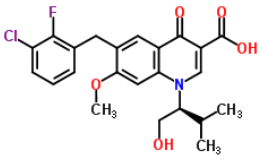	$C_{23}H_{23}ClFNO_5$ 6-(3-Chloro-2-fluorobenzyl)-1-[(2S)-1-hydroxy-3-methyl-2-butanyl]-7-methoxy-4-oxo-1,4-dihydro-3-quinolinecarboxylic acid	Vitekta
	Raltegravir (raltegravir potassium, RAL)	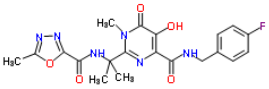	$C_{20}H_{21}FN_6O_5$ 1,3-Thiazol-5-ylmethyl [(2R,5R)-5-{[(2S)-2-({[(2-isopropyl-1,3-thiazol-4-yl)methyl](methyl)carbamoyl}amino)-4-(4-morpholinyl)butanoyl]amino}-1,6-diphenyl-2-hexanyl]carbamate	Isentress

Type	Molecules(Brand name)	Structure	IUPAC Name	Brand name
Pharmacokinetic enhancer	Cobicistat (COBI)	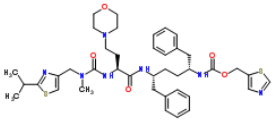	$C_{40}H_{53}N_7O_5S_2$ N-(4-Fluorobenzyl)-5-hydroxy-1-methyl-2-(2-{[(5-methyl-1,3,4-oxadiazol-2-yl)carbonyl]amino}-2-propanyl)-6-oxo-1,6-dihydro-4-pyrimidinecarboxamide	Tybost

Categories of FDA-Approved HIV Medicines for HIV		
NRTIs	Nucleoside Reverse Transcriptase Inhibitors	NRTIs block reverse transcriptase, anenzyme HIV needs to make copies of itself.
NNRTIs	Non-Nucleoside Reverse Transcriptase Inhibitors	NNRTIs bind to and later alter reverse transcriptase, an enzyme HIV needs to make copies of itself.
Pis	Protease Inhibitors	Pis block HIV protease, an enzyme HIV needs to make copies of itself
Fis	Fusion Inhibitors	Fusion inhibitors block HIV from entering theCD4 cells of the immune system
Eis	Entry Inhibitors	Entry inhibitors block proteins on the CD4 cells that HIV needs to enter the cells.
Iis	Integrase Inhibitors	Integrase inhibitors block HIV integrase, an enzyme HIV needs to make copies of itself.
PKE	Pharmacokinetic Enhancers	Pharmacokinetic enhancers are used in HIV treatment to increase the effectiveness of an HIV medicine included in an HIV regimen.
CombD	Combination HIV Medicines	Combination HIV medicines contain two or more HIV medicines from one or more drug classes.

Combination HIV drugs	
abacavir and lamivudine (abacavir sulfate / lamivudine, ABC / 3TC)	Epzicom
abacavir, dolutegravir, and lamivudine (abacavir sulfate / dolutegravir sodium / lamivudine, ABC / DTG / 3TC)	Triumeq
abacavir, lamivudine, and zidovudine (abacavir sulfate / lamivudine / zidovudine, ABC / 3TC / ZDV)	Trizivir
atazanavir and cobicistat (atazanavir sulfate / cobicistat, ATV / COBI)	Evotaz

Combination HIV drugs (contd.)	
emtricitabine, rilpivirine, and tenofovir disoproxil fumarate (emtricitabine / rilpivirine hydrochloride / tenofovir disoproxil fumarate, emtricitabine / rilpivirine / tenofovir, FTC / RPV / TDF)	Complera
emtricitabine and tenofovir disoproxil fumarate (emtricitabine / tenofovir, FTC / TDF)	Truvada
lamivudine and zidovudine (3TC / ZDV)	Combivir
lopinavir and ritonavir (ritonavir-boosted lopinavir, LPV/r, LPV / RTV)	Kaletra

darunavir and cobicistat (darunavir ethanolate / cobicistat, DRV / COBI)	Prezcobix
efavirenz, emtricitabine, and tenofovir disoproxil fumarate (efavirenz / emtricitabine / tenofovir, efavirenz / emtricitabine / tenofovir DF, EFV / FTC / TDF)	Atripla
elvitegravir, cobicistat, emtricitabine, and tenofovir alafenamide fumarate (elvitegravir / cobicistat / emtricitabine / tenofovir alafenamide, EVG / COBI / FTC / TAF)	Genvoya
elvitegravir, cobicistat, emtricitabine, and tenofovir disoproxil fumarate (QUAD, EVG / COBI / FTC / TDF)	Stribild

COBI : Cobicistat
DRV : Darunavir
DRV/c DRV-boosted COBI
FDA : Food and Drug Administration
FTC : Emtricitabine
RTV : Ritonavir
TAF : Tenofovir alfenamide
TDF : Tenofovir disoproxil fumarate

FDCs : Fixed-dose combinations
NRTIs : Nucleoside/nucleotide RTIs
Pis : Protease inhibitors
RAM : Resistance-associated mutation
RTIs : Reverse transcriptase inhibitors
STR : Single tablet regimen.

Drug	Used in combination with	mg/day
Lamivudine	✓ zidovudine and abacavir	2 x 150
Azidothymidine		
Tenofovir disoproxil	✓ lamivudine and efavirrenz ☠ Not with lamivudine plus abacavir	1 x 300
Zalcitabine:	HIV drugs ; ☠ not with didanosine If un responsive to zidovudine	
Stavudine	✓ Advanced HIV HIV drugs	2 x 40
Didanosine	Other HIV drugs	2 x 200
Emtricitabine	✓ tenofovir disoproxil fumarate	1 x 200
disoproxil	✓ lamivudine and efavirrenz	1 x 300
Abacavir	✓ zidovudine and limivudine	2 x 300 3 x 200

APPENDIX -3
Schrodinger suit for biochemical and chemical research (SSBCR)

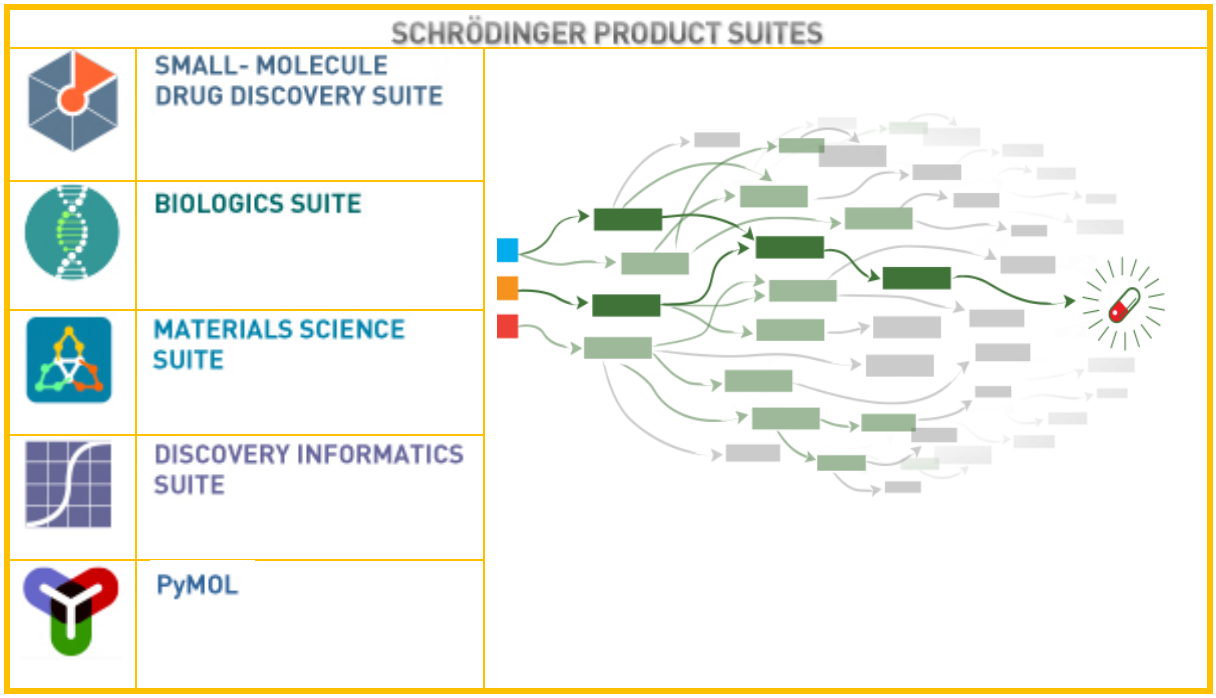

Typical features of Jaguar 8.0 version	
Hartree–Fock	RHF UHF ROHF
Density functional theory	LDA Gradient-corrected Dispersion-corrected Hybrid functionals
Local second-order Møller–Plesset perturbation theory (LMP2)	
Generalized valence bond perfect-pairing	GVB-PP GVB-LMP2 calculations
Prediction of excited states	Configuration interaction (CIS) Time-dependent DFT (TDDFT)
Geometry optimization	
Transition state search	
Solvation	Poisson–Boltzmann equation
Spectra	Infrared (IR) Nuclear magnetic resonance (NMR) Ultraviolet (UV)

Tasks in Jaguar

Computational tasks	
Optimization	Relaxed Coordinate Scan Rigid Coordinate Scan Transition State Search Reaction Coordinate Initial Guess Only
Single Point Energy	
Properties	PKa Hydrogen Bond

Chemical Tasks

- Reaction thermochemistry and reaction path exploration
- Rate constants for reactions and transport from transition state theory
- Validated models for calculating oxidation and reduction potentials
- Accurate heats of formation and atomization energies for larger systems
- Reliable properties for systems containing transition metals

	Vibrational circular dichroism (VCD) spectra
pKa prediction	
molecular surfaces	Electrostatic Potential Electron Density Molecular Orbitals
molecular properties	Multipole Moments Polarizabilities Vibrational Frequencies

- Efficient calculation of electric field dependent properties
- Prediction of vibrational and electronic spectra for complex systems
- Multiple pre-defined calculation modes representing tested simulation parameters
- Balancing speed and accuracy
- Energies and redox properties

Optoelectronics and reactive systems

- ✓ Automated calculation of complex properties, such as hole/electron reorganization
- ✓ Excited states and optical adsorption spectra
- ✓ Electronic structure and orbital visualization
- ✓ Reaction energy screening to identify systems with desired stability and activity

Transition State (TS)

The search for transition state is performed by quadratic synchronous transit (QST) or non-QST methods. The range of distances of linear synchronous transit (LST) transition-state initial guess between reactant and product geometries is 0.0 to 1.0. An eigenvector highly correlated with that followed previously or a new Eigen vector is chosen for each iteration of optimization. The transition vector is lowest Hessian eigenvector, lowest non-torsional eigenvector,lowest stretching eigenvector or eigenvector best representing reaction path.

Computation of Standard redox potential

Input : Oxidized and reduced states

- Cal CQC ground-state electronic energies at B4LYP level in vacuum
- Cal zero-point vibrational energies for the vibrational ground state (ZPE)
- Cal free energies for the thermal excited states at 298 K

	Difference of energies between reduced and oxidized states
$\Delta G°g$	vacuum
$\Delta\Delta G°sol$	Solvation
F	23.06 kcal · mol-1 V-1
N	Number of electrons transfered in redox proocess
E°_{SHE}	-4.36 eV

$$\Delta G^{\circ}_{s} = \Delta G^{\circ}_{g} + \Delta\Delta G^{\circ}_{sol}$$

$$E^{\circ} = E^{\circ}_{SHE} - \frac{\Delta G^{\circ}_{s}}{n * F}$$

Ana Patricia Ga´miz-Herna´ndez, Artur S. Galstyan, and Ernst-Walter Knapp J. Chem. Theory Comput. **2009**, 5, 2898–2908

Understanding Rubredoxin Redox Potentials: Role of H-Bonds on Model Complexes

Schrodinger modules software (SMS)

CombiGlide	Combinatorial Library Design
Glide	Ligand Docking
Impact	MD Simulation
Induced Fit	Ligand Docking
Jaguar	Quantum Mechanics
Liaison	Predicts Binding Affinity

- Small-Molecule Drug Discovery
- Biologics
- Materials Science
- Discovery Informatics
- PyMOL

LigPrep	2D to 3D Ligand Conversion
Macro-Model	Molecular Modeling
Maestro	Graphical User Interface
Phase	Pharmacophore Modeling
Prime Prime X	Protein Structure Prediction
QikProp	ADME Properties
Qsite	Reaction Mechanism (QM/MM)
Strike	Structural Activity Relationship

- Canvas
- ConfGen
- Core Hopping
- CovDOck
- Desmond
- Epik
- Fieldbased QSAR
- Induced Fit
- KNIME Extensions
- Protein preparation wizard
- QM-Polarized Ligand Docking
- Shape Screening
- SARvision | SM
- SARvision | Biologics

Dynamics of convergence process in geometric optimization by Jaguar		
Convergence.Quality	**KB**	**Indicator. Jaguar**
$$$ convergence to an optimal structure		
Monotonic		0
Non-monotonic	+ Converged to an optimal structure ++ No erratic convergence detected	1:
Erratic	! ! but optimization converged to an optimal structure	2
Convergeence to a		
Non-optimal structure **	- Abs(converged energy - minimal energy) < 0.1 kcal/mole	3
	-- Abs(converged energy - minimal energy) > 0.1 kcal/mole	4
	**Geometry optimization is NOT OK.	

Interpretation of results of convergence analysis		
If	Categories 0-2	
Then	successful convergence	
If	Category 3	
	If	optimization in solution
	Then	successful convergence
	else	Borderline convergence
	endif	
endif		
	.	
If	category 4	
Then	convergence should be scrutinized for potential problems	
	Remedy: might consider starting from a different initial guess or using different geometry optimization settings	
If	Geometry optimization is not OK &	
	numberOfImaginaryFrequencies = 0	
Then	Reoptimize geometric structure &	
	Repeat Frequency analysis with optimized structure	
While	Geometry optimization is not OK &	
	Reoptimize geometric structure	
endwhile		
While	Frequency analysis is not satisfactory	
	Repeat frequency analysis with different BS, Level theory	
endwhile		

KB. BasisSet.Jaguar		
If	User chooses basis set	
Then	Jaguar uses it	
else		
	If	basis functions for 6-31G** are available for all atoms in the molecule
	Then	Jaguar default basis set : 6-31G**
	else	LACVP** basis set
	endIf	
endIf		

If	KeyWord.GeoOpt. Optverdict = 0
Then	geometry optimization analysis disabled
If	KeyWord.GeoOpt. Optverdict = 2
Then	geometry optimization analysis for every iteration

Typical CQC packages with information regarding type of orbitals and computer language

CQC software package	Category of orbitals	Computer Language used
ABINIT	PW	Fortran
ACES	GTO	Fortran/C++
ADF	STO	Fortran
AMPAC	Unknown	Unknown
Atomistix ToolKit(ATK)	NAO/EHT	C++/Python
BigDFT	Wavelet	Fortran
CADPAC	GTO	Fortran
CASINO (QMC)	GTO / PW /	Fortran 95

CQC software package	Category of orbitals	Computer Language used
FHI-aims	NAO	Fortran
Firefly / PC GAMESS	GTO	Fortran, C,Assembly
FLEUR	FP-(L)APW+lo	Fortran 95
FreeON	GTO	Fortran 95
GAMESS (UK)	GTO	Fortran
GAMESS (US)	GTO	Fortran
Gaussian	GTO	Fortran
GPAW	Grid / NAO / PW	Python / C

	Spline / Grid / STO	
CASTEP	PW	Fortran 95/ Fortran 2003
CFOUR	GTO	Fortran
COLUMBUS	GTO	Fortran
CONQUEST	NAO/Spline	Fortran 90
CP2K	Hybrid GTO / PW	Fortran 95
CPMD	PW	Fortran
CRYSTAL	GTO	Fortran
DACAPO	PW	Fortran
DALTON	GTO	Fortran
deMon2k	GTO	Fortran
DFT++	PW / Wavelet	C++
DFTB+	NAO	Fortran 95
DIRAC	GTO	Fortran 77, Fortran 90, C
DMol3	NAO	Fortran 90
ELK	FP-LAPW	Fortran 95
Empire	Minimal STO	Fortran
ErgoSCF	GTO	C++
ERKALE	GTO	C++
EXCITING	FP-LAPW	Fortran 95

HiLAPW	FLAPW	Unknown
HORTON	GTO	Python / C++
Jaguar	GTO	Fortran / C
JDFTx	PW	C++ / CUDA
LOWDIN	GTO	Fortran 95/03
MADNESS	Wavelet	C++
MISSTEP	PW	C++
MOLCAS	GTO	Fortran
MolDS	STO/GTO	C++
MOLPRO	GTO	Fortran
MONSTERGAUSS	GTO	Fortran
MOPAC	Minimal GTO	Fortran
MPQC	GTO	C++
NRLMOL	GTO	Fortran
NTChem	GTO	Unknown
NWChem	GTO, PW	Fortran 77 / C
Octopus	Grid	Fortran 95, C,OpenCL
ONETEP	PW	Fortran
OpenAtom	PW	Charm++ (C++)
OpenMX	NAO	C
ORCA	GTO	C++

CQC software package	Category of orbitals	Computer Language used
PLATO	NAO	Unknown
PQS	Unknown	Unknown
Priroda-06	GTO	C
PSI	GTO	C / C++
PUPIL	GTO, PW	Fortran / C
PWscf[6]	PW	Fortran
PyQuante	GTO	Python
PySCF	GTO	Python
Q-Chem	GTO	Fortran / C++
QMCPACK (QMC)	GTO / PW / Spline / Grid / STO	C++ / CUDA
QSite	GTO	Unknown
Quantemol-N	GTO	Fortran

CQC software package	Category of orbitals	Computer Language used
RMG	Grid	C/C++
RSPt	FP-LMTO	Fortran / C
SCIGRESS	GTO	C++, C, Java,Fortran
Siam Quantum	GTO	C
SIESTA	NAO	Fortran
Spartan	GTO	Fortran / C / C++
TB-LMTO	LMTO	Fortran
TERACHEM	GTO	C/CUDA
TURBOMOLE	GTO	Fortran
VASP	PW	Fortran
WIEN2k	FP-(L)APW+lo	Fortran / C
Yambo Code	PW	Fortran

Quantum ESPRESSO	PW	Fortran

Appendix 4:
Classification and solution methods of mathematical equations (CSMME)

	EqnWorld (World of Eqns.)	
Eqns. Algebraic Equation Differential Difference Integral Functional	**Eqns.Algeb.** Matrix Eqns. Tensor Eqns.	**DE.** ODE PDE
PDF. Linear Non-linear Non-linear Delay	**PDF.NonLinear** First order Second order: Parabolic, Elliptical, Hyperbolic Higher order Fourth order: biharmonic, Nonhomogeneous	**PDF.solution.** Analytical Numerical Decomposition
PDF. Solution.Numerical Finite differencce Finite element Finite volume Monte Carlo Variational Spectral Method of Generalized Separation of Variables Method of Functional Separation of Variables Differential Constraints Method Nonlocal symmetries and genaration of solutions for partial differential equations	**PDF.solution.** Generalized finite element method (GFEM) Extended finite element method (XFEM) Spectral finite element method (SFEM) Meshfree finite element method Discontinuous Galerkin finite element method (DGFEM) Element-Free Galerkin Method (EFGM) Interpolating Element-Free Galerkin Method (IEFGM)	**PDF. Solution. Numerical. Spectral.Pseudospectral** **PDF. Solution.Numerical. Spectral** FFT

REFERENCES

Anti-Cancer drugs

[1] E. Lattmann, F. Low, H. Singh, M.J.Tisdale D.Kinchinaton, *Cancer Science*, **2015,** 1, 1, 1-7.
Chlorinated Pyridazin-3-(2H)-ones as Novel Anti-Cancer Agents

[2] K.Basore, Y.Cheng, A.K. Kushwaha, S.T. Nguyen S.A. Desai, *Frontiers in Pharmacology*, **2015,** 6, 91, 1-7.
How do antimalarial drugs reach their intracellular targets?

[3] O. Olayinka, Ajani, J.T. Isaac, T.F. Owoeye A.A. Akinsiku, *International Journal of Biological Chemistry*, **2015,** 9, 4, 148-177.
Exploration of the Chemistry Biological Properties of Pyrimidine as a Privilege Pharmacophore in Therapeutics

[4] C.Zhu, K.B.Nigam, R.C. Date, K.T. Bush, Stevan, Springer, M.H. Saier, Jr., W.Wu, S.K. Nigam, *PLOS ONE* ,**2015,**1-20.
Evolutionary Analysis Classification of OATs, OCTs, OCTNs, Other SLC22, Transporters: Structure-Function Implications Analysis of Sequence Motifs

[5] B. K.Douglas, *Trends in Pharmacological Sciences*, **2015,** 36, 1, 15-21.
What would be the observableconsequences if phospholipid bilayer diffusion of drugs into cells is negligible?

[6] R.S. K.Rayappa, *World Journal Of Pharmacy Pharmaceutical Sciences*, **2015,** 4, 6, 1729-1740.
Synthesis, Characterization Biological Evaluation Of 6-Amino-5-[2-(5-Substituted-2-Phenyl-1hindol-3-Yl)-4-Oxothiazolidin-3-Yl]-1,3-Dimethylpyrimidine-2,4-Dione.

[7] B.K.Douglas S.G.Oliver, *FrontiersinPharmacology | DrugMetabolismTransport*, **2014,** 5, 231.
How drugs get into cells: tested testable predictions to help discriminate between transporter-mediated uptake lipoidal bilayer diffusion

[8] Z.L.Johnson, J.H.Lee, K.Lee, M.Lee, D.Y.Kwon, J.Hong, S.Y.Lee, *Life*, **2014,** 3, 1-19.
Structural basis of nucleoside nucleoside drug selectivity by concentrative nucleoside transporters

[9] M.Mirzaei, R.S.Ahangari, *Superlattices Microstructures*, **2014,** 65, 375-379.
Formations of CNT modified 5-(halogen) uracil hybrids: DFT studies

[10] A.Meščić, S.Krištafor, I.Novaković, A.Osmanović, U. Müller, D.Završnik, S.M. Ametamey, L.Scapozza S.R.Malić, *Molecules*, **2013,** 18, 5104-5124.
C-5 Hydroxyethyl Hydroxypropyl Acyclonucleosides asSubstrates for Thymidine Kinase of Herpes Simplex VirusType 1 (HSV-1 TK): Syntheses Biological Evaluation

[11] S.Balaz, *Drug Discov Today.*, **2012,** 17, 1920, 1079-1087.
Does transbilayer diffusion have a role in membrane transport of drugs?

[12] M.Yarim, M.Koksal, I.Durmaz R.Atalay, *Int. J. Mol. Sci.*, **2012,** 392, 8071-8085.
Cancer Cell Cytotoxicities of1-(4-Substitutedbenzoyl)-4-(4-chlorobenzhydryl) piperazine Derivatives

[13] H.Sajiki, Y.Iida, K (Yasunaga) Ikawa, Y.Sawama, Y.Monguchi, Y.Kitade, Y.Maki, H.Inoue, K.Hirota, *Molecules*, **2012,** 17, 6519-6546.
Development of Diversified Methods for Chemical Modificationof the 5,6-Double Bond of Uracil Derivatives Depending on Active Methylene Compounds

[14] H.U.Istanbullu, I.A.Zupk´O, V.A.U.Un, E.C.Erc¨iyas, *Turk J Chem*, **2012,** 36, 583-592.
Synthesis cytotoxic evaluation of uracil C-MannichBases

[15] S.Baroniya, Z.Anwer, P.K. Sharma, R.Dudhe, N.Kumar, *Der Pharmacia Sinica*, **2010**, 1 (3), 172-182.
Recent advancement in imidazole as anti-cancer agents: A review

[16] R. Singh, S. Jaiswal, M. Kumar, P. Singh, G. Srivastav, R.A. Yadav, *Spectrochimica Acta*, **2010,** 75, 267–276.
DFT study of molecular geometries and vibrational characteristics of uracil and its thio-derivatives and their radical cations

[17] S. D.Shewach, R.D. Kuchta, *Chemical Reviews*, **2009,** 109, 7, 2859-2861.
Introduction to Cancer Chemotherapeutics

[18] S. Prachayasittikul, N. Sornsongkhram, R. Pingaew, A.Worachartcheewan, S.Ruchirawat V. Prachayasittiku, *Molecules*,**2009,** 14, 2768-2779.
Synthesis of N-Substituted 5-Iodouracils as Antimicrobial Anticancer Agents

[19] J.Xiong, H.F. Zhu, Y.J.Zhao, Y.J. Lan, J.W.Jiang, J.J.Yang S.F.Zhang, *Molecules*, **2009,** 14, 3142-3152.
Synthesis Antitumor Activity of Amino Acid EsterDerivatives Containing 5-Fluorouracil

[20] N.Zhang, Y.Yin, S.J.Xu W.S.Chen, *Molecules*, **2008,** 13, 1551-1569.
5-Fluorouracil: Mechanisms of Resistance Reversal Strategies

[21] V.E. Semenov, A.D. Voloshina, E.M. Toroptzova, N.V. Kulik, V.V. Zobov, R.K. Giniyatullin, A.S. Mikhailov, A.E. Nikolaev, V.D. Akamsin, V.S. Reznik, *European Journal of Medicinal Chemistry*, **2006,** 41, 1093–1101.
Antibacterial antifungal activity of acyclic macrocyclic uracilderivatives with quaternized nitrogen atoms in spacers

[22] Z. Brzozowski, F. S.Czewski, M. Gdaniec, *Eur. J. Med. Chem.*, **2002,** 37, 285-293.
Synthesis, molecular structure anticancer activity of1-allyl-3-amino-2-(4-chloro-2-mercapto benzenesulphonyl) guanidine derivatives

[23] K.H.Lee, B.R.Huang, C.C. Tzeng, *Bioorganic & Medicinal Chemistry Letters*, 9 (1999) 241-244, **1999,** 9, 241-244.
Synthesis anticancer evaluation of certain c-methylene-t-(4-substituted phenyl)-y-butyrola ctone bearing thymine, uracil, 5-bromouracil

[24] J.L.Bernier, J.Pierre, H.Bnichart, V.Warin, C.Trentesaux, J.C.Jardilliero, *Journal of Medicinal Chemistry*, **1985,** 28, 4, 497-502.
5-Cinnamoyl-6-aminouracil Derivatives as Novel Anticancer Agents. Synthesis, Biological Evaluation, Structure-Activity Relationships

Drugs for HIV

[25] S. N.Mikhail, R.W.Buckheit Jr., K.Temburnikar, A.L. Khazhinskaya, A.V.Ivanov, K.L.Seley-Radtke,*Bioorganic & Medicinal Chemistry*, **2010,** 18, 8310-8314.
1-Benzyl derivatives of 5-(arylamino) uracils as anti-HIV-1 anti-EBV agents

[26] Y.Yoshimura, Y.Yamazaki, Y.Saito, Y.Natori, T.Imamichi, H.Takahata, Bioorganic & Medicinal Chemistry Letters, **2011,** 21, 3313-3316.
Synthesis of 5-thiodidehydropyranylcytosine derivatives as potential anti-HIVAgents

[27] O.Putcharoen, T.Do, A.Avihingsanon, K.Ruxrungtham, Drug Design, Development Therapy, **2015,** 9, 5763-5769.
Rationale clinical utility of the darunavir–cobicistat combination in the treatment of HIV /AIDS

[28] A.Pałasz, D.Cie_, European Journal of Medicinal Chemistry, **2015,** 97, 582-611.

In search of uracil derivatives as bioactive agents. Uracils fused uracils: Synthesis, biological activity applications

[29] V.Malik, P.Singh S.Kumar, Tetrahedron, **2006,** 62, 5944-5951.
Unique chlorine effect in regioselective one-pot synthesis of 1-alkyl-/allyl-3-(o-chlorobenzyl) uracils: anti-HIV activity of selected uracil derivatives

[30] N.Sakakibara, T.Hamasaki, M.Baba, Y.Demizu, M.Kurihara, K.Irie, M.Iwai, E.Asada, Y.Kato, T.Maruyama, Bioorganic & Medicinal Chemistry, **2013,** 21, 5900-5906.
Synthesis evaluation of novel 3-(3,5-dimethylbenzyl)uracil analogs as potential anti-HIV-1 agents

[31] G.Ghasemi, M.Nirouei, S.Shariati, P.Abdolmaleki, Z.Rastgoo, Arabian Journal of Chemistry.
A quantitative structure–activity relationship studyon HIV-1 integrase inhibitors using genetic algorithm, artificial neural networks different statistical methods

[32] B.Barmana, A.Mukhopadhyay, Procedia Technology, **2013,** 10, 450-456.
Construction of GA-optimized Radial Basis Neural Network from HIV-1 Vpr Mutant Microarray Gene Expression Data

[33] R.Darnag, B.Minaoui, M.Fakir, Arabian Journal of Chemistry, **2014,** Doi: 10.1016/j. arabjc. 2012. 10.021
QSAR models for prediction study of HIV protease inhibitors using support vector machines, neural networks multiple linear regression

Schrodinger

Application of Jaguar in bio-chemical material science research

[34] N. A. Migues, Adina Muskat, Scott M. Auerbach, W. Sherman, S. Vaitheeswaran, Catal., **2015,** 5, 2859−2865.
On the Rational Design of Zeolite Clusters

[35] Horbert R, B Pinchuk, E Johannes, J Schlosser, D Schmidt, D Cappel, F Totzke, C Schächtele, C Peifer *J Med Chem*, **2015**, 58, 1, 170–182.
Optimization of Potent DFG-in Inhibitors of Platelet Derived Growth Factor Receptorβ (PDGF-Rβ) Guided by Water Thermodynamics

[36] I. T.Brohman, W. Sherman; M. Repasky; T. Beuming, *J. Chem. Inf. Model.*, **2015**, 53, 7, 1689-1699.
Improved docking of polypeptides with Glide

[37] D. Cappel, S.L Dixon, W. Sherman, J.Duan, *J. Comput. Aided Mol. Des.*, **2015**, 29, 2 165-182.
Exploring conformational search protocols for lig-based virtual screening 3-D QSAR modeling

[38] M. Unger; AM Eichhoff; L Schumacher; M Strysio; M Menzel,; C Schwan; V Alzogaray; V Zylberman; M Seman,; J Brner; H Rohde,; K Zhu,; F Haag,; H Mittrücker,; F Goldbaum,; K Aktories; F K. Nolte, *Scientific Reports*, **2015**, 7850, 5 1-10.
Selection of Nanobodies that Block the Enzymatic Cytotoxic Activities of the Binary Clostridium Difficile Toxin CDT

[39] A. Chatterjee; S.J Cutler; R.J Doerksen; I.A Khan; J.S Williamson, *Bioorg. Med. Chem*, **2014**, 22, 6409-6421.
Discovery of thienoquinolone derivatives as selective ATP non-competitive CDK5/p25 inhibitors by structure-based virtual screening

[40] D.J.Weldon; F.Shah; A.G.Chittiboyina; A. Sheri; R.R.Chada; J.Gut; P.J.Rosenthal, D. Shivakumar; W.Sherman,; P.Desai; J. C. Jung; A.M.Avery *Bioorg. Med. Chem. Lett*, **2014**, 24, 5, 1274-1279.

Synthesis, biological evaluation, hydration site thermodynamics, chemical reactivity analysis of α-keto substituted peptidomimetics for the inhibition of Plasmodium falciparum

[41] D. Wang; O. Wiest; P.Helquist; H. L. Hargest; N.L.Wiech, *Bioorg. Med. Chem. Lett.*, **2014**, 14, 707-711.
QSAR studies of PC-3 cell line inhibition activity of TSA SAHA-like hydroxamic acids

[42] A.I. Foudah; A.A Sallam; M.R Akl; K.A.El Sayed, *Eur. J. Med. Chem*, **2014**, 73, 310-324.
Optimization, pharmacophore modeling 3D-QSAR studies of sipholanes as breast cancer migration proliferation inhibitors

[43] MR. A.I.Foudah; H.Y. Ebrahim; S.A.Meyer; K.A.E. Sayed, *Mar. Drugs*, **2014**, 12, 6, 2282-2304.
The marine-derived sipholenol A-4-O-3′,4′-dichlorobenzoate inhibits breast cancer growth motility in vitro in vivo through the suppression of Brk FAK signaling

[44] G. Madhavi Sastry, V. S. Seep Inakollu, Woody Sherman, *J. Chem. Inf. Model.*, **2013,** 53, 1531−1542.
Boosting Virtual Screening Enrichments with Data Fusion: Coalescing Hits from Two-Dimensional Fingerprints, Shape, Docking

[45] D. A Bochevarov, E T F Harder, Hughes, J R. Greenwood, D A. Braden, D M. Philipp, D Rinaldo, M D. Halls, J Zhang, R A. Friesner, *International Journal of Quantum Chemistry*, **2013,** 113, 2110–2142.
Jaguar: A High-Performance Quantum Chemistry Software Program with Strengths in Life Materials Sciences

[46] B. Breiten, MR Lockett, W Sherman, S Fujita, M Al-Sayah, H Lange, CM Bowers, A Heroux, G Krilov, GM.Whitesides, *J Am Chem Soc* ,**2013**, 135, 41, 15579–15584.
Water networks contribute to enthalpy/entropy compensation in protein-lig binding

[47] G.M. Sastry; V.S Inakollu; W Sherman, *J. Chem. Inf. Model*, 2013, 53, 1531-1542.
Boosting virtual screening enrichments with data fusion: Coalescing hits from two-dimensional fingerprints, shape, docking

[48] D. Pala; T Beuming; W Sherman; A Lodola; S Rivara; M Mor, *J. Chem. Inf. Model*, 2013, 53, 4 821-835.
Structure-based virtual screening of MT_2 melatonin receptor: Influence of template choice structural refinement

[49] C. J. Hillar, LH Lim, Journal of the ACM, **2013,** 60, 645.
Most Tensor Problems Are NP-Hard

[50] V.Myrianthopoulos; M. Kritsanida; N. G. Kolar; P. Magiatis; Y. Ferin; E. Durieu; O. Lozach; D. Cappel;M. Soundararajan; P. Filippakopoulos; W. Sherman; S. Knapp; L.Meijer; E. Mikros; A.L.Skaltsounis, *Med Chem Lett*, 2013, 4, 122-26.
Novel inverse binding mode of indirubin derivatives yields improved selectivity for DYRK kinases

[51] A.A. Sallam; W.E Houssen; C.R.Gissendanner; K.Y. Orabi; A.I Foudah; K.A El Sayed, *Med. Chem. Commun*, **2013**, 4, 1360-1369.
Bioguided discovery pharmacophore modeling of the mycotoxic indole diterpene alkaloids penitrems as breast cancer proliferation, migration, invasion inhibitors

[52] D H. Mathew, P. J Djurovich, D. J Giesen, A. Goldberg, J.Sommer, E. McAnally, M. E Thompson, New Journal of Physics, **2013,** 15, 105029-105044.
Virtual screening of electron acceptor materialsfor organic photovoltaic applications

[53] R.A. Pearlstein, W Sherman, R Abel.*Proteins*, **2013**, 81, 9 1509–1526.

Contributions of water transfer energy to protein-lig association dissociation barriers

[54] Q.T. Tran; S. Williams; R. Farid; G. Erdemli; R.Pearlstein*Proteins*, **2013**, 81, 2, 291-299.
The translocation kinetics of antibiotics through porin OmpC: Insights from structure-based solvation mapping using WaterMap

[55] J. Fu; P Si; M Zheng; L Chen; X Shen; Y Tang; W Li, *Bioorg. Med. Chem. Lett*, **2012**, 22, 6848-6853.
Discovery of new non-steroidal FXR ligs via a virtual screening workflow based on Phase shape induced fit docking

[56] A. Galstyan, A. Robertazzi, E. W. Knapp, *J. Am. Chem. Soc*., **2012,** 134, 7442−7449.
Oxygen-Evolving Mn Cluster in Photosystem II: The ProtonationPattern Oxidation State in the High-Resolution Crystal Structure

[57] F. Shah; G. Jiri; J. Legac; D. Shivakumar; W. Sherman; P.J. Rosenthal; M.Avery, *J. Chem. Inf. Model*, **2012**, 52, 3, 696-710.
Computer-aided drug design of falcipain inhibitors: Virtual screening, structure-activity relationships, reactivity analysis

[58] O. Kalid, D.T.Warshaviak, S Shechter.; W, Sherman, S. Shacham, *J. Comput.Aided Mol. Des.*, **2012**, 26, 1217–1228.
Consensus Induced Fit Docking (cIFD): Methodology, validation, application to the discovery of novel Crm1 inhibitors

[59] D. Lupyan, Y.A Abramov, W Sherman, *J. Comput. Aided Mol. Des*,**2012,** 26, 1195-1205.
Close intramolecular sulfur–oxygen contacts: Modified force field parameters for improved conformation generation

[60] A.H.Newman; T. Beuming; A.K. Banala; P. Donthamsetti; K. Pongetti; A. L. Bounty; B. Levy; J. Cao; M. Michino; R.P. Luedtke; J.A.Javitch; L. Shi, *J. Med. Chem*, **2012**, 55, 15, 6689–6699.
Molecular determinants of selectivity efficacy at the dopamine D3 receptor

[61] M.A. Brodney; G Barreiro; K Ogilvie; E H. Korcsok; J Murray ; F Vajdos; C Ambroise; C Christoffersen; K Fisher; L Lanyon; J Liu; C. E Nolan;, J. M Withka; K. A Borzilleri;, I Efremov; C. E Oborski; A Varghese; B O'Neill, *J. Med. Chem*, **2012**, 55, 9224-39.
Spirocyclic sulfamides as β-secretase 1 (BACE-1) inhibitors for the treatment of Alzheimer's disease: Utilization of structure based drug design, WaterMap, CNS penetration studies to identify centrally efficacious inhibitors

[62] M.C. Lousada, A.J, Johansson, T Brinck, M Jonsson, *J. Phys. Chem. C.*, **2012,** 116, 9533–9543.
Mechanism of H_2O_2 decomposition on transition metal oxide surfaces

[63] R. C. Liu, L. Panetta, P. Yang, Journal of Quantitative Spectroscopy & Radiative Transfer, **2012,** 113, 1728-1740.
Application of the pseudo-spectral time domain method to compute particle single-scattering properties for size parameters up to 200

[64] C. Coletti, L. Gonsalvi, A. Guerriero, L. Marvelli, M. Peruzzini, G. Reginato, N. Re Organometallics, **2012,** 31, 57-69.
Electron-Poor Rhenium Allenylidenes Their Reactivity toward Phosphines: A Combined Experimental Theoretical Study

[65] H Fu, Blacksburg, Virginia Ph.D. thesis, **2012.**
Modeling of Plasma Irregularities Associated with Articially Created Dusty Plasmas in the Near-Earth Space Environment

[66] T.F. Hughes, J. N Harvey, R. A. Friesner, *Phys. Chem. Chem. Phys.*, **2012,** 14, 7724-7738.
A B3LYP-DBLOC empirical correction scheme for lig removal enthalpies of transition metal complexes: Parameterization against experimental CCSD(T)-F12 heats of formation

[67] Q.T.Tran, S Williams, R Farid, G Erdemli, R Pearlstein, *Proteins*, **2012**, 81, 2, 291-299.
The translocation kinetics of antibiotics through porin OmpC: Insights from structure-based solvation mapping using watermap

[68] T. Beuming; Y Che; R Abel; B Kim; V Shanmugasundaram; W Sherman, *Proteins*, **2012**, 80, 871-83.
Thermodynamic analysis of water molecules at the surface of proteins applications to binding site prediction characterization

[69] R. Abel, N.K.Salam, J.Shelley, R. Farid, R.A. Friesner, W. Sherman, *Chem Med Chem*, **2011**, 6 1049-1066.
Contribution of explicit solvent effects to the binding affinity of small-molecule inhibitors in blood coagulation factor serine proteases

[70] K. Ohno, K Mori, M Orita, M Takeuchi, *Curr. Med. Chem*, 2011, 18, 220-233.
Computational Insights into Binding of Bisphosphates to Farnesyl Pyrophosphate Synthase

[71] R. R. Naredla, C. Zheng, S.O. N. Lill, D. A. Klumpp, *J. Am. Chem. Soc*., **2011,** 133, 13169–13175.
Charge Delocalization Enhanced Acidity in Tricationic Superelectrophiles

[72] L. Klaić, P.C Trippier, R. K Mishra, R.I Morimoto, R.B Silverman, *J. Am. Chem. Soc*., **2011,** 133, 19634–19637.
Remarkable Stereospecific Conjugate Additions to the Hsp90 Inhibitor Celastrol

[73] T.H. Yu, Y Sha, W.G Liu, B.V Merinov, P Shirvanian, W.A Goddard, J. Am. Chem. Soc., **2011,** 133, 19857–19863.
Mechanism for Degradation of Nafion in PEM Fuel Cells from Quantum Mechanics Calculations

[74] D. Wu, Q. Wang, R.S. Assary, L.J. Broadbelt, G. Krilov, *J. Chem. Inf. Model*, **2011**, 51, 1634-47.
A computational approach to design evaluate enzymatic reaction pathways: application to 1-butanol production from pyruvate

[75] G.M. Sastry, S.L.Dixon, W. Sherman, *J. Chem. Inf. Model*, 2011, 51, 2455-2466.
Rapid Shape-Based Lig Alignment Virtual Screening Method Based on Atom/Feature-Pair Similarities Volume Overlap Scoring

[76] S. Durdagi,, H.J Duff., S.Y Noskov, *J. Chem. Inf. Model*, 2011, 51, 463-74.
Combined receptor lig-based approach to the universal pharmacophore model development for studies of drug blockade to the hERG1 pore domain

[77] J. Du, H Sun, L Xi, J L., Y Yang, H Liu, X Yao. *J. Comp. Chem*, 2011, 32, 13 2800-2809.
Molecular modeling study of checkpoint kinase 1 inhibitors by multiple docking strategies Prime / MM-GBSA calculation

[78] J.D.Charrier, A. Miller., D. P. Kay, G. Brenchley, H.C.Twin, P.N.Collier, S.Ramaya, S.B. Keily., S.J. Durrant, R. M. Knegtel, R. M*J. Med. Chem*, **2011**, 54, 2341-2350.
Discovery structure-activity relationship of 3-aminopyrid-2-ones as potent selective interleukin-2 inducible T-cell kinase (Itk) inhibitors

[79] F. Caporuscio, G Rastelli, C.Imbriano, A D. Rio, *J. Med. Chem*, **2011**, 54, 4006–4017.
Structure-based design of potent aromatase inhibitors by high-throughput docking

[80] H.M.H.G. Albers, L.J.D. Hendrickx, R.J.P van Tol, J Hausmann,, A Perrakis, H Ovaa, *J. Med. Chem*, **2011**, 54, 4619-26.
Structure-based design of novel boronic acid-based inhibitors of autotaxin

[81] A.D. William, A.C.-H Lee, S Blanchard, A.Poulsen, E.L Teo, H Nagarajet al, *J. Med. Chem*, **2011**, 54, 4638-4658.
Discovery of the macrocycle 11-(2-Pyrrolidin-1-yl-ethoxy)-14,19-dioxa-5,7,26-triaza-tetra cyclo [19.3.1.1(2,6).1(8,12)]heptacosa-1(25),2(26),3,5,8,10,12(27),16,21,23-decaene (SB1518), a potent Janus kinase 2/fms-Like tyrosine kinase-3 (JAK2/FLT3) Inhibitor for the treatment of myelofibrosis lymphoma

[82] V. S. Bryantsev, V. Giordani, W. Walker, M. Blanco, S. Zecevic, K. Sasaki, J. Uddin, D. Addison, G. V. Chase, *J. Phys. Chem. A*, **2011,** 115, 12399–12409.
Predicting Solvent Stability in Aprotic Electrolyte LiAir Batteries: Nucleophilic Substitution by the Superoxide Anion Radical (O2•)

[83] T.F. Hughes, R.A., Friesner, *J. Phys. Chem. B*, **2011,** 115, 8597-8608.
"(rac)-1, 1'-binaphthyl-based simple receptors designed for fluorometric discrimination of maleic fumaric acids"

[84] R. E Pellicciari. Camaioni, A.M. Gilbert, A. Macchiarulo, J.A.Bikker, F.Shah, J. Bard, G. Costantino, A. Gioiello, G.M. Robertson et al, *Med. Chem. Commun*, **2011**, 2, 559-565.
Discovery characterization of novel potent PARP-1 inhibitors endowed with neuroprotective properties: From TIQ-A to HYDAMTIQ,"

[85] R. M.A. Knegtel, D.D.Robinson, *Mol. Inf*, 2011, 30, 950–959.
A role for hydration in interleukin-2 inducible T-cell kinase (Itk) selectivity

[86] P.W.Snyder, J. Mecinović, D.T.Moustakas, MR. SW. Thomas III, M.Harder, E.T.Mack, MR Lockett, A Héroux, W Sherman, G M Whitesides *PNAS*, 2011, 108, 17889-17894.
Mechanism of the hydrophobic effect in the biomolecular recognition of arylsulfonamides by carbonic anhydrase

[87] D.D.Robinson, W. Sherman, R. Farid *Chem Med Chem*, 2010, 5, 618-627.
Understing kinase selectivity through energetic analysis of binding site waters

[88] A. D. Bochevarov, R. A. Friesner, S. J. Lippard, *J Chem Theory Comput*, **2010,** 6, 123735–3749.
The prediction of 57Fe Mössbauer parameters by the densityfunctional theory: a benchmark study

[89] T. Wang, G. Brudvig, V. S. Batista, *J Chem Theory Comput*, **2010,** 29, 3755–760.
Characterization of proton coupled electron transfer in abiomimetic oxomanganese complex: Evaluation of the DFTB3LYP level of theory

[90] I. Kendrick, D. Kumari, A. Yakaboski, N. Dimakis, E. S. Smotkin, *J. Am. Chem. Soc*., **2010,** 132, 917611–17616.
Elucidating the Ionomer-Electrified Metal Interface

[91] C.R. Guimarães, A M Mathiowetz, *J. Chem. Inf. Model*, 2010, 50, 547-559.
Addressing limitations with the MM-GB/SA scoring procedure using the WaterMap method free energy perturbation calculations

[92] R.Abel, L Wang, R.A.Friesner, B.J. Berne, *J. Chem. Theory Comput*, 2010, 6 2924-2934.
A displaced-solvent functional analysis of model hydrophobic enclosures

[93] H. D. King, Z Meng, J. A. Deskus, C.P. Sloan, Q Gao, B R. Beno, E S. Kozlowski, M. A. LaPaglia, G. K. Mattson, T. F. Molski, M. T. Taber, N. J. Lodge, R. J. Mattson, J. E. Macor, *J. Med. Chem.*, **2010,** 53, 7564–7572.

Conformationally Restricted Homotryptamines. Part 7: 3-cis-(3-Aminocyclopentyl)indolesAs Potent Selective Serotonin Reuptake Inhibitors

[94] J. E. Chrencik, A Patny, I. K Leung, B Korniski, T.L. Emmons, T Hall, R.A Weinberg, J A,Gormley. J.M Williams, J. E Day et al, *J. Mol. Biol*, 2010, 400, 413-433.
Structural thermodynamic characterization of the TYK2 JAK3 kinase domains in complex with CP-690550 CMP-6

[95] E. Farber, J. Herget, Jose A. Gascon, A. R. Howell, *J. Org. Chem*., **2010,** 75, 7565–7572.
Unexpected Cleavage of 2-Azido-2-(hydroxymethyl)oxetanes: Conformation Determines Reaction Pathway?

[96] V. Georgiev, H. Noack, T. Borowski, R. A. Margareta, Blomberg, P. E. M. Siegbahn, *J. Phys. Chem. B*, **2010,** 114, 5878–5885.
DFT Study on the Catalytic Reactivity of a Functional Model Complex forIntradiol-Cleaving Dioxygenases

[97] I. Chen, N.Foloppe, *J.Chem. Inf. Model*, 2010, 50, 822-839.
Drug-like Bioactive Structures Conformational Coverage with the LigPrep/ConfGen Suite: Comparison to Programs MOE Catalyst

[98] R.A. M Blomberg, Per E. M. Siegbahn, *Journal of Computational Chemistry*, **2010,** 27, 121374-1384.
Quantum Chemistry Applied to the Mechanisms of Transition Metal Containing Enzymes—Cytochrome c Oxidase, a Particularly Challenging Case.

[99] C. Higgs, T. Beuming, W.Sherman, *Med. Chem. Lett*, **2010**, 1, 160-164.
Hydration site thermodynamics explain SARs for Triazolylpurines Analogues Binding to the A2A Receptor

[100] D.J.Huggins, G.J. McKenzie, D.D.Robinson, A.J. Narváez, B. Hardwick, M. R. Thomson, A.R.Venkitaraman, G.H. Grant, M.C.Payne, *PLoS Comput. Biol*, **2010,** 8, e1000880.
Computational analysis of phosphopeptide binding to the polo-box domain of the mitotic kinase PLK1 using molecular dynamics simulation

[101] L. Wang, B. J Berne, R. A Friesner, *Proc. Natl. Acad. Sci. U S A*, **2010**, 108, 1326-30.
Lig binding to protein-binding pockets with wet dry regions

[102] S. Han, R.P. Zaniewski, E.S.Marr, B. M Lacey, A. P Tomaras, A Evdokimov, J. R Miller, V Shanmugasundaram, *Proc. Natl. Acad. Sci. U S A*, **2010**, 107, 22002-7.
Structural basis for effectiveness of siderophore-conjugated monocarbams against clinically relevant strains of Pseudomonas aeruginosa

[103] R. A. Pearlstein, Q.Y Hu, J Zhou, D Yowe, J Levell, B Dale, V.K. Kaushik, D Daniels, S Hanrahan, W Sherman, R Abel *Proteins*, **2010**, 78, 2571-2586.
New hypotheses about the structure-function of proprotein convertase subtilisin/kexin type 9: Analysis of the epidermal growth factor-like repeat A docking site using WaterMap

[104] J. F.Recio, M.J.E.Sternberg, *Proteins*, **2010**, 78, 3065-3066.
The 4th meeting on the Critical Assessment of Predicted Interaction (CAPRI) held at the Mare Nostrum, Barcelona

[105] Z Pipirou, V Guallar, J Basran, C L. Metcalfe, E J. Murphy, A R. Bottrill, S C. Mistry, E L Raven, Biochemistry, **2009,** 48, 3593–3599.
Peroxide-Dependent Formation of a Covalent Link between Trp51 the Heme in Cytochrome c Peroxidase

[106] S. T. Schneebeli, M. L. Hall, R. Breslow, R.Friesner J. Am. Chem. Soc., **2009,** 131, 3965–3973.
Quantitative DFT Modeling of the Enantiomeric Excess for Dioxirane-Catalyzed Epoxidations

[107] L. Wang, R Abel, R Friesner, B. J Berne *J. Chem. Theory Comput*, **2009**, 5, 1462-1473.
Thermodynamic Properties of Liquid Water: An Application of a Nonparametric Approach to Computing the Entropy of a Neat Fluid

[108] A. Patricia G. Herna´ndez, Artur S. Galstyan, E.W Knapp J. Chem. Theory Comput., **2009,** 5, 2898–2908.
Understing Rubredoxin Redox Potentials: Role of H-Bonds on Model Complexes

[109] L Tian R A. Friesner, *J. Chem. Theory Comput*, **2009,** 5, 1421–1431.
QM/MM Simulation on P450 BM3 Enzyme Catalysis Mechanism

[110] R.P.Clausen,, P.Naur., A.S. Kristensen, J.R.Greenwood, M.Strange, H.B.Osborne, A.A. Jensen, A.S. Nielsen, U. Geneser, L.M. Ringgaard et.al*J. Med. Chem*, **2009**, 52, 4911-4922.
The glutamate receptor GluR5 agonist (S)-2-amino-3-(3-hydroxy-7,8-dihydro-6H-cyclohepta[d]isoxazol-4-yl)propionic acid the 8-methyl analogue: synthesis, biostructural characterization

[111] S´ Katarzyna widerek, A Panczakiewicz, A Bujacz, G Bujacz, P Paneth, *J. Phys. Chem. B*, **2009,** 113, 12782–12789.
Modeling of Isotope Effects on Binding Oxamate to Lactic Dehydrogenase

[112] T. Wang R. A. Friesner, *J. Phys. Chem. C*, **2009,** 113, 2553–2561.
Computational Modeling of the Electronic Structure of Oligothiophenes with Various Side Chains

[113] T. Beuming, R. Farid W. Sherman *Protein Sci*, **2009**, 18, 1609-1619.
High-energy water sites determine peptide binding affinity specificity of PDZ domains

[114] G.Y. Chuang, D. Kozakov, R. Brenke, S.R. Comeau, S. Vajda *Biophys. J*, **2008**, 95, 4217-4227.
DARS (Decoys As the Reference State) Potentials for Protein-Protein Docking

[115] R. Abel, T.Young, R. Farid, B.J. Berne, R.A. Friesner, *J Am Chem Soc*, **2008**, 130, 2817-2831.
The role of the active-site solvent in the thermodynamics of factor Xa lig binding

[116] W. Brooks, K Daniel, S Sung, W Guida, *J. Chem. Inf. Model*, **2008**, 48, 639-645.
Computational Validation of the Importance of Absolute Stereochemistry in Virtual Screening

[117] C. Ko, D.K Malick, D.A Braden, R.A Friesner, T.J Martínez J. Chem. Phys, **2008,** 128, 104103-104111.
Pseudospectral time-dependent density functional theory

[118] A.C. Good, T. I.Oprea, *J. Comput.Aided Mol. Des*, **2008**, 22, 169-178.
Optimization of CAMD techniques 3. Virtual screening enrichment studies: a help or hindrance to tool selection

[119] Y Wang, O Haze, J P. Dinnocenzo, S Farid, R S. Farid, I R. Gould, *J. Phys. Chem. A*, **2008,** 112, 13088–13094.
Bonded Exciplex Formation: Electronic Stereoelectronic Effects

[120] A. D. Pissarnitski, T Asberom, T A. Bara, A V. Buevich, J W. Clader, W J. Greenlee, H. S. Guzik, H. B. Josien, W. Li, M. McEwan, B. A. McKittrick, T. L. Nechuta, E. M. Parker, L. Sinning, E. M. Smith, L. Song, H. A. Vaccaro, J. H. Voigt, L. Zhang, Q. Zhangd Z. Zhao Bioorganic & Medicinal Chemistry Letters, **2007,** 17, 57–62.
2, 6-Disubstituted N-arylsulfonyl piperidines as c-secretase inhibitors

[121] A. J Keith, D C. Behenna, J T. Mohr, S Ma, S C. Marinescu, J Oxgaard, B M. Stoltz, W A. Goddard, *J. Am. Chem. Soc.*,**2007,** 129, 11876-11877.

The Inner-Sphere Process in the Enantioselective Tsuji Allylation Reactionwith (S)-t-Bu-phosphinooxazoline Ligs

[122] J. Quinn, F Foss, L Venkataraman., M Hybertsen., R Breslow, *J. Am. Chem. Soc*., **2007,** 129, 6714-6715.
Single-Molecule Junction Conductance through Diaminoacenes

[123] G. Barreiro, C.R.W. Guimaraes, I. T.Brohman, T.M.Lyons, J. T.Rives, W.L. Jorgensen*J. Chem. Inf. Model*, **2007**, 47, 2416-2428.
Search for Non-Nucleoside Inhibitors of HIV-1 Reverse Transcriptase Using Chemical Similarity, Molecular Docking, MM-GB/SA Scoring

[124] M. Hao, O Haq, I Muegg, *J. Chem. Inf. Model*, **2007,** 47, 2242-2252.
Torsion angle preference energetics of small-molecule ligs bound to proteins

[125] P.K. Gadakar, S. Phukan, P. Dattatreya, V.N.Balaji, *J. Chem. Inf. Model*., 2007, 47, 1446-1459.
Pose prediction accuracy in docking studies enrichment of actives in the active site of GSK-3β

[126] A.Bortolato, S. Moro, *J. Chem. Info. Model*, **2007**, 47, 572-582.
In silico binding free energy predictability by using the linear interaction energy (LIE) method: bromobenzimidazole CK2 inhibitors as a case study

[127] C.Dzierba, A. Tebben, R. Wilde, A. Takvorian, M.Rafalski, P.K. Polam, J.D.Klaczkiewicz, A.D.Pechulis, A.L.Davis, M.P.Sweet, A.M.Woo, Z.Yang, S.M.Ebeltoft, T.F.Molski, G.Zhang, R.C.Zaczek, G.L.Trainor, A.P. Combs, Gil, *J. Med. Chem*, **2007**, 50, 2269-2272.
Dihydropyridopyrazinones Dihydropteridinones as Corticotropin-Releasing Factor-1 Receptor Antagonists: Structure-Activity Relationships Computational Modeling

[128] A Szczepanska, J L Espartero, A J. M Vargas, A T. Carmona, I Robina, *J. Org. Chem*., **2007,** 72, 6776-6785.
Synthesis Conformational Analysis of Novel Trimeric Maleimide Cross-Linking Reagents

[129] Y. Wang, O.Haze, J.P Dinnocenzo., S Farid., R.S Farid, I.R Gould, *J. Org. Chem*., **2007,** 72, 6970-6981.
Bonded Exciplexes. A New Concept in Photochemical Reactions

[130] C. Berrios, G C. Jiron, J Marco, C Gutierrez, M. U. Zanartu, *J. Phys. Chem. A*, **2007,** 111, 2706-2714.
Theoretical Spectroscopic Study of Nickel(II) Porphyrin Derivatives

[131] M J Cheng, K Chenoweth, J Oxgaard, A van Duin, W A. Goddard, *J. Phys. Chem. C*, **2007,** 111, 5115-5127.
Single-Site Vanadyl Activation, Functionalization, Reoxidation Reaction Mechanism for Propane Oxidative Dehydrogenation on the Cubic V4O10 Cluster

[132] K. Siddiquee, S Zhang, W.C Guida, M.A Blaskovich, B Greedy, H.R Lawrence, M.L Yip, R Jove, M.M McLaughlin, N.J Lawrence, S.M Sebti, Turkson, *J. Proc. Natl. Acad. Sci.*,2007, 104, 7391–7396.
Selective chemical probe inhibitor of Stat3, identified through structure-based virtual screening, induces antitumor activity

[133] L. Venkataraman, Y Park, A Whalley, C Nuckolls, M Hybertsen, M Steigerwald, Nano Letter, **2007,** 7, 502-506.
Electronics Chemistry: Varying Single-Molecule Junction Conductance Using Chemical Substituents

[134] J. B Jordan, M A. Pollier, L A. Miller, C Tiernan, G Clavier, P Audebert, V M. Rotello, *Org. Lett*., **2007,** 9, 152835-2538.
Redox-Modulated Recognition ofTetrazines Using Thioureas

[135] S. Hagmayer, A Früh, T Haas, M Drexler, H, Fischer, *Organometallics*, **2007,** 26, 3791-3801.
Unprecedented Formation of Azulenylidene Ligs by Reaction of the Vinylidene Lig in Arylvinylidene Pentacarbonyl Complexes of Chromium Tungsten with Alkoxyacetylenes

[136] M. Dede, M Drexler, H Fischer, *Organometallics*, **2007,** 26, 4294-4299.
Heptahexaenylidene Complexes: Synthesis Characterization of the First Complexes with an M=C=C=C=C=C=C=CR2 Moiety (M = Cr, W)

[137] T. Young, R.Abel, Kim, B., B.J Berne, R.A Friesner, *Proc. Natl. Acad. Sci (U S A)*, 2007, 104, 808-813.
Motifs for molecular recognition exploiting hydrophobic enclosure in protein–lig binding

[138] W.L.Jorgensen, J. R. Caro., J. T. Rives, A. Basavapathruni,, K.S. erson, A.D. Hamilton, *Bioorg. Med. Chem. Lett*, 2006, 16, 663-667.
Computer-aided design of non-nucleoside inhibitors of HIV-1 reverse transcriptase

[139] S. Wang, Z. Wu, Y. Cheng, L. Da, Computational Methods In Engineering Science EPMESC X, **2006,** 942-945.
The Pseudo-spectral Method Matlab Implement

[140] S. Werner, P. Iyer, M.Fodor, C.Coleman, L.Twining, B.Mitasev, K.M.Brummond, *J. Comb. Chem*, 2006, 8, 368-380.
Solution-Phase Synthesis of a Tricyclic Pyrrole-2-Carboxamide Discovery Library Applying a Stetter-Paal-Knorr Reaction Sequence

[141] V. Kenyon, I Chorny, W Carvajal, T Holman, M. Jacobson, *J. Med. Chem*, 2006, 49, 1356-1363.
Novel Human Lipoxygenase Inhibitors Discovered Using Virtual Screening with Homology Models

[142] R.A. Margareta, Blomberg, Per E. M. Siegbahn, *Journal of Computational Chemistry*, **2006,** 27, 1373–1384.
Quantum Chemistry Applied to the Mechanismsof Transition Metal Containing Enzymes—Cytochromec Oxidase, a Particularly Challenging Case

[143] E.M. Per Siegbahn, M Lundberg, *Journal of Inorganic Biochemistry*, **2006,** 100, 1035–1040.
Hydroxide instead of bicarbonate in the structure ofthe oxygen evolving complex

[144] D.Kozakov, R.Brenke, S.R. Comeau, S. Vajda, *Proteins*, 2006, 65, 392-406.
PIPER: An FFT-based protein docking program with pairwise potentials

[145] G. Dukovic, B. E White, Z. Y Zhou, F Wang, S Jockusch., M. L Steigerwald, T. F Heinz, R. A Friesner, N. J Turro., L. E.Brus, *J. Am. Chem. Soc*., **2004,** 126, 15269–15276.
Reversible surface oxidation efficient luminescence quenching in semiconductor single-wall carbon nanotubes

[146] Z Zhou., S M teigerwald, M Hybertsen, L Brus, R. A Friesner, *J. Am. Chem. Soc*., **2004,** 126, 3597–3607.
Electronic Structure of Tubular Aromatic Molecules derived from the Metallic (5, 5) Armchair Single Wall Carbon Nanotube

[147] J. Lu, K. Crimin., J. Goodwin, P. Crivori, C. Orrenius, L. Xing, P.J. Tler, T.J.Vidmar, B.M.Amore, A.G.Wilson, P.F.Stouten, P.S.Burton, *J. Med. Chem*, 2004, 47, 6104-6107.
Inluence of Molecular Flexibility Polar Surface Area Metrics on Oral Bioavailability in the Rat

[148] G.A. Kaminski, H. A Stern, B. J Berne, R. A.Friesner, *J. Phys. Chem. A*, **2004,** 108, 621–627.
Development of an Accurate Robust Polarizable Molecular Mechanics Force Field from Ab Initio Quantum Chemistry

[149] K.T. Rim, T Muller, J.P Fitts., K Adib, N Camillone, R.M Osgood, E. R Batista, R. A., Friesner, S. A Joyce, G. W Flynn, *J. Phys. Chem. B*, **2004,** 108, 16753–16760.
Scanning tunneling microscopy theoretical study of competitive reactions in the dissociative chemisorption of CCl4 on iron oxide surfaces

[150] J.F. R. Silva, A F. Riveros, M.Berrondo, *Int. J. Quantum Chem*, **2003,** 94, 105–112.
DFT study of 1-D Li6Gd(BO3)(3)

[151] L. Tang, E. T Papish, G. P Abramo, J. R Norton, M Baik, R. A Friesner, A Rappé, *J. Am. Chem. Soc*., **2003,** 125, 10093–10102.
Kinetics Thermodynamics of H• Transfer From (h5-C5R5)Cr(CO)3H to Methyl Methacrylate Styrene

[152] Z. Zhou, R. A Friesner, L Brus, *J. Am. Chem. Soc*., **2003,** 125, 15599–15607.
Electronic Structure of 1 to 2 nm Diameter Silicon Core/Shell Nanocrystals: Surface Chemistry, Optical Spectra, Charge Transfer Doping

[153] B.F. Jensen, M.D. Sørensen, A.M.Kissmeyer, F.Björkling, K.Sonne, S.B.Engelsen, L.Nørgaard, *J. Comput. Aided Mol. Des*, **2003**, 17, 849-859.
Prediction of in vitro metabolic stability of calcitriol analogs by QSAR

[154] G.A. Kaminski, R. A Friesner, R.Zhou, *J. Comput. Chem*, **2003,** 24, 267–276.
A Computationally Inexpensive Modification of the Point Dipole Electrostatic Polarization Model for Molecular Simulations

[155] M. Baik, R. A Friesner, S.Lippard, *J. Inorg. Chem*, **2003,** 42, 8615–8617.
cis-{Pt(NH3)2(L)}2+/+ (L = Cl, H2O, NH3) Binding to Purines CO: Does p-Back-Donation Play a Role?

[156] Z. Zhou, L Brus, R. A Friesner, *Nano Letters*, **2003,** 3, 163–167.
Electronic Structure Luminescence of 1.1- 1.4-nm Silicon Nanocrystals: Oxide Shell versus Hydrogen Passivation

[157] J. R. Greenwood, M Begtrup, *Theor. Chem. Acc*, **2003,** 109, 200–205.
Action of HCl on 3-hydroxypyrazolo(iso)quinolines to give 1-chloropyrazoles: evidence for an addition-elimination mechanism by ab initio calculations in gas phase water

[158] W.L.Jorgensen, E.M. Duffy, *Adv. Drug Deliv. Rev*, 2002, 54, 355-366.
Prediction of drug solubility from structure

[159] H. Tony, M Baik, B. M Bridgewater, J. H Shin, D. G Churchill, R. A Friesner, G. F Parkin, *Chemical Communications, (British Royal Society)*, **2002,** 22, 2644–2645.
A non-classical hydrogen bond in the molybdenum arene complex [η6-C6H5C6H3(Ph)OH]Mo(PMe3)3: evidence that hydrogen bonding facilitates oxidative addition of the O–H bond

[160] M. Baik, J. B Crystal, R. A Friesner, *Inorg. Chem*, **2002,** 41, 5926–5927.
Ab Initio Quantum Calculation of the Diabatic Coupling Matrix Elemetns for the Self-Exchange Redox Couples M(Cp)2 0/+(M=Fe, Co, Cp=C5H5)

[161] V. Guallar, B. F Gherman, W. H Miller, S. J Lippard, R.A Friesner, *J. Am. Chem. Soc.*, **2002,** 124, 3377–3384.
Dynamics of alkane hydroxylation at the non-heme diiron center in methane monooxygenase

[162] G.A Kaminski, H. A Stern, B. J Berne, R. A Friesner, Y X. Cao, R. B Murphy, R Zhou, T. A. Halgren, *J. Comput. Chem*, **2002,** 23, 1515–1531.
Development of a polarizable force field for proteins via ab initio quantum chemistry: First generation model gas phase tests

[163] J.J Klicic, R. A Friesner, S Y Liu., W. C Guida, *J. Phys. Chem. A*, **2002,** 106, 1327–1335.
Accurate prediction of acidity constants in aqueous solution via density functional theory self-consistent reaction field methods

[164] J. Crystal, L. Y Zhang, R. A Friesner, G Flynn, *J. Phys. Chem. A*, **2002,** 106, 1802–1814.
Computational Modeling for Scanning Tunneling Microscopy of Physisorbed Molecules via Ab Initio Quantum Chemistry

[165] M.H. Baik, R.A Friesner, *J. Phys. Chem. A*, **2002,** 106, 7407–7412.
Computing redox potentials in solution: Density functional theory as a tool for rational design of redox agents

[166] R.A. Friesner, B. D Dunietz, *Accounts of Chemical Research*, **2001,** 34, 351–358.
Large Scale Ab Initio Quantum Chemical Calculations on Biological Systems

[167] P. T. Snee, C. K Payne., T Kotz, K., H Yang, C. B Harris, *J. Am. Chem. Soc*., **2001,** 123, 2255–2264.
High Spin Reactivity Under Ambient Conditions: An Ultrafast UV-Pump IR-Probe Study

[168] B. F. Gherman, B. D Dunietz, D.A Whittington, S. J Lippard, R. A Friesner, *J. Am. Chem. Soc.*, **2001,** 123, 3836–3837.
Activation of the C-H bond of methane by intermediate Q of methane monoozygenase: A theoretical study

[169] H. Yang, P. T Snee, K. T Kotz, C. K Payne, C. B Harris. *J. Am. Chem. Soc*., **2001,** 123, 4204.
Femtosecond Infrared Study of the Dynamics of Solvation Solvent Caging

[170] J. El Yazal, F.G Prendergast, D. E Shaw, Y. P Pang, *J. Am. Chem. Soc.*, **2000,** 122, 11411–11415.
Protonation states of the chromophore of denatured green fluorescent proteins predicted by ab initio calculations

[171] E.M.Duffy, W.L. Jorgensen, *J. Am. Chem. Soc.*, **2000**, 122, 2878-88.
Prediction of Properties from Simulations: Free Energies of Solvation in Hexadecane, Octanol, Water

[172] R. Baltensperger, M. R. Trummer Siam, *J. Sci. Comput*., **2006**,24, 5 1465–1487.
Spectral differencing with a twist

CQC

[173] K. RamaKrishna, Ch.V. Kameswara Rao, V. Ananta Ramam, R. Sambasiva Rao, *Journal of Applicable Chemistry*, **2015,** 4(3), 637-800.
Computational Quantum Chemistry (CQC) Part 1: Evolution of a computational tool into an instrumental probe

[174] Ch. V. Kamewara Rao, M.Phil thesis, **2012**, Acharya Nagarjuna University, Nagarjuna Nagar, AP
Computational quantum chemistry (CQC) models of isonicotinic acid hydrazide, its valence isomers their isopropyl derivatives

[175] K Rama Krishna, Ch V Kameswara Rao, V Ananta Ramam, R Sambasiva Rao, M. Venkata Subba Rao, *Ind. J. Chem.*, **2012**, *51A*, 571-579.
Model chemistries of hydrazides III: SEMO computations of isonicotinic acid hydrazide, its valence isomers their isopropyl derivatives

[176] I. Suryanarayana, V. Ananta Ramam, K.M.M.Krishna Prasad R.Sambasiva Rao, *Ind. J. Chem.*, **2008**, *47A*, 199-206.
Model chemistries of hydrazides I. Electronic parameters of aliphatic hydrazides with AM1 PM3 Hamiltonians

[177] V Ananta Ramam, V.V. Panakala Rao, K Rama Krishna R. Sambasiva Rao, *Ind J Chem*, **2006**, 45A, 100-105 (Special issue).
Model chemistries of hydrazides II. Electronic structure of five membered aromatic hydrazides

[178] K. Ramakrishna, R. Sambasiva Rao, *Manuscript under preparation*.
(a) Impact of experimental design NNs in CQC, (b) Prospects of quaternions in quantum physics (PQQP), (c) Are CQC and Experimental chemistry mutually exclusive or two sides of same coin?

[179] K. Ramakrishna, B. Venkata Sasidhar, Bioorganic and Medicinal Chem. (communicated), (b) Patent IP (India)Appl.No: 3933/CHE/2014; 5135/CHE/2015 A;(c) R. Sambasiva Rao, (unpublished).

AIDS

[180] K Suryanarayana, R Sambasiva Rao, Deccan chronicle December5, **1994**,
A new dimension in AIDs prevention

Neural networks

[181] K RamaKrishna, Ch. V. Kameswara Rao, V. Anantha Ramam, R. Sambasiva Rao, *J. Applicable Chem.*, **2014,** 3, 6, 2209-2311.
Mathematical Neural Network (MaNN) Models, Part VI: Single-layer perceptron [SLP] and Multi-layer perceptron [MLP] Neural networks in ChEM- Lab.

[182] K RamaKrishna, V.Anantha Ramam, R. Sambasiva Rao, *J. Applicable Chem.*, **2014,** 3, 5, 1807-1893**.**
Mathematical Neural Network (MaNN) Models, Part V: Radial basis function (RBF) neural networks (NNs) in Chemometrics, Envirometrics and Medicinometrics 3D-fns.

[183] K RamaKrishna, V. Anantha Ramam, R. Sambasiva Rao, *J. Applicable Chem.*, **2014**, 3 (4) 1337-1422**.**
Mathematical Neural Network (MaNN) Models Part IV: Recurrent Neural networks (RecNN) in bio-/chemical- tasks.

[184] K RamaKrishna, V. Anantha Ramam, R. Sambasiva Rao, *J. Applicable Chem.*, **2014**, 3 (3) 919-989.
Mathematical Neural Network (MaNN) Models, Part III: ART and ARTMAP in OMNI_METRICS.

[185] K RamaKrishna, V. Anantha Ramam, R. Sambasiva Rao, *J. Applicable Chem.*, **2014**, 3 (2) 834-884.
Mathematical Neural Network (MaNN) Models, Part II: Self Organizing Maps. (SOMs) in chemical sciences.

[186] I. Suryanarayana, A. Braibanti, R. Sambasiva Rao, V. AnantaRamam, D. Sudarsan, G. Nageswara Rao, *Fisheries Research*, **2008**, 92, 115-139.
Neural networks in fisheries research

E-man

[187] K RamaKrishna and R Sambasiva Rao, *J. Applicable Chem.*, **2015**, 4(6), 1597-1690.
Evolution of Mimics of Algorithms of Nature (E-man) Part 6: Research Tutorial on bat and Mosquito algorithms

[188] K. RamaKrishna, G. Ramkumar and R. Sambasiva Rao, *J. Applicable Chem.*, **2013,** 2, 6, 1413-1458.
Evolution of Mimics of Algorithms of Nature (E-man) Part 5: Tutorial on Big_Bang–Big_Crunch algorithm.

[189] K. RamaKrishna, Ch. V. Kameswara Rao and R. Sambasiva Rao, *J. Applicable Chem.*, **2013,** 2, 5, 1007-1034.
E-man Part 4: Tutorial on prospects of charged system search (CSS) algorithm in chemical sciences.

[190] K. RamaKrishna, Ch. V. Kameswara Rao, R. Sambasiva Rao, *J. Applicable Chem.*, **2013,** 2, 4, 698-713.
Eman-Part III: Tutorial on gravitational algorithm in Structure activity relationships (SXR).

[191] K. Viswanath, R. Sambasiva Rao, Ch. V. Kameswara Rao, K. Rama Krishna, B. Rama Krishna and G. E. G. Santhosh, *J. Applicable Chem.*, **2012,** 1, *1*, 109-124.
Eman (Evolution of Mimics of Algorithms of Nature)-Part II: Application of neural networks for classification of bauxite.

Swarm Intelligence

[192] K. RamaKrishna, R. Sambasiva Rao, *J. Applicable Chem*., **2014**, 3 (2) 449-492.
Swarm_Intelligence (SI)-State-of-Art (SI-SA), Part I: Tutorial on Firefly algorithm

Hot_Ice

[193] K. RamaKrishna, R. Sambasiva Rao, *J. Applicable Chem*. (Communicated)
HotIce: Hands-on-tutorial for intelligent computational Evolution Part 1: Quaternions in Omnimetrics (QuO)

Sup.Inf. 01:
Typical input/output formats in vogue in CQC packages

Alc	Alchemy file
prep	AMBER PREP file
bs	Ball and Stick file
bgf	MSI BGF file
car	Biosym .CAR file
boog	Boogie file
caccrt	Cacao Cartesian file
cadpac	Cambridge CADPAC file
charmm	CHARMm file
c3d1	Chem3D Cartesian 1 file
c3d2	Chem3D Cartesian 2 file
cssr	CSD CSSR file
fdat	CSD FDAT file
gstat	CSD GSTAT file
dock	Dock Database file
dpdb	Dock PDB file
feat	Feature file
fract	Free Form Fractional file
gamout	GAMESS Output file

gzmat	Gaussian Z-Matrix file
gauout	Gaussian 92 Output file
g94	Gaussian 94 Output file
gr96A	GROMOS96 (A) file
gr96N	GROMOS96 (nm) file
hin	Hyperchem HIN file
sdf	MDL Isis SDF file
jagin	Jaguar Input file
jagout	Jaguar Output file
m3d	M3D file
macmol	Mac Molecule file
macmod	Macromodel file
micro	Micro World file
mm2in	MM2 Input file
mm2out	MM2 Output file
mm3	MM3 file
mmads	MMADS file
mdl	MDL MOLfile file
molen	MOLIN file
mopcrt	Mopac Cartesian file

mopint	Mopac Internal file
mopout	Mopac Output file
pcmod	PC Model file
pdb	PDB file
psin	PS-GVB Input file
psout	PS-GVB Output file
msf	Quanta MSF file
schakal	Schakal file
shelx	ShelX file
smiles	SMILES file
spar	Spartan file
semi Spartan	Semi-Empirical file
spmm	Spartan Molecular Mechanics file
mol	Sybyl Mol file
mol2	Sybyl Mol2 file
wiz	Conjure file
unixyz	UniChem XYZ file
xyz	XYZ file
xed	XED file

Babel program of Jaguar

→ Reads (about 40) of input and output file formats

→ Writes both Cartesian and Z-matrix notations

Sup.Inf. 02:
Exerts from geometric optimization and vibrational frequency calculation by Jaguar

```
Job jaguar_2 started on SO800 at Sun Jan 11 17:39:31 2015
jobid: SO800-0-54b236c2

 +-----------------------------------------------------------------+
 |  Jaguar version 8.5, release  13

   Copyright Schrodinger, Inc.
   All Rights Reserved.

   The following have contributed to Jaguar (listed alphabetically):
   Mike Beachy, Art Bochevarov, Dale Braden, Yixiang Cao,
   Chris Cortis, Rich Friesner, Bill Goddard, Hod Greeley,
   Tom Hughes, Jean-Marc Langlois, Daniel Mainz, Rob Murphy,
   Dean Philipp, Tom Pollard, Murco Ringnalda.

   Use of this program should be acknowledged in publications as:

   Jaguar, version 8.5, Schrodinger, Inc., New York, NY, 2014.

   A. D. Bochevarov, E. Harder, T. F. Hughes, J. R. Greenwood,
   D. A. Braden, D. M. Philipp, D. Rinaldo, M. D. Halls,
   J. Zhang, R. A. Friesner, "Jaguar: A High-Performance Quantum
   Chemistry Software Program with Strengths in Life and Materials
   Sciences", Int. J. Quantum Chem., 2013, 113(18), 2110-2142.
 +-----------------------------------------------------------------+
```

start of program pre

```
 Job name: jaguar_2
 Executables used: /app/schrodinger/SCHRODINGER_2014-3/jaguar-v85013/bin/Linux-x86_64
 Temporary files : /app/schrodinger/tmp/inoue/jaguar_2#SO800-0-54b236c2
 Maestro file (input):  jaguar_2.mae
 Maestro file (output): jaguar_2.01.mae


 basis set:            6-31g**
 net molecular charge:    0
 multiplicity:            1

 Running   2 MPI processes

 Master MPI process running on SO800
  Slave MPI process   1 running on SO800

 Using up to   2 threads per process

  number of basis functions....          284
```

```
Molecular weight:     233.05 amu

 Stoichiometry: C7N3H11SO4
 Molecular Point Group: C1
 Point Group used: C1
```

```
Number of optimization coordinates:    78
Number of independent coordinates:     78
Number of non-redundant coordinates:   72
Number of frozen coordinates:          0
Number of harmonic constraints:        0

Number of geometric degrees of freedom:    72
Maximum geometric degrees of freedom:      72
 " " " " " excluding dummy atoms:          72
```

```
Non-default options chosen:
   SCF calculation type: UDFT(b3lyp)
UDFT=Becke_3_Parameter/HF+Slater+Becke88+VWN+LYP (B3LYP)
   Geometry will be optimized in redundant internal coordinates
   Maximum number of SCF iterations:  100
   Electrostatic potential fit to point charges on atomic centers
   Molecular orbitals will be written to .vis files
   Mulliken populations computed by atom
   Store KE, NAI, and pt. chg. terms separately
```

```
                                    start of program onee
smallest eigenvalue of S:    1.218E-03
number of canonical orbitals.....          284

end of program onee
```

```
                                    start of program hfig

  initial wavefunction generated automatically from atomic wavefunctions
  orbitals   20 through   61
  using Mulliken Atomic Population Localization

  --------------------
  Alpha orbital space
  --------------------

  Irreducible     Total no   No of occupied orbitals
  representation  orbitals   Shell_1  Shell_2    ...
  No Symm          284        61
  -------------------------
  Orbital occupation/shell    1.000

  -------------------
  Beta orbital space
  -------------------

  Irreducible     Total no   No of occupied orbitals
  representation  orbitals   Shell_1  Shell_2    ...
  No Symm          284        61
  -------------------------
  Orbital occupation/shell    1.000



    Unrestricted Spin Properties ...
    Sz*(Sz+1) .............     0.000
<S**2> of initial guess      0.000
```

```
end of program hfig

start of program grid
grid      grid set  grid #  grid sym
 ------    --------  ------  --------
 coarse        0        0        1
 medium        2        1        1
 fine          0        0        1
 ultrafine     4        2        1
 charge       -1        3        1
 gradient      4        2        1
 density       0        0        1
 DFT-fine    -11        4        1
 DFT-med.    -10        5        1
 DFT-grad    -12        6        1
 DFT-der2      0        0        1
 DFT-cphf      0        0        1
 LMP2-enrg     4        2        1
 LMP2-grad     2        1        1
 DFT-cphf2     0        0        1
 PBF-dens      0        0        1
 plotting     -7        7        1
 Rel-grad    -17        0        1


 number of gridpoints:
    atom        N1       C2       N3       C4       C5       C6       O7
 grid # 1       99       97       99       95       98       96      123
 grid # 2      347      354      346      339      370      358      502
 grid # 3      235      240      232      191      166      235     1280
 grid # 4     4304     4304     4304     4304     4304     4304     4304
 grid # 5     1192     1192     1192     1192     1192     1192     1192
 grid # 6     5226     5226     5226     5226     5226     5226     5226

                                start of program scf

 number of electrons..........        122
 number of alpha electrons....         61
 number of beta electrons.....         61
 number of alpha orbitals.....        284
 number of beta orbitals......        284
 number of alpha occupied orb..        61
 number of alpha virtual orb...       223
 number of beta occupied orb...        61
 number of beta virtual orb....       223
 SCF type: UDFT=Becke_3_Parameter/HF+Slater+Becke88+VWN+LYP (B3LYP)


                                start of program rwr

 dpptrf failed in rinv with info = 185
 switching to SVD for RwR matrix   1 for grid  2

 end of program rwr

start of program der1b
forces (hartrees/bohr) : total
end of program der1b
                                start of program geopt
```

```
geometry optimization step  1
  energy:          -1136.66132081521 hartrees
....
predicted energy change:  -2.2888E-02
  step size:     0.30088
  trust radius:  0.30000

  molecular structure not yet converged...

  ---------------------------------------------------
 /  end of geometry optimization iteration   1   /
 ---------------------------------------------------
```

```
 ....
```

```
geometry optimization step  2
  energy:          -1136.67996406800 hartrees
  predicted energy change:  -4.7250E-03
  step size:     0.30077
  trust radius:  0.30000

  molecular structure not yet converged...
.....
```

```
  start of program geopt

  geometry optimization step 15
  energy:          -1136.69146425541 hartrees

  energy change:         -1.8334E-05 *  (  5.0000E-05 )
  gradient maximum:        3.1016E-04 *  (  4.5000E-04 )
  gradient rms:           7.6608E-05 *  (  3.0000E-04 )
  displacement maximum:    1.4078E-02 .  (  1.8000E-03 )
  displacement rms:        2.8850E-03 .  (  1.2000E-03 )

  predicted energy change:  -2.3898E-06
  step size:     0.02548
  trust radius:  0.30000

  molecular structure not yet converged...
```

```
start of program geopt

  geometry optimization step 16
  energy:          -1136.69148669926 hartrees

  energy change:         -2.2444E-05 *  (  5.0000E-05 )
  gradient maximum:        2.3999E-04 *  (  4.5000E-04 )
  gradient rms:           5.4653E-05 #  (  3.0000E-04 )
  displacement maximum:    4.7513E-03 .  (  1.8000E-03 )
  displacement rms:        1.1361E-03 *  (  1.2000E-03 )

  predicted energy change:  -7.2053E-07
  step size:     0.01003
  trust radius:  0.30000

  ***********************************************************
  **          Geometry optimization complete           **
  ***********************************************************

  Checking the geometry optimization convergence pattern ...
```

```
best                worst
==0=====1=====2=====3=====4==
```

Convergence category 1: non-monotonic convergence to an optimal structure.
Geometry optimization was OK.

Number of imaginary frequencies: 0

Cartesian Format for Geometry Input

```
O    0.000000    0.000000   -0.113502
H1   0.000000    0.753108    0.454006
H2   0.000000   -0.753108    0.454006
```

Variables in Cartesian Input

```
O    0.000000    0.000000   -0.113502
H1   0.000000    ycoor       zcoor
H2   0.000000   -ycoor       zcoor
ycoor=0.753108   zcoor=0.454006
```

```
O    0.000000    0.000000   -0.113502
H1   0.000000    ycoor       zcoor
H2   0.000000   -ycoor       zcoor
Z-variables
ycoor=0.753108
zcoor=0.454006
```

```
O    0.000000    0.000000   -0.113502
H1   0.000000    ycoor       zcoor#
H2   0.000000   -ycoor       zcoor#
ycoor=0.753108   zcoor=0.454006
```

```
N1
C2   N1   1.4589
```

Variables and Dummy Atoms in Z-Matrix Input

CH3OH

```
C
O     C    1.421
H1    C    1.094    O    107.2
X1    C    1.000    O    129.9    H1   180.0
H2    C    1.094    X1    54.25   H1    90.0
H3    C    1.094    X1    54.25   H1   -90.0
H4    O    0.963    C    108.0    H1   180.0
```

	Constraining Z-Matrix Bond Lengths or Angles
If	geometry optimization
	bond lengths or angles are to be frozen
Then	add a # sign after the coordinate values
Ex.	O H1 O 0.9428 H1 O 0.9428 H1 106.0#
Ex.	chbond=1.09# HCHang=109.47

To freeze during a geometry optimization

Sup.Inf. 02b:

Typical screendumps of Jaguar.Schrodinger suit

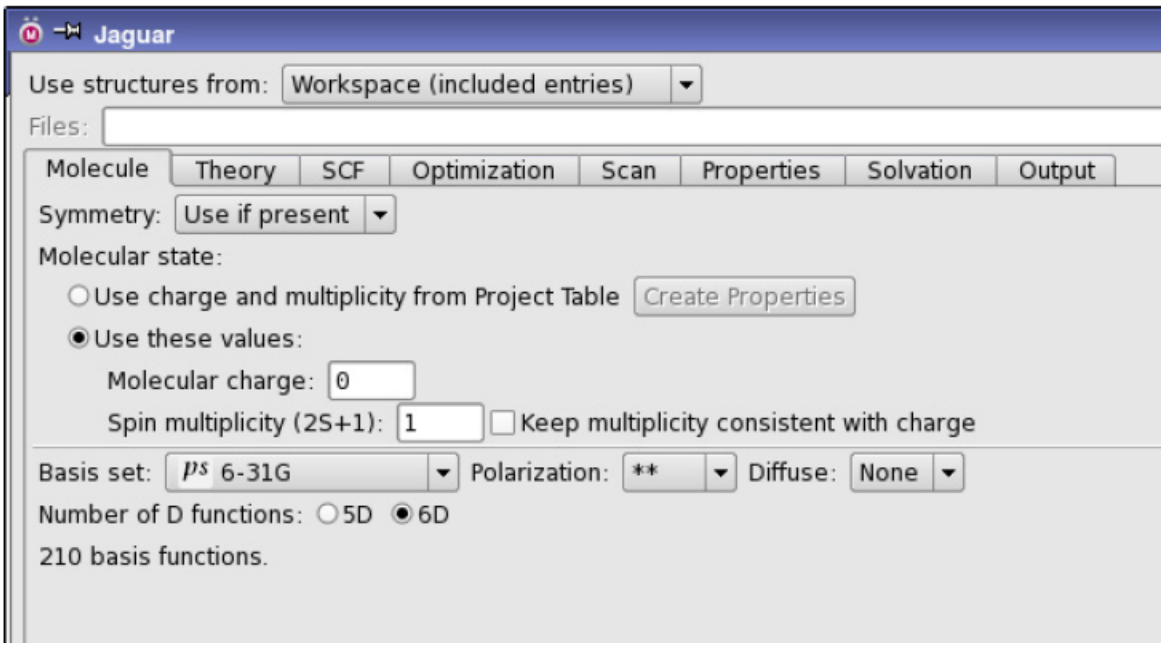

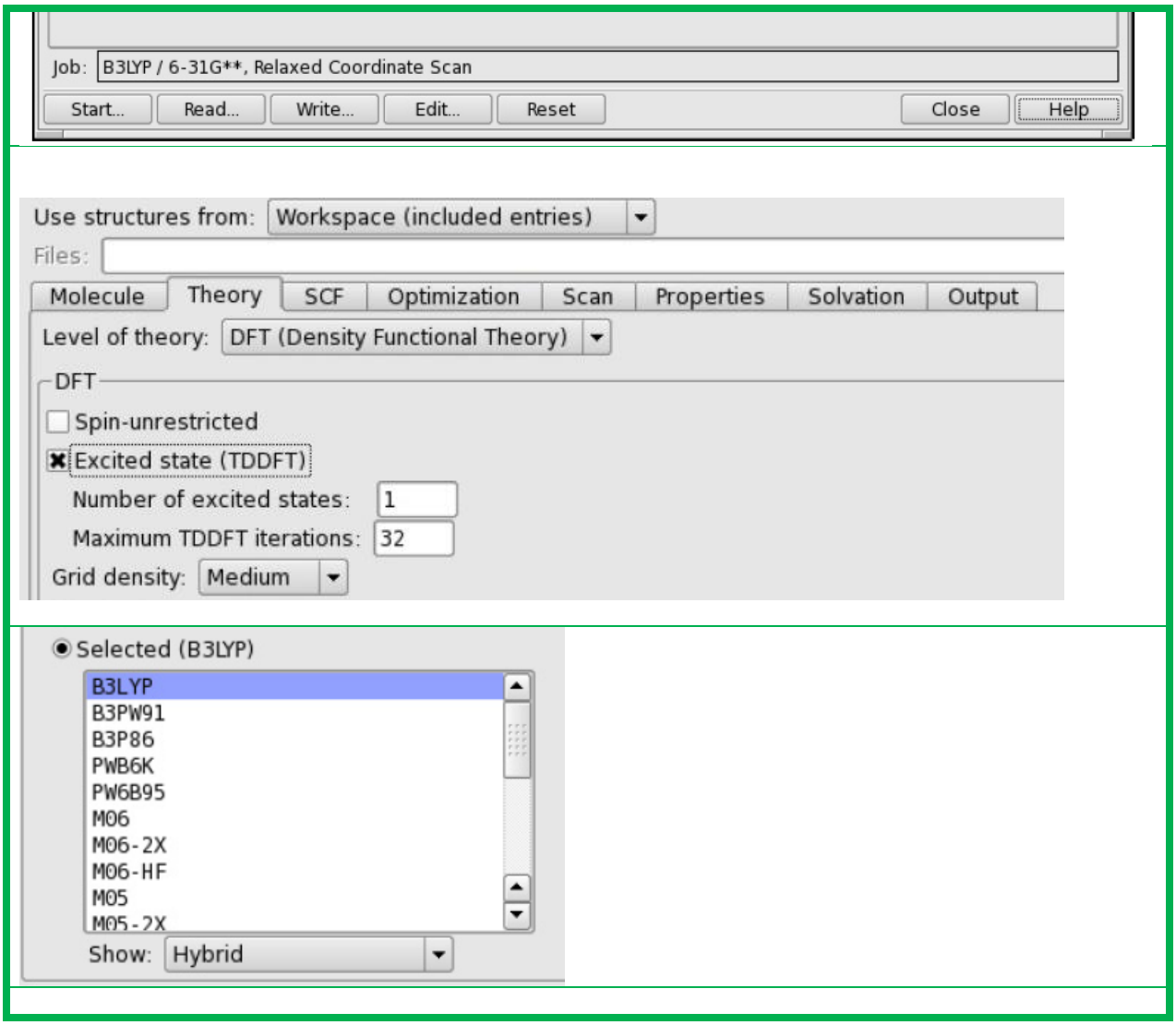

Sup.Par 01:
Optimized XYZ co-ordinates

9* Ethyl,1-((2,4-dioxo-1,2,3,4-tetrahydropyrimidin-5-yl)sulfonyl)piperidine-4-carboxylate

atom	x	y	z
N1	-0.5032515963	0.2290728374	0.6525051370
C2	0.7123919793	-0.3359244761	0.3116048200
N3	1.5664727665	0.5676597011	-0.3305477869

start of program geopt

geometry optimization step 12
energy: -1366.53823028710 hartrees

energy change: -8.2644E-08 ! (5.0000E-05)
gradient maximum: 3.1798E-04 * (4.5000E-04)
gradient rms: 7.1390E-05 * (3.0000E-04)

```
displacement maximum:    6.6348E-03 .  (  1.8000E-03 )
displacement rms:        1.4581E-03 .  (  1.2000E-03 )

predicted energy change:  -1.7657E-06
step size:     0.01564
trust radius:  0.30000
```

```
Comp -2

Energy components, in hartrees:
  (A)  Nuclear repulsion............    1448.39184130558
  (E)  Total one-electron terms.....   -4539.28665283178
  (F)    Electron-nuclear...........   -5744.39934282256
  (H)    Kinetic....................    1205.11268999078
  (I)  Total two-electron terms.....    1876.77773210543
  (L)  Electronic energy............   -2662.50892072635  (E+I)
  (M)  -V/T........................       2.00747182359  (-(A+F+I)/H)
  (N)  Total energy................   -1214.11707942077  (A+L
```

```
Exchange+Corr.
 Total two-electron terms    1876.77773210543    2011.46409262681    -134.68636052137
   Hamiltonian  1........     957.90018039839    1005.73204631340     -47.83186591501
   Hamiltonian  2........     957.90018039839    1005.73204631340     -47.83186591501
```

```
 Atomic charges from Mulliken population analysis:

 Atom      N1          C2          N3          C4          C5
 Charge   -0.60523     0.75020    -0.56474     0.17543    -0.28418

 Atom      C6          O7          O8          S9          N10
 Charge    0.63132    -0.45882    -0.48134     1.25209    -0.66744
```

```
                              Natural Population                Natural
          Natural    ---------------------------------------------  Spin
  Atom No    Charge        Core      Valence    Rydberg      Total      Density
 ----------------------------------------------------------------------------------
    N  1   -0.68268     1.99934     5.67264    0.01070     7.68268     0.00000
    C  2    0.82601     1.99943     3.13185    0.04271     5.17399    -0.00000
```

```
Natural Population
 -------------------------------------------------------
   Core                    49.98447 ( 99.9689% of   50)
   Valence                109.40584 ( 99.4599% of  110)
   Natural Minimal Basis  159.39030 ( 99.6189% of  160)
   Natural Rydberg Basis    0.60970 (  0.3811% of  160)
 -------------------------------------------------------
```

```
Atom No         Natural Electron Configuration
 ------------------------------------------------------------------------
     N  1      [core]2s( 1.30)2p( 4.37)3p( 0.01)
     C  2      [core]2s( 0.71)2p( 2.42)3p( 0.03)3d( 0.01)
```

```
N 3    [core]2s( 1.27)2p( 4.35)3p( 0.01)
C 4    [core]2s( 0.93)2p( 3.00)3p( 0.01)
C 5    [core]2s( 1.01)2p( 3.44)3p( 0.02)
```

Natural Population

Atom No	Natural Charge	Core	Valence	Rydberg	Total
N 1	-0.34134	0.99967	2.83632	0.00535	3.84134
C 2	0.41301	0.99972	1.56592	0.02135	2.58699
N 3	-0.31716	0.99967	2.81159	0.00590	3.81716
C 4	0.02695	0.99948	1.96378	0.00978	2.97305

Sup.Knowledge:01

Drugs for typical cancers

Drug	Used for	Drug	Used for
Afinitor	Advanced pancreatic neuroendocrine tumors	Lonsurf (trifluridine and tipiracil)	Metastatic colorectal cancer
Anexsia	Chronic pain	Lupron Depot (leuprolide acetate for depot suspension)	Prostate cancer
	For the prevention of chemotherapy-induced nausea and vomiting	Lupron Depot (leuprolide acetate for depot suspension)	Advanced prostate cancer
Afinitor	Renal cell carcinoma	Lynparza (olaparib)	Previously treated BRCA mutated advanced ovarian cancer
Anzemet	Treatment for the prevention of nausea and vomiting associated with chemotherapy and surgery Emesis	Marqibo (vinCRIStine sulfate LIPOSOME injection)	Ph- acute lymphoblastic leukemia August
Alecensa alectinib	ALK-positive metastatic non-small cell lung cancer	Mekinist (trametinib)	Unresectable or metastatic melanoma with BRAF V600E or V600K mutations May of
Arimidex Anastrozole	Advanced breast cancer in postmenopausal women	Miraluma test	Test for breast cancer
Afinitor everolimus	Renal angiomyolipoma associated with tuberous sclerosis complex Hormone receptor-positive HER2-negative breast cancer Advanced pancreatic neuroendocrine tumors Renal cell carcinoma	Mozobil (plerixafor injection)	Non-Hodgkin's lymphoma and multiple myeloma
Arranon nelarabine	T-cell acute lymphoblastic leukemia and T-cell lymphoblastic lymphoma	Mylotarg (gemtuzumab ozogamicin)	CD33 positive acute myeloid leukemia (AML)

Aloxi palonosetron	For the prevention of nausea and vomiting associated with emetogenic cancer chemotherapy		Neulasta	Treatment to decrease the chance of infection by febrile neutropenia in patients receiving chemotherapy
Aredia pamidronate disodium for injection	Osteolytic bone metastases of breast cancer		Neumega	Thrombocytopenia
Alimta pemetrexed for injection	Malignant pleural mesothelioma		Neupogen	Slow white blood cell recovery following chemotherapy Approval
			Neutroval (tbo-filgrastim)	For the reduction in the duration of severe chemotherapy-induced neutropenia August
Abraxane (paclitaxel protein-bound particles for injectable suspension)	Non-small cell lung cancer		Nexavar (sorafenib)	For the Treatment of Renal Cell Carcinoma
Abstral (fentanyl sublingual tablets)	Breakthrough cancer pain in opioid-tolerant patients		Ninlaro (ixazomib)	Multiple myeloma
Actiq	Treatment for Cancer Pain		Nolvadex	Breast cancer
Adcetris (brentuximab vedotin)	Hodgkin lymphoma and anaplastic large cell lymphoma		Odomzo (sonidegib)	Locally advanced basal cell carcinoma
Arzerra (ofatumumab)	Chronic lymphocytic leukemia		Onivyde (irinotecan liposome injection)	Metastatic pancreatic cancer following gemcitabine-based therapy
Avastin (bevacizumab)	Renal cell carcinoma		Onsolis (fentanyl buccal)	For the management of breakthrough cancer pain
Avastin (bevacizumab)	Metastatic carcinoma of the colon or rectum		Opdivo (nivolumab)	Metastatic squamous non-small cell lung cancer March
Beleodaq (belinostat)	Relapsed or refractory peripheral T-cell lymphoma		Opdivo (nivolumab)	Unresectable or metastatic melanoma
Bexxar	Patients with CD20 positive follicular non-Hodgkin's lymphoma following chemotherapy relapse		Perjeta (pertuzumab)	For the first-line treatment of HER2+ metastatic breast cancer
Blincyto (blinatumomab)	Philadelphia chromosome-negative relapsed /refractory B cell precursor acute lymphoblastic leukemia		Photodynamic Therapy	Photodynamic therapy device for the treatment of esophageal cancer January
Bosulif (bosutinib)	Ph+ chronic myelogenous leukemia		Photofrin	Early-stage microinvasive endobronchial non-small cell lung cancer
Bromfenac	Management of acute pain		Picato (ingenol mebutate) gel	Actinic keratosis
Busulflex	For use in combination for the treatment of leukemia		Plenaxis (abarelix for injectable suspension)	For treatment of advanced prostate cancer
Campath	Injectable treatment of B-cell chronic lymphocytic leukemia		Pomalyst (pomalidomide)	Relapsed and refractory multiple myeloma
Campostar	Metastatic colorectal cancer		Portrazza (necitumumab)	Metastatic squamous non-small cell lung cancer
Camptosar	Colon or Rectal Cancer		Premarin (conjugated estrogens)	For the prevention of postmenopausal osteoporosis and treatment of vasomotor menopause symptoms of

CEA-Scan	☠	Diagnostic imaging product for colorectal cancer		Proleukin	☠	Metastatic melanoma
Cervarix [Human Papillomavirus Bivalent (Types 16 and 18) Vaccine Recombinant	☠	For the prevention of cervical cancer and cervical intraepithelial neoplasia caused by HPV types 16 and 18		Provenge (sipuleucel-T)	☠	Hormone refractory prostate cancer
Clolar (clofarabine)	☠	Acute lymphoblastic leukemia in pediatric patients		Quadramet (Samarium Sm 153 Lexidronam Injection)	☠	Pain associated with bone cancer
Cometriq (cabozantinib)	☠	Metastatic medullary thyroid cancer		Revlimid (lenalidomide)	☠	Mantle cell lymphoma
Cotellic (cobimetinib)	☠	BRAF V600E or V600K melanoma		Rituxan	☠	Non-hodgkin's lymphoma
Cyramza (ramucirumab)	☠	Gastric cancer		Sancuso (granisetron)	☠	Chemotherapy-induced nausea and vomiting
Darzalex (daratumumab)	☠	Multiple myeloma		Sclerosol Intrapleural Aerosol	☠	Malignant pleural effusions
Degarelix (degarelix for injection)	☠	Prostate cancer of		SecreFlo (secretin)	☠	To aid in the diagnosis of pancreatic dysfunction and gastrinoma
Doxil (doxorubicin HCl liposome injection)	☠	Ovarian cancer that is refractory to other first-line therapies		Self-examination breast pad	☠	Self-examination breast pad on 22
Eligard (leuprolide acetate)	☠	For the palliative treatment of advanced prostate cancer		Sensipar (cinacalcet)	☠	Secondary hyperparathyroidism and hypercalcemia in parathyroid carcinoma patients
Elitek (rasburicase)	☠	For the management of plasma uric acid levels in adults with malignancies		Sprycel (dasatinib)	☠	Imatinib-resistant chronic myeloid leukemia
Ellence	☠	Epirubicin hydrochloride		Stivarga (regorafenib)	☠	Gastrointestinal stromal tumor
Elliotts B Solution (buffered intrathecal electrolyte/dextrose injection)	☠	Treatment of meningeal leukemia or lymphocytic lymphoma		Stivarga (regorafenib)	☠	Previously treated patients with metastatic colorectal cancer
Eloxatin (oxaliplatin/5-fluorouracil/leucovorin)	☠	Colon or rectum carcinomas		Subsys (fentanyl sublingual spray)	☠	Breakthrough cancer painof
Emend (aprepitant)	☠	Nausea and vomiting associated with chemotherapy		Sutent (sunitinib malate)	☠	Pancreatic neuroendocrine tumors
Empliciti (elotuzumab)	☠	Patients with multiple myeloma who have received prior therapies		Sutent (sunitinib)	☠	Kidney cancer and gastrointestinal stromal tumors
Erbitux (cetuximab)	☠	EGFR-expressing metastatic colorectal cancer		Sylatron (peginterferon alfa-2b)	☠	Melanoma
Erivedge (vismodegib)	☠	Basal cell carcinoma January		Synribo (omacetaxine mepesuccinate)	☠	Chronic or accelerated phase chronic myeloid leukemia
Erwinaze (asparaginase Erwinia chrysanthemi)	☠	Acute lymphoblastic leukemia of		Tafinlar (dabrafenib)	☠	Unresectable or metastatic melanoma with BRAF V600E mutation May
Ethyol (amifostine)	☠	Xerostomia (dry mouth) due to radiation		Tagrisso (osimertinib)	☠	EGFR T790M mutation positive non-small cell lung cancer
Ethyol (amifostine)	☠	Treatment to reduce renal		Tarceva (erlotinib	☠	Advanced refractory metastatic

		toxicity associated with chemotherapy in subjects with advanced ovarian cancer 8		OSI 774)	non-small cell lung cancer November
Eulexin (flutamide)	☠	Prostate cancer		Tasigna (nilotinib hydrochloride monohydrate)	☠ Chronic myelogenous leukemia
Evista (raloxifene hydrochloride)	☠	For the treatment/prevention of osteoporosis and reduction of breast cancer risk in postmenopausal women		Taxol	☠ AIDS-related Kaposi's Sarcoma
Farydak (panobinostat)	☠	Multiple myeloma February		Taxotere (Docetaxel)	☠ Locally advanced or metastatic breast cancer
Faslodex (fulvestrant)	☠	Hormone receptor positive metastatic breast cancer		Temodar	☠ Refractory anaplastic astrocytoma
Femara (letrozole)	☠	First-line treatment of postmenopausal women with locally advanced or metastatic breast cancer		Torisel (temsirolimus)	☠ Renal cell carcinoma
Femara (letrozole)	☠	Breast cancer		Treanda (bendamustine hydrochloride)	☠ Chronic lymphocytic leukemia and B-cell non-Hodgkin's lymphoma
Feridex I.V.	☠	Contrast agent for magnetic resonance imaging of liver lesions		Trelstar Depot (triptorelin pamoate)	☠ For the palliative treatment of advanced prostate cancer
Folotyn (pralatrexate injection)	☠	Peripheral T-cell lymphoma		Trelstar LA (triptorelin pamoate)	☠ Intramuscular injection for the treatment of advanced stage prostate cancer
Fusilev (levoleucovorin)	☠	For rescue after high-dose methotrexate therapy in osteosarcoma and to reduce the toxicity of methotrexate of		Trisenox (arsenic trioxide)	☠ For the induction of remission and consolidation in patients with acute promyelocytic leukemia (APL)
Gardasil (quadrivalent human papillomavirus (types 6 11 16 18) recombinant vaccine)	☠	For the prevention of cervical cancer associated with human papillomavirus		Tykerb (lapatinib)	☠ Breast cancer
GastroMARK	☠	Contrast agent for magnetic resonance imaging of the gastrointestinal tract		UltraJect	☠ Chronic pain
Gazyva (obinutuzumab)	☠	Previously untreated chronic lymphocytic leukemia of		Unituxin (dinutuximab)	☠ Pediatrics with high-risk neuroblastoma
Gemzar (gemcitabine HCL)	☠	Lung cancer		UroXatral (alfuzosin HCl extended-release tablets)	☠ Of the signs and symptoms of benign prostatic hyperplasia
Gemzar (gemcitabine HCL)	☠	Pancreatic cancer		UVADEX Sterile Solution	☠ Treatment of the skin manifestations of cutaneous T-cell lymphoma (CTCL)
Gilotrif (afatinib)	☠	Metastatic non-small cell lung cancer with EGFR mutations		Valchlor (mechlorethamine) gel	☠ Stage IA/IB mycosisfungoides-type cutaneous T-cell lymphoma August
Gleevec (imatinib mesylate)	☠	Gastrointestinal stromal tumors (gists)		Valstar	☠ Bladder cancer
Gleevec (imatinib mesylate)	☠	Oral therapy for the treatment of chronic myeloid leukemia		Vandetanib (vandetanib)	☠ Thyroid cancer
Gliadel Wafer (polifeprosan 20 with carmustine implant)	☠	Brain cancer		Varubi (rolapitant)	☠ For the prevention of delayed nausea and vomiting associated with chemotherapy

Halaven (eribulin mesylate)	Metastatic breast cancer		Vectibix (panitumumab)	Colorectal cancer
Herceptin	Metastatic breast cancer		Velcade (bortezomib)	Injectable agent for the treatment of multiple myeloma patients who have received at least two prior therapies.
Herceptin (trastuzumab)	Gastric cancer		Viadur (leuprolide acetate implant)	For pain relief in men with advanced prostate cancer
Hycamtin (topotecan hydrochloride)	Small cell lung cancer		Visipaque (iodixanol)	Diagnostic contrast agent
Hycamtin (topotecan hydrochloride)	Metastatic ovarian cancer		Votrient (pazopanib)	Soft tissue sarcoma
Ibrance (palbociclib)	ER-positive HER2-negative breast cancer		Votrient (pazopanib)	Renal cell carcinoma of
Iclusig (ponatinib)	Chronic myeloid leukemia and Philadelphia chromosome positive acute lymphoblastic leukemia		Xalkori (crizotinib)	ALK+ non-small cell lung cancer of
Imbruvica (ibrutinib)	Chronic lymphocytic leukemia		Xeloda	Oral chemotherapy for the treatment of metastatic colorectal cancer
Imbruvica (ibrutinib)	Mantle cell lymphoma of		Xeloda	Advanced breast cancer tumors
Imlygic (talimogene laherparepvec)	Unresectable recurrent melanoma October		Xgeva (denosumab)	Giant cell tumor of bone
Inform HER-2/neu breast cancer test	Breast cancer prediction		Xgeva (denosumab)	For the prevention of skeletal-related events in patients with bone metastases from solid tumors
Inlyta (axitinib)	Advanced renal cell carcinoma		Xofigo (radium Ra 223 dichloride)	Prostate cancer with bone metastases
Intron A (interferon alfa-2b recombinant)	Non-Hodgkin's lymphoma		Xtandi (enzalutamide)	Metastatic castration-resistant prostate cancer August
Intron A (Interferon alfa-2b recombinant)	An adjuvant treatment to surgery in subjects at high risk for systemic recurrence of malignant melanoma		Yervoy (ipilimumab)	Metastatic melanoma
Iressa (gefitinib)	For the second-line treatment of non-small-cell lung cancer		Yondelis (trabectedin)	Liposarcoma or leiomyosarcoma
Istodax (romidepsin)	Cutaneous T-cell lymphoma		Zaltrap (ziv-aflibercept)	Metastatic colorectal cancer
Ixempra (ixabepilone)	Breast cancer		Zelboraf (vemurafenib)	BRAF + melanoma of
Jevtana (cabazitaxel)	Prostate cancer		Zevalin (ibritumomab tiuxetan)	Non-Hodgkin's lymphoma
Kadcyla (ado-trastuzumab emtansine)	HER2-positive metastatic breast cancer		Zofran	The prevention of chemotherapy and radiation-induced nausea
Kadian	Chronic moderate to severe pain		Zofran	Postoperative vomiting and nausea in adults
Keytruda (pembrolizumab)	Unresectable or metastatic melanoma		Zoladex (10.8 mg goserelin acetate implant)	Advanced prostate cancer
Kyprolis (carfilzomib)	Multiple myeloma		Zometa (zoledronic acid)	Multiple myeloma and bone metastases from solid tumors
Kytril (granisetron) solution	For the prevention of nausea and vomiting associated with cancer therapy		Zometa (zoledronic acid)	Hypercalcemia of malignancy

Kytril (granisetron) tablets	Prevention of nausea and vomiting associated with chemotherapy		Zuplenz (ondansetron oral soluble film)	For the prevention of post-operative chemotherapy and radiotherapy induced nausea and vomiting
Lazanda (fentanyl citrate) nasal spray	For the management of breakthrough cancer pain		Zydelig (idelalisib)	Relapsed CLL follicular B-cell NHL and small lymphocytic lymphoma
Lenvima (lenvatinib)	Thyroid cancer		Zykadia (ceritinib)	ALK+ metastatic non-small cell lung cancer
Leukine (sargramostim)	The replenishment of white blood cells		Zytiga (abiraterone acetate)	Prostate cancer
Leukine (sargramostim)	Mobilizing peripheral blood progenitor cells for use after transplantation. On november 24			

Sup.Knowledge:02 (SK2)

BiochemicalPathway of HIV-replication

(Red arrows: virus reactions, blue arrows: host reactions)

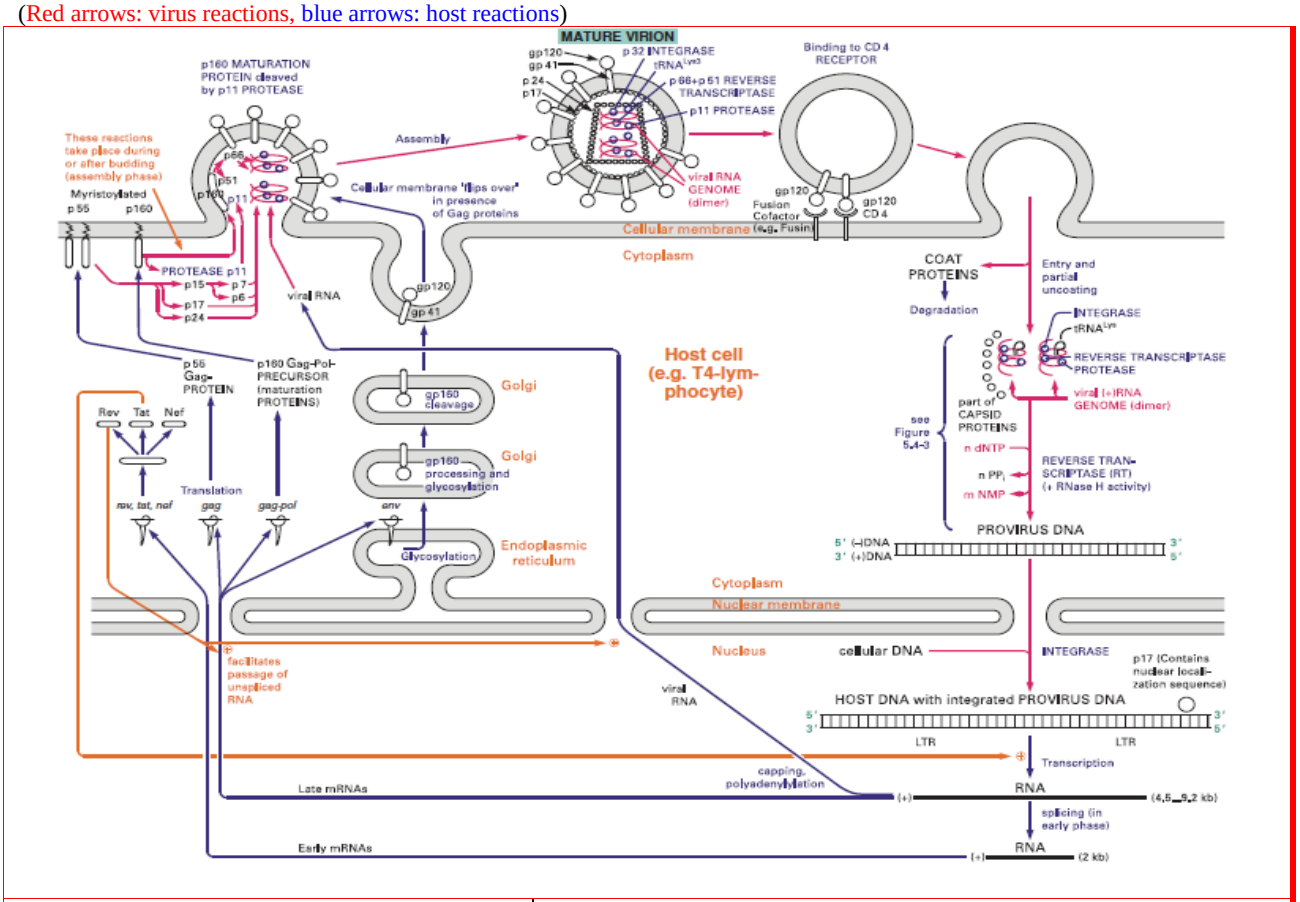

Attachment	Transcription (Viral protein expression
Fusion and capsid disassembly	Virus assembly
Reverse transcription (DNA synthesis)	Virus budding

- Nuclear import and integration
- Virus maturation

Courtesy of Gerhard Michal, Dietmar Schomburg (Editors), 2012, Biochemical pathways:An atlas of biochemistry and Molecular biology(Second Edition) , A John Wiley & Sons, Inc., New Jersey.

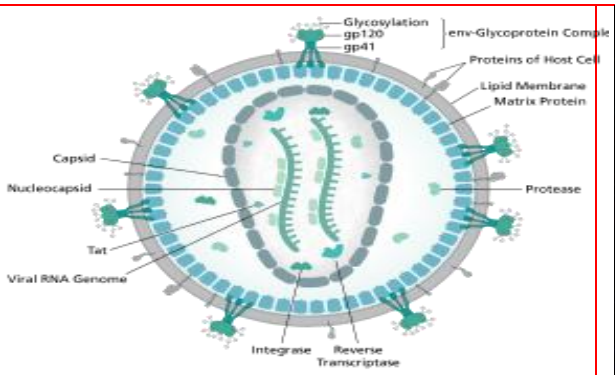

- HIV virion
  - Core proteins
    - ✓ Reverse transcriptase
    - ✓ Genome
  - Lipid envelope (100 nm in diameter)
    - ✓ Dense cylindrical nucleoid
    - ✓ Proteins gp41, gp120,
    - ✓ Nucelocapsid proteins
      - p24, p17, p9, p7

Sequence similar to non-cell-transforming lentiviridae

- Visna and caprine encephalitis viruses

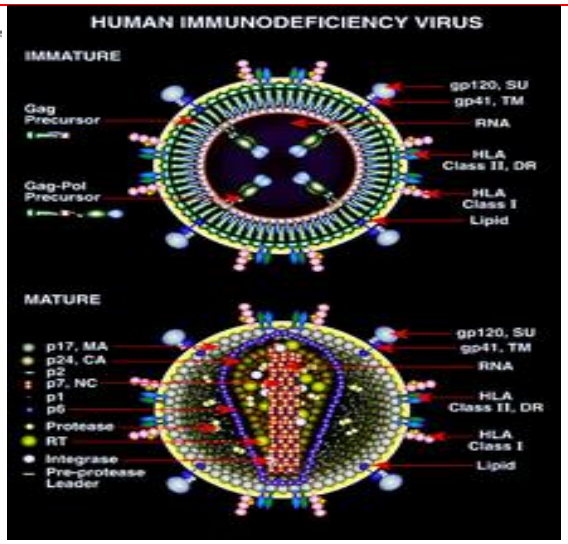

Diagram of the immature and mature forms of HIV

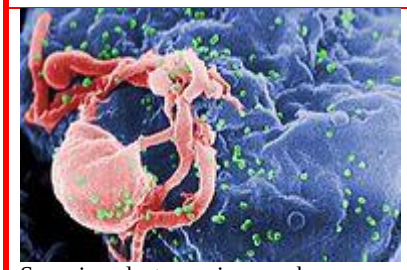

Scanning electron micrograph
Green dots: HIV-1 budding from cultured lymphocyte.
Multiple round bumps on cell surface: sites of assembly

Group	: Group VI (ssRNA-RT)
Order	: Unassigned
Family	: Retroviridae
Subfamily	: Orthoretrovirinae
Genus	: Lentivirusand budding of virions

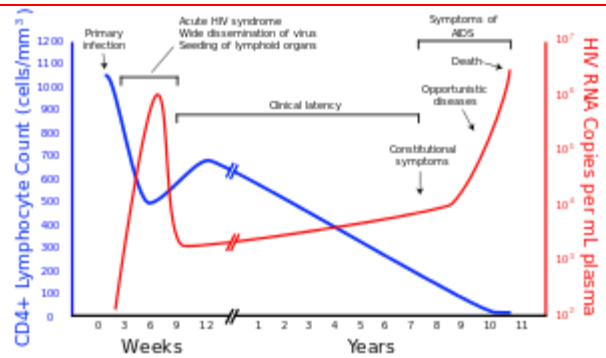

y	x
CD4+ T cell count (cells per µL)	Time of untreated patient
HIV RNA copies per mL of plasma	

Courtesy of WikiPedia

AUTHORS' ADDRESSES

1. **K RamaKrishna**
Department of Chemistry,
Gitam Institute of Science,
Gitam University,
Visakhapatnam, A.P
E-mail:karipeddirk@gmail.com

2. **R. Sambasiva Rao**
School of Chemistry,
Andhra University,
Visakhapatnam 530 003, A.P
E-mail:rsr.chem@gmail.com

3. **B. Venkata Sasidhar**
Department of Chemistry,
Gitam Institute of Science,
Gitam University,
Visakhapatnam, A.P